Markus Gerold Schröfl, BSc

Quark Masses and Flavour Mixing in a minimal, parameterized Ultraviolet Completion of the Standard Model

MASTER'S THESIS

to achieve the university degree of

Master of Science

Master's degree programme: Physics

submitted to

Graz University of Technology

Supervisor

Univ.-Prof. Dr.rer.nat. Reinhard Alkofer

Institut für Physik der Karl-Franzens-Universität Graz

Graz, December 2019

AFFIDAVIT

I declare that I have authored this thesis independently, that I have not used other than the declared sources/resources, and that I have explicitly indicated all material which has been quoted either literally or by content from the sources used. The text document uploaded to TUGRAZonline is identical to the present master‘s thesis.

Date

Signature

Abstract

We study the renormalization group flow of the Standard Model of Elementary Particle Physics gauge-Yukawa sector including minimal, parametrized, antiscreening contributions from new physics which render the Standard Model ultraviolet complete. Besides the gauge sector, we consider a two generation quark Yukawa sector where we take flavour mixing effects into account. The competition between the Standard Model running and the antiscreening new-physics terms results in a sophisticated system of fixed point solutions. We explore to what extent the observed low energy flavour structure of the standard model can be deduced from the renormalization group evolution of this model. We show that there exist fixed point solutions which put constraints on the mass spectrum of the quarks in the infrared while yielding phenomenologically viable renormalization group trajectories.

Kurzfassung

Wir untersuchen den Renormierungsgruppenfluß des Eich-Yukawa-Sektors im Standardmodell der Elementarteilchenphysik unter Einbindung von minimalen, parametrisierten, anti-abschirmenden Beiträgen neuer Physik, welche eine Ultraviolettvervollständigung des Standardmodells ermöglichen. Neben dem Eichsektor berücksichtigen wir einen Yukawasektor mit zwei Quarkgenerationen inklusive Flavourmischungseffekten. Das Zusammenspiel von Standardmodell und anti-abschirmenden Termen erzeugt ein komplexes System von Fixpunktlösungen. Wir untersuchen in welchem Ausmaß die beobachteten Niedrigenergieflavourstrukturen des Standardmodells von der Renormierungsgruppenentwicklung dieses Modells abgeleitet werden können. Wir zeigen, dass es Fixpunktlösungen gibt, welche das Massenspektrum der Quarks im Infraroten einschränken und gleichzeitig eine phänomenologisch brauchbare Renormierungsgruppentrajektorie liefern.

This page is intentionally left blank.

Contents

This page is intentionally left blank.

1. Introduction

The Standard Model (SM) of particle physics is a quantum gauge field theory (QFT) which describes the weak, strong and electromagnetic interactions between all experimentally known elementary particles employing non-Abelian and Abelian gauge groups. Even though there is an astounding agreement between experiment and theory, the SM cannot be viewed as a fundamental theory of nature. Besides others, one of the reasons for this is the fact that the SM is not valid at arbitrary high energy scales. At the perturbative level, the renormalization group (RG) running of the Abelian gauge coupling leads to a Landau pole, where the gauge coupling becomes infinite and perturbation theory breaks down [1]. A similar phenomenon occurs in the Yukawa sector of the SM [2]. There are hints that the impossibility of finding a suitable ultraviolet (UV) completion of the SM persists even beyond perturbation theory[1], a circumstance which would render the SM *trivial*. Hence, the SM should be considered an *effective field theory*: A QFT which is valid in a certain range of energies, but fails to describe physics at any other scale. In order to render the SM fundamental, i.e., valid at *all* scales, new beyond-the-standard-model (bSM) physics have to be incorporated into the theory, which alter the RG flow of the SM couplings. Such bSM physics could be, for example, gravity, dark matter, grand unified theories etc.

Besides the lack of a suitable UV completion, the SM suffers from an "aesthetic" problem: It contains a large number of free parameters whose values have to be fixed by comparing them to experimental data and cannot be derived from first principles. The majority of these parameters stem from the Yukawa sector of the SM and are on account of the fermionic matter content. The fermions in the SM are grouped into three generations of quarks and leptons, adding up to a total of 12 particles. The masses of these particles range from sub-meV (neutrinos) over the sub-MeV domain (e.g. the electron mass: $m_e \approx 0.511\,\mathrm{MeV}$) to more than a hundred GeV (top quark mass: $m_t \approx 173\,\mathrm{GeV}$). The SM itself neither explains the individual masses of the particles nor the large disparity between them. In addition to this intriguing mass spectrum, another phenomenon arises from the Yukawa sector of the SM: From experiment, we conclude that the eigenstates of the weak interaction are not equal to mass (or energy) eigenstates but rather linear superpositions of them. This is known as *flavour mixing*. Just like for the mass spectrum, we do not have an explanation for the observed mixing patterns. There have been several attempts in the past to derive both the mass spectrum of the fermions in the SM as well as the observed mixing patterns, but so far none of these have been entirely successful.

In this thesis, we study whether a minimalistic parametrization of new physics can

[1] see, e.g., [3–5]

provide a phenomenologically viable UV completion of the SM and explore to what extent the characteristics of the fermionic mass spectrum and mixing patterns can be deduced from the RG evolution of the respective SM couplings. We will focus on a toy model with two generations of quarks rather than the full SM, as this is sufficient to demonstrate the central findings we have made. An extension to three generations of quarks has been started in [6] and the investigation of a model containing the leptonic sector of the SM is subject to future works.

The cornerstone of this thesis is a modification of the SM β-functions of the form[2] [7–9]

$$\beta(g) = \beta^{\mathrm{SM}}(g) - \mathfrak{f}_g g \tag{1.1}$$

where g is a SM coupling constant and $\mathfrak{f}_g$ parametrizes the new physics contribution to the RG running of g. This new physics contribution is effectively decoupled from the SM at low energies, but becomes significant once a mass threshold M_{NP} is exceeded. In this thesis, we will assume that this new physics scale coincides or almost coincides with the Planck scale, $M_{\mathrm{NP}} \approx M_{\mathrm{Planck}}$. Even though the bSM term $-\mathfrak{f}_g g$ originally stems from a study of asymptotically safe quantum gravity coupled to the SM[3], we stress that in this thesis we do *not* specify the actual physics that generate such terms. We simply suppose that there is some new physics which renders the SM in this way UV complete, while describing the observed physics in the infrared (IR). The interplay between the SM β-functions $\beta^{\mathrm{SM}}(g)$ and the bSM contribution $-\mathfrak{f}_g g$ gives rise to an intricate system of RG fixed point (FP) solutions, the study of which will be the main part of this work. Not only does it provide a UV completion of the theory, it also puts constraints on the flavour structure, i.e., the mass spectrum and mixing pattern, in the IR.

The bSM term in Eq. (1.1) is linear in the coupling g and is hence the dominant term for $g \ll 1$, as the leading term of the SM β-function $\beta^{\mathrm{SM}}(g)$ is $\mathcal{O}(g^3)$. Furthermore, we assume that the bSM contribution to the running of the SM couplings is *antiscreening*, i.e., $-\mathfrak{f}_g < 0$ for $\mu > M_{\mathrm{NP}}$. This has, as discussed in Section 3.1, the effect that now there exists an asymptotically safe RG trajectory for the Abelian gauge coupling – a crucial feature of our model, as an interacting fixed point of the Abelian gauge coupling not only solves its Landau pole problem but also breaks the symmetry of the system of β-functions of the quark Yukawa couplings with respect to an exchange of up- and down-type flavour indices. This, in turn, extends to the fixed point solutions as well, with a given FP solution no longer being necessarily symmetric for up- and down-type quarks. Besides, the bSM contributions to the running of the SM couplings are minimal and universal in the sense that the contribution in the gauge sector is parametrized by one parameter f_g, and the contribution in the Yukawa sector is parametrized by one parameter f_y, which is equal for all quarks. This means that the assumed new physics part in the running of the couplings is completely parametrized by two free parameters, f_g and f_y.

This thesis is organized as follows: In Chapter 2 we lay out the fundamentals on

[2] Throughout this thesis, we will use perturbative one-loop β-functions for $\beta^{\mathrm{SM}}(g)$. A short overview of the effects of the respective two-loop terms is given in Chapter 5.

[3] see [7–9] and references therein.

which this work is build. We start with a discussion of the fermionic matter content of the SM and continue with a review of the Yukawa sector, where we introduce quark flavour mixing described by the Cabibbo-Kobayashi-Maskawa (CKM) matrix [10, 11]. We proceed with a recapitulation of the renormalization group in QFT. Here, we will be predominantly concerned with the concept of RG fixed points and their implications for the predictivity of a quantum field theory. The chapter will be concluded with the derivation of the necessary perturbative one-loop β-functions of the gauge and Yukawa couplings in the SM as well as of the CKM matrix elements.

In Chapter 3 we will introduce the major features of our approach by reviewing the study of a top-bottom-system as performed in [9]. We will demonstrate how low energy values of coupling constants can be calculated from non-vanishing UV fixed points, an important observation that places significant constraints on the IR values of – otherwise free – couplings. Specifically, we show how a modification of the SM β-functions of the form Eq. (1.1) can provide an asymptotically safe RG trajectory of the Abelian gauge coupling. As a consequence, the difference in the weak hypercharges of up- and down-type quarks generates unequal interacting UV fixed points for the top and bottom quarks. We then show that there exists a RG trajectory which connects this UV fixed point with IR values that are – to a great degree – phenomenologically viable.

Chapter 4 forms the main part of this thesis. We extend the study of the previous gauge-Yukawa system to a model with two generations of quarks, which we will study in detail. Mixing effects now have to be taken into account, which will introduce a new layer of complexity to the theory. After exploring the fixed point solutions of this model, a phenomenologically viable RG flow – extending the discussions of Chapter 3 to two generations – will be presented. The chapter will be concluded by a discussion of the poles appearing in the β-functions of the squared moduli of the CKM matrix elements – a non-perturbative property of the RG evolution of the CKM matrix, stemming from its unitarity, which further restrains the values of the SM couplings in the IR.

We will conclude this thesis in Chapter 5, where we summarize our findings and give an interpretation of our results. We also provide a brief outlook on the study of a system containing three generations of quarks, based on the studies in [6], and on future possible extensions of this work. The Appendices contain additional information as well as details on the calculations performed in the main text.

The main results of this thesis are – together with some extensions to three generations – published in [6], which has been prepared by a collaboration including the author and the supervisor of this thesis.

2. Basic Concepts

2.1. Standard Model of Particle Physics

The Standard Model (SM) of particle physics is a non-Abelian gauge theory based on the symmetry group[1] $\mathsf{SU}(N_c)_\mathsf{C} \otimes \mathsf{SU}(2)_\mathsf{L} \otimes \mathsf{U}(1)_\mathsf{Y}$ [12]. It constitutes the theoretical description of all known elementary particles and their interactions via the strong and electroweak forces. In the following, we will give a brief overview of those sections of the SM which will concern us the most in the upcoming chapters. We start by reviewing the fermionic matter content of the SM.

2.1.1. Fermionic Matter Content

The fermionic matter fields in the SM consist of quarks and leptons and are organized into three generations (cf. Tab. 2.1). Each generation contains two quarks (up- and down-type quark) and two leptons (charged lepton and neutrino), where the difference between up- and down-type quarks and charged leptons and neutrinos lies in the $\mathsf{U}(1)_\mathsf{Y}$ hypercharge of the respective right-handed $\mathsf{SU}(2)_\mathsf{L}$ singlets. Quarks are strongly interacting particles and transform as colour-triplets under $\mathsf{SU}(3)_\mathsf{C}$, while the leptons do not interact via the strong force and hence transform as singlets under $\mathsf{SU}(3)_\mathsf{C}$ transformations. As the SM is a chiral theory, the fermion fields are split into left-handed (l.h.) and right-handed (r.h.) Weyl-spinors. The left-handed fields transform as doublets under $\mathsf{SU}(2)_\mathsf{L}$ transformations, while the right-handed fields transform as singlets. A summary of the transformation properties of the fermion fields present in the SM is given in Tab. 2.2. For later use the respective properties of the Higgs particle are included.

The three generations of fermions in the SM are identical in terms of their gauge group representations. Their difference lies solely in their flavour quantum numbers and

[1] In the SM, $N_c = 3$.

Generation	up-type	down-type	charged lepton	neutrino
1	up (u)	down (d)	electron (e)	electron neutrino (ν_e)
2	charm (c)	strange (s)	muon (μ)	muon neutrino (ν_μ)
3	top (t)	bottom (b)	tau (τ)	tau neutrino (ν_τ)

Table 2.1.: Generation structure of fermions in the SM [13].

particle	chirality	gauge group representation
up-type	l.h.	$(3,2)_{\frac{1}{6}}$
	r.h.	$(3,1)_{\frac{2}{3}}$
down-type	l.h.	$(3,2)_{\frac{1}{6}}$
	r.h.	$(3,1)_{-\frac{1}{3}}$
charged lepton	l.h.	$(1,2)_{-\frac{1}{2}}$
	r.h.	$(1,1)_{-1}$
neutrino	l.h.	$(1,2)_{-\frac{1}{2}}$
	r.h.	$(1,1)_0$
Higgs	complex scalar	$(1,2)_{\frac{1}{2}}$

Table 2.2.: The matter content of the $\mathsf{SU}(N_c)_\mathsf{C}\otimes\mathsf{SU}(2)_\mathsf{L}\otimes\mathsf{U}(1)_\mathsf{Y}$ Standard Model (cf. [12]), given for $N_c = 3$. In the third column, the gauge group representations of the respective particles are given in the form $(a,b)_c$. Here, a is the representation of the colour group $\mathsf{SU}(3)_\mathsf{C}$ under which the particle transforms: 3 means the particle transforms as a colour-triplet, i.e. in the fundamental representation of $\mathsf{SU}(3)_\mathsf{C}$ and 1 means the field transforms as a colour-singlet, i.e. it is invariant under $\mathsf{SU}(3)_\mathsf{C}$-transformations. b denotes the representation of $\mathsf{SU}(2)_\mathsf{L}$, where 2 corresponds to the fundamental representation (left-handed doublets) and 1 means the fields transform as singlets (right-handed singlet). The subscript c represents the $\mathsf{U}(1)_\mathsf{Y}$ hypercharge of the respective particle.

– an observation that is of central interest to us – the masses of the respective quarks and leptons [13]. In Tab. 2.3, we list the most recent quark[2] mass estimates from the particle data group booklet [14]. As one can see, the mass spectrum of quarks in the SM spans a range of five orders of magnitude: the heaviest quark, the top quark, is approximately 10^5 times heavier than the lightest quark, the up quark. The mass ratios within generations vary as well: $m_u/m_d \approx 0.5$, $m_c/m_s \approx 13$ and $m_t/m_b \approx 40$. Notice that in the first generation, the up-type quark is *lighter* than the down-type quark, a circumstance that is not present in the other two generations. The SM does not yield an explanation for the masses of fermions observed in the laboratory. They are free parameters of the theory and are fixed by comparing them to experiment. The fermionic mass spectra – together with the mixing patterns – remain one of the most intriguing enigmas of the SM. In this thesis, we will infer potential constraints on the mass spectrum and mixing patterns of quarks by studying RG fixed point solutions of a minimally parametrized bSM model.

[2]From now on, we will focus on quarks and ignore leptons for the most part.

quark	mass / MeV
up (u)	$2.16 \pm 0.49 \pm 0.26$
down (d)	$4.67 \pm 0.48 \pm 0.17$
charm (c)	$1\,270 \pm 20$
strange (s)	$95 \pm 11 \pm 5$
top (t)	$172\,900 \pm 400$
bottom (b)	$4\,180 \pm 30 \pm 20$

Table 2.3.: Quark mass estimates taken from [14]. The masses are calculated in the $\overline{\text{MS}}$ scheme at a renormalization scale of $\mu = 2\,\text{GeV}$ for light quarks (u, d, s) and $\mu = m_Q$ for heavy quarks (c, b). The value of the top quark mass is the particle data group's (PDG) average of direct measurements from LHC and Tevatron Runs (see [14] for details). The first given error is statistical, the second (if given) is systematic.

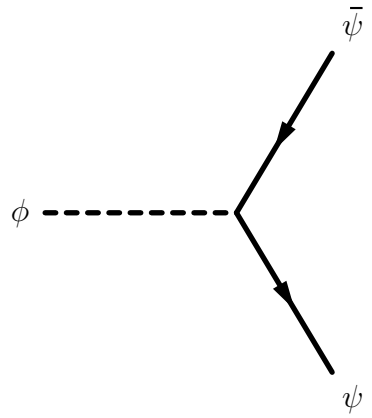

Figure 2.1.: Yukawa interaction vertex.

2.1.2. Yukawa Sector[3]

Yukawa couplings describe interactions between a scalar field and a fermion and are of the form $\sim y\phi\bar{\psi}\psi$, where y is the coupling constant of the interaction (cf. Fig. 2.1). In the SM, fermions acquire their masses through their coupling to the Higgs via the so-called Brout-Englert-Higgs effect [16–18]. A general Yukawa Lagrangian describing a theory with N_g generations of fermions reads [19–21]

$$\mathscr{L}_{\text{YUK}} = \overline{Q}_{\text{L}}\tilde{\Phi}\boldsymbol{\mathcal{Y}}_u u_{\text{R}} + \overline{Q}_{\text{L}}\Phi\boldsymbol{\mathcal{Y}}_d d_{\text{R}} + \overline{l}_{\text{L}}\Phi\boldsymbol{\mathcal{Y}}_e e_{\text{R}} + \overline{l}_{\text{L}}\tilde{\Phi}\boldsymbol{\mathcal{Y}}_\nu \nu_{\text{R}} + \text{h.c.} \tag{2.1}$$

where the Yukawa coupling matrices $\boldsymbol{\mathcal{Y}}_{u,d,e}$ are general complex, non-Hermitian $N_g \times N_g$ matrices

$$\boldsymbol{\mathcal{Y}}_{u,d,e,\nu} \in \mathbb{C}^{N_g \times N_g} \tag{2.2}$$

[3]For a comprehensive review of the topics presented in this section the reader may refer to [12, 13, 15].

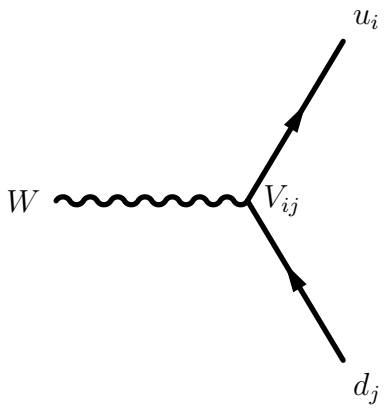

Figure 2.2.: Weak charged current interaction vertex.

and $\tilde{\Phi} \equiv i\sigma_2\Phi^*$ is the conjugate Higgs doublet. $\overline{Q}_\mathrm{L}$ and $\overline{l}_\mathrm{L}$ are the left-handed $\mathsf{SU}(2)_\mathsf{L}$ doublets of the quarks and leptons, respectively, and u_R, d_R, e_R and ν_R are the right-handed $\mathsf{SU}(2)_\mathsf{L}$ singlets. Note that generational indices are suppressed in Eq. (2.1).

The fact that the Yukawa matrices are general, rather than diagonal, matrices has far reaching consequences: Phenomenology tells us that – in the SM – the eigenstates of the weak interactions[4] are *not* equal to the mass (or energy) eigenstates. The eigenstates of the weak interactions are those states which are produced in weak interactions like, e.g., weak charged current interactions (cf. Fig. 2.2). Those states form an orthonormal basis and – in the most general case – the Yukawa matrices will be general complex $N_g \times N_g$ matrices with respect to this basis. After spontaneous symmetry breaking, we expect to have mass terms of the form $\sim m_{(i)}\bar{\psi}_i\psi_i$ in the Lagrangian. Hence, the general, complex Yukawa matrices $\boldsymbol{\mathcal{Y}}_{u,d,e,\nu}$ have to be diagonalized, i.e., a change of basis has to be performed. The eigenstates with respect to this basis are the mass (or energy) eigenstates, i.e., the propagating states. The disparity between the flavour and mass eigenstates gives rise to phenomenons such as flavour mixing and flavour oscillations, which we will discuss in the following.

In order to diagonalize the Yukawa matrices, we notice that one can always write a complex matrix as a product of a Hermitian and a unitary matrix [13]:

$$\boldsymbol{\mathcal{Y}}_i = \boldsymbol{\mathcal{H}}_i\,\boldsymbol{\mathcal{U}}_i = \boldsymbol{U}_i^\dagger\,\mathscr{Y}_i\,\boldsymbol{U}_i\,\boldsymbol{\mathcal{U}}_i\ , \qquad i \in \{u,\, d,\, e,\, \nu\}\ . \tag{2.3}$$

Here, $\boldsymbol{\mathcal{H}}_i$ is a Hermitian matrix, $\boldsymbol{U}_i$ and $\boldsymbol{\mathcal{U}}_i$ are unitary matrices and $\mathscr{Y}_i$ is a diagonal matrix. The diagonal matrices $\mathscr{Y}_{u,d}$ contain the physical quark Yukawa couplings

$$\mathscr{Y}_u = \mathrm{diag}\,(y_u, y_c, y_t, \ldots)\ , \qquad \mathscr{Y}_d = \mathrm{diag}\,(y_d, y_s, y_b, \ldots)\ , \tag{2.4}$$

which are – after SSB – related to the physical fermion masses via [21]

$$\mathscr{Y}_u = \frac{\sqrt{2}}{v}\,\mathrm{diag}\,(m_u, m_c, m_t, \ldots)\ , \quad \mathscr{Y}_d = \frac{\sqrt{2}}{v}\,\mathrm{diag}\,(m_d, m_s, m_b, \ldots)\ , \tag{2.5}$$

[4] also referred to as flavour eigenstates

where v is the vacuum expectation value of the Higgs, $v = 246$ GeV.

In general, it is not possible to diagonalize all Yukawa matrices simultaneously, i.e.

$$\boldsymbol{U}_u \neq \boldsymbol{U}_d \,, \qquad \boldsymbol{U}_e \neq \boldsymbol{U}_\nu \,. \tag{2.6}$$

This has a net effect on the weak charged current interactions. For example, the terms in the Lagrangian that generate the charged current interactions between a up- and a down-type quarks are of the form [13]

$$\bar{u}_\mathrm{L} d_\mathrm{L} = \bar{u}'_\mathrm{L} \boldsymbol{U}_u \boldsymbol{U}_d^\dagger d'_\mathrm{L} = \bar{u}'_\mathrm{L} \boldsymbol{V} d'_\mathrm{L} \,, \tag{2.7}$$

where primed fields are fields in the mass basis and $\boldsymbol{V}$ is the Cabibbo-Kobayashi-Maskawa (CKM) matrix[5] [10, 11] defined as [12, 24]

$$\boldsymbol{V} \equiv \boldsymbol{U}_u \boldsymbol{U}_d^\dagger \,. \tag{2.8}$$

The charged current vertices are proportional to the elements of this matrix (cf. Fig. 2.2). The $W^\pm$ bosons now couple any up-type quark with all down-type mass eigenstate quarks because the weak doublet partner of u_i is a superposition of down-type mass eigenstates[6] :

$$\begin{pmatrix} d \\ s \\ b \end{pmatrix} = \begin{pmatrix} V_{11} & V_{12} & V_{13} \\ V_{21} & V_{22} & V_{23} \\ V_{31} & V_{32} & V_{33} \end{pmatrix} \begin{pmatrix} d' \\ s' \\ b' \end{pmatrix} = \begin{pmatrix} V_{ud} & V_{us} & V_{ub} \\ V_{cd} & V_{cs} & V_{cb} \\ V_{td} & V_{ts} & V_{tb} \end{pmatrix} \begin{pmatrix} d' \\ s' \\ b' \end{pmatrix} \,. \tag{2.9}$$

This phenomenon is called *flavour mixing*. Flavour eigenstates produced in weak interactions are hence a superposition of mass eigenstates. As we know from quantum mechanics, a state that is a superposition of energy eigenstates is generally no longer a stationary state. For states produced in weak interaction, this gives rise to a phenomenon which is called *flavour oscillation*[7].

The CKM matrix $\boldsymbol{V}$ is a $N_g \times N_g$ unitary matrix. It therefore has N_g^2 independent real parameters. In case of $\boldsymbol{V}$ however, we can absorb some of those parameters into unobservable global quark phases [12]. With two quarks per generation, we can redefine $2N_g$ parameters as quark phases, leaving us with $2N_g - 1$ relative and 1 global phase, hence reducing the number of independent CKM parameters to $(N_g - 1)^2$. In the usual parametrizations, those are $N_g(N_g-1)/2$ rotation angles and $(N_g-1)(N_g-2)/2$ complex phases.

In case of $N_g = 2$, the CKM matrix reduces to a rotation matrix characterized by a single parameter: the Cabibbo angle θ_C [10]. In case of $N_g = 3$, the CKM matrix is usually parametrized by 3 rotation angles and 1 $\mathcal{CP}$ violating complex phase. In Sec. 2.3,

[5] An analogous effect in the leptonic sector is described by the so called Pontecorvo-Maki-Nakagawa-Sakata (PMNS) matrix [22, 23]

[6] It is purely conventional to define the matrix in terms of down-type flavour and mass eigenstates. A definition in terms of up-type eigenstates would be just as valid.

[7] see, e.g., [13] for a review on this topic.

we will derive, following the argumentation of Sasaki [25], the one-loop β-functions of the quadratic matrix elements $|V_{ij}|^2$. This is convenient, as the matrix elements $|V_{ij}|^2$ also appear in the β-functions of the physical Yukawa couplings. Furthermore, the quadratic entries $|V_{ij}|^2$ are, unlike the angles and phases, convention independent. In order to see that the knowledge of the quadratic entries $|V_{ij}|^2$ is equivalent to the knowledge of the angles and phases, we recall the unitarity conditions for a $N_g \times N_g$ matrix:

$$\sum_i V_{ij} V_{ik}^* = \delta_{jk} \,, \qquad \sum_j V_{ij} V_{kj}^* = \delta_{ik} \,, \qquad \forall\, i,j,k = 1,\ldots,N_g \,. \tag{2.10}$$

From the N_g^2 real parameters $|V_{ij}|^2$, the above unitarity conditions show that only $(N_g - 1)^2$ of them are independent. Therefore, there are just as much independent quadratic entries $|V_{ij}|^2$ as there are independent angles and phases in $\boldsymbol{V}$ [25].

As stated above, generally it is not possible to diagonalize all Yukawa matrices simultaneously (cf. Eq. (2.6)). Hence, the CKM matrix is – in the general case – not equal to the unit matrix:

$$\boldsymbol{V} \neq \mathbb{1} \,. \tag{2.11}$$

The PDG lists the experimentally determined magnitudes of the CKM matrix elements as[8] [14]:

$$\{|V_{ij}|\} = \begin{pmatrix} 0.97420 \pm 0.00021 & 0.2243 \pm 0.0005 & (3.94 \pm 0.36) \times 10^{-3} \\ 0.218 \pm 0.004 & 0.997 \pm 0.017 & (42.2 \pm 0.8) \times 10^{-3} \\ (8.1 \pm 0.5) \times 10^{-3} & (39.4 \pm 2.3) \times 10^{-3} & 1.019 \pm 0.025 \end{pmatrix} \,. \tag{2.12}$$

It turns out that the CKM matrix is diagonally dominant and close to – but not equal to – the unit matrix. While there have been efforts in the past to explain this observed structure[9], so far there has been no completely successful attempt. In this thesis, we study whether the RG evolution of a minimally parametrized bSM theory can provide further insight into this problem.

2.2. Renormalization Group

In this section, we will introduce the renormalization group (RG). We will derive the notion of running couplings, β-functions, fixed points and RG flows in theory space, which will allow us to make statements about the predictivity of quantum field theories. Though most of the presented concepts are general features of the renormalization group, we will start with the RG in the context of perturbative calculations in QFT [1, 29–31], as the RG β-functions used in this work will be calculated within perturbation theory. For a more complete introduction to these topics see, e.g., [32–37].

[8] for details, see [14]

[9] An example would be, e.g., [26–28]

2.2.1. Renormalization Group Equations

In the perturbative calculation of n-point correlation functions within a given QFT, divergent integrals over virtual loop momenta may occur, which render the perturbation expansion ill-defined [36]. In order to find a well-defined perturbation expansion[10], one first needs to *regularize* the divergent integrals by, e.g., introducing a momentum cut-off Λ or by analytic continuation of the space-time dimension d [38, 39]. The regularization procedure has the effect that the (formerly divergent) coefficient functions of the perturbative expansion are now finite as long as the regulator is not removed. These coefficient functions can be split into a finite, regular part and a "singular" part, which is that part that diverges if the regulator is removed. As a next step, one *renormalizes* the theory by introducing suitable counter-terms in the Lagrangian. This causes a reparametrization of the theory: All the bare parameters of the theory (couplings and masses) can be expressed in terms of (multiplicative) renormalization constants and (finite) renormalized couplings. In addition, the fields themselves are rescaled as well. The counter-terms are chosen such that they exactly cancel the singular parts of the coefficient functions when one calculates the – now finite – renormalized correlation functions from the renormalized Lagrangian. As the singular parts cancel exactly, the regulator can be removed after the renormalization step.

The counter-terms themselves are divergent as well and can also be split into a singular and a regular part. While the singular part is fixed by requiring the renormalized correlation functions to be finite, the regular parts are completely arbitrary. A *renormalization scheme* is a prescription for choosing these finite parts [40]. As the choice of renormalization scheme is arbitrary, physical quantities must not depend on it. Yet, the results of calculations change if the finite parts of the counter-terms are altered. This apparent problem can be solved by realizing that a change of renormalization scheme can be compensated by changing the values of the renormalized parameters of the theory [40]. Hence, a change of renormalization scheme changes the *parametrization* of the theory rather than the theory itself [33]. One way of changing the renormalization scheme is to vary the value of μ, the dimensionful *renormalization scale* which is generically introduced in the renormalization procedure. The invariance of a theory with respect to a change in the renormalization scale μ is described by the *renormalization group*[11] (RG) [1, 29–31, 42–45].

In order to fully determine the theory, one fixes the renormalized couplings and masses at a renormalization point μ such that one recovers experimental results. If the theory is perturbatively renormalizable, the number of required experimental data is finite and one needs exactly as much data points as there are free parameters in the theory[12]. The theory is then described by a set of parameters at a scale μ: $(\mu; \{g_i\}, m)$. What happens if we change this (arbitrary) scale, i.e., perform a *scale transformation* $\mu \to \mu'$? We remember that a change in scale is nothing but a change of the finite parts of

[10] we assume the theory is, in fact, (perturbatively) renormalizable.

[11] Generally speaking, the RG is only a *semigroup*, as the RG transformations employed are not necessarily invertible [41].

[12] cf. Sec. 2.2.2

the counter-terms, i.e., a change in regularization scheme. Hence, as discussed above, physical quantities (like, e.g., S-Matrix elements) have to be invariant under such a scale transformation. From this requirement, we can infer that the numerical values of the parameters of the theory have to change in order to ensure that physical quantities are indeed invariant if μ is changed [33]:

$$(\mu; \{g_i\}, m) \;\rightarrow\; (\mu'; \{g_i'\}, m') \;, \tag{2.13}$$

$$\mathcal{F}(\{g_i\}, m; \mu) = \mathcal{F}(\{g_i'\}, m'; \mu') \;, \tag{2.14}$$

where $\mathcal{F}$ is some physical quantity.

We are now going to derive the renormalization group equations (RGE) that describe the change of the parameters under a change in the scale μ, such that the theory itself stays invariant. The renormalized n-point correlation functions G_n defined by

$$G_n(x_1, \ldots, x_n; \{g_i\}, m, \mu) \;\equiv\; \langle \mathcal{T}\phi(x_1) \ldots \phi(x_n) \rangle \;, \tag{2.15}$$

where $\mathcal{T}$ is the time-ordering operator and which are related to the bare n-point correlation functions via

$$G_n(x_1, \ldots, x_n; \{g_i\}, m, \mu) \;= Z_\phi^{-\frac{n}{2}} G_n^B\left(x_1, \ldots, x_n; \left\{g_i^B\right\}, m^B\right) \tag{2.16}$$

with Z_ϕ the field renormalization constant defined by

$$\phi = Z_\phi^{-\frac{1}{2}} \phi^B \;. \tag{2.17}$$

Now assume an infinitesimal change in the renormalization scale:

$$\mu \;\rightarrow\; \mu' = \mu + \mathrm{d}\mu \;. \tag{2.18}$$

From Eq. (2.14) we conclude

$$\mu \frac{\mathrm{d}\mathcal{F}}{\mathrm{d}\mu} = \frac{\mathrm{d}\mathcal{F}}{\mathrm{d}t} = 0 \;, \tag{2.19}$$

where we defined the dimensionless *renormalization group time* $t \equiv \log(\mu/\Lambda)$ with Λ some reference scale. The total derivative with respect to t can be expressed as [33]

$$\frac{\mathrm{d}}{\mathrm{d}t} = \frac{\partial}{\partial t} + \sum_i \frac{\partial g_i}{\partial t} \frac{\partial}{\partial g_i} + \frac{\partial m}{\partial t} \frac{\partial}{\partial m} \;. \tag{2.20}$$

Given that the bare correlation functions are independent of the renormalization scale μ, i.e., they are renormalization group invariant, we end up with the following equation[13]

[13] Here, we assumed only a single field ϕ on the right-hand side of Eq. (2.15). If there are several kinds of fields ϕ_i with different field renormalization constants Z_{ϕ_i}, the total pre-factor on the right-hand side of Eq. (2.16) has the form $\prod_i Z_{\phi_i}^{-n_i/2}$ where n_i is the number of fields ϕ_i appearing in the correlation function $G_{n_1 \ldots n_m}$. Accordingly, an additional sum appears in the Callan-Symanzik equation Eq. (2.22).

[33];

$$\begin{aligned}\frac{\mathrm{d}G_n}{\mathrm{d}t} &= \frac{\mathrm{d}}{\mathrm{d}t}\left(Z_\phi^{-\frac{n}{2}} G_n^B\right) \\ &= \left(\frac{\mathrm{d}}{\mathrm{d}t} Z_\phi^{-\frac{n}{2}}\right) G_n^B \\ &= \left(-\frac{n}{2} Z_\phi^{-\frac{n}{2}} Z_\phi^{-1} \frac{\mathrm{d}Z_\phi}{\mathrm{d}t}\right) G_n^B \\ &= -\frac{n}{2}\frac{\mathrm{d}\log Z_\phi}{\mathrm{d}t} G_n \ . \end{aligned} \tag{2.21}$$

Using Eq. (2.20) then yields the *Callan–Symanzik equation* [29–31]:

$$\left[\frac{\partial}{\partial t} + \sum_i \beta\left(g_i\right)\frac{\partial}{\partial g_i} + \gamma_m m \frac{\partial}{\partial m} + \frac{n}{2}\gamma\right] G_n\left(x_1, \ldots, x_n; \{g_i\}, m, \mu\right) = 0 \ . \tag{2.22}$$

Here, we defined the following renormalization group coefficients[14]:

$$\beta\left(g_i\right) \equiv \frac{\partial g_i}{\partial t} \ , \tag{2.23}$$

$$\gamma_m \equiv \frac{1}{m}\frac{\partial m}{\partial t} \ , \tag{2.24}$$

$$\gamma \equiv \frac{\mathrm{d}\log Z_\phi}{\mathrm{d}t} \ . \tag{2.25}$$

The β-functions defined in Eq. (2.23) are of special importance to us. They describe the running of the couplings in the Lagrangian, i.e., their dependence on the renormalization scale μ. The β-functions can be calculated either using perturbation theory or non-perturbatively, using, e.g., the functional renormalization group [47–51]. They constitute a system of differential equations, the solution of which describes a RG trajectory in theory space, i.e., a set of equivalent parametrizations of the theory. RG trajectories and RG fixed points are the topics of the next subsection.

We finish this subsection with a few comments on the renormalization scale μ. In order to fully determine a renormalized theory, one has to fix the renormalized coupling constants. This is typically done by defining a renormalized coupling as the value of a matrix element at some arbitrary renormalization point, e.g., at some specific kinematic configuration of the external momenta [52]. The matrix element depends on some energy scale Q that is characteristic for the process: a center-of-mass energy, a set of Mandelstam variables, a momentum transfer, etc. As the renormalization scale μ is completely arbitrary, there is no a priori correspondence with the energy scale of a

[14] If a mass independent renormalization (MIR) scheme, i.e. a renormalization scheme where the counter-terms are independent of the renormalized mass m, is applied, these functions only depend on the coupling constants $\{g_i\}$ and are independent of m [46]. Furthermore, they only implicitly depend on μ via the couplings. An example of a MIR scheme is the (modified) minimal subtraction ($\overline{\mathrm{MS}}$) scheme [38, 39].

process. However, in order to preserve the validity of the perturbative expansion, one is advised to choose μ to be of order Q.

In order to see this, we note that dimensional analysis tells us that the powers of the coupling constants in the perturbative expansion are accompanied by logarithmic terms[15] of the form $\sim \log \mu/Q$. Hence, the condition that the coupling is small, i.e. $g \ll 1$, is *not* sufficient to guarantee that higher order terms are negligible. Rather, the combination of coupling and logarithmic term has to be small:

$$\left| g \log \frac{\mu}{Q} \right| \ll 1 \ . \tag{2.26}$$

This is the case if – in addition to the smallness of g – the renormalization scale μ is chosen[16] to be of order Q:

$$\mu \sim \mathcal{O}(Q) \ . \tag{2.27}$$

The renormlization scale μ can then be thought of as being indicative of a "typical" energy scale of a process.

Substituting the bare couplings with renormalized couplings defined at some renormalization scale μ has the consequence that the integrals over virtual loop momenta are effectively cut off around μ [52]. This bridges the gap to the Wilsonian idea of the renormalization group [43–45]. The fact that we have to keep $\mu \sim \mathcal{O}(Q)$ in order to keep the perturbative expansion valid is not a coincidence but reflects a general property of the renormalization group: The physics happening at a certain scale is best described by the degrees of freedom present at this scale. The dynamics of such *effective* degrees of freedom are described by an *effective theory* [37]. Hence, phenomena at a scale μ are conveniently described by subsuming degrees of freedom of higher energies into a reparametrization of the theory, i.e. of the coupling constants and masses. In Wilsonian RG, phenomena at a length scale $\sim k^{-1}$ are described by integrating out high energy modes with momenta $p > k$. This results in an effective theory which governs the dynamics of the low energy modes with $p < k$. We will employ some ideas of the Wilsonian version of the RG in the following subsection.

2.2.2. Theory space, Fixed Points, and Predictivity

A *renormalization group flow* or renormalization group trajectory is a solution to Eq. (2.23). It constitutes a subset of the *theory space* of the respective QFT. The theory space of a given theory is defined as the space spanned by coupling constants $\{g_i\}$ representing all interactions[17] allowed by symmetries and field content of the theory. This space is in general infinitely dimensional.

Renormalization group *fixed points* (FP) are special elements of a theory space. At a RG fixed point, all β-functions vanish simultaneously and the theory becomes scale

[15] for details and constraints on this assertion see, e.g., [33, 36, 52].

[16] An example of this would be to define $\mu^2 \stackrel{!}{=} s^2 = t^2 = u^2$ in some $2 \to 2$ process.

[17] In the context of QFT, it is the space spanned by all possible operators of the field(s), which are invariant with respect to the theory's symmetry group [51].

invariant:

$$\beta_i\left(\{g_j\}\right)\Big|_\star = \left.\frac{\partial g_i}{\partial t}\right|_\star = 0 \qquad \forall\, i\ , \tag{2.28}$$

where a subscript $\star$ indicates that the expression is to be evaluated at a FP. One distinguishes between two kinds of fixed points: If the point where all couplings vanish ($g_i = 0\ \forall\, i$) is a FP, it is called a non-interacting FP, as it corresponds to a free theory. As the (Euclidean) path integral is then Gaußian, this FP is also called a Gaußian FP. Contrary to this, a FP where the coupling constants take finite values is called an interacting or non-Gaußian FP. If some, but not all couplings at a FP are (non-)vanishing, one also speaks of partially (non-)Gaußian FPs.

A FP can either be located in the IR or in the UV. In this thesis, we will be predominantely concerned with UV fixed points. A theory that posseses an UV FP of any kind is said to be UV-complete and is well-behaved and predictive at all scales [53]. The notion of a QFT with a fixed point in the UV leads to the concept of *asymptotic safety* [54]. A special case of asymptotic safety is *asymptotic freedom* [55–57], where the RG flow emanates from a Gaußian FP in the UV, i.e., all interactions are dynamically switched off at high energies. This is the case for, e.g., non-Abelian gauge theories in four space-time dimensions.

In the vicinity of a FP, we can linearize[18] the β-functions [58–60]:

$$\begin{aligned}\beta_i\left(\{g_{j\star} + \delta g_j\}\right) &= \beta_i\left(\{g_{j\star}\}\right) + \mathcal{M}_{ij}\delta g_j + \mathcal{O}\left(\delta g_j^2\right) \\ &= \mathcal{M}_{ij}\delta g_j + \mathcal{O}\left(\delta g_j^2\right)\end{aligned} \tag{2.29}$$

with $\mathcal{M}_{ij}$ the *stability matrix* defined as

$$\mathcal{M}_{ij} \equiv \left.\frac{\partial \beta_i}{\partial g_j}\right|_\star\ . \tag{2.30}$$

Choosing a basis $\sigma_i = \left(T^{-1}\right)_{ij}\delta g_j$ in which $\mathcal{M}_{ij}$ is diagonal,

$$\sum_{ij}\left(T^{-1}\right)_{ai}\mathcal{M}_{ij}T_{jb} = \delta_{ab}\vartheta_b\ , \tag{2.31}$$

the linearized β-functions can be written as [53]:

$$\frac{\partial \sigma_i}{\partial t} = \vartheta_i\sigma_i \quad \Rightarrow \quad \sigma_i\left(t\right) \propto e^{\vartheta_i t} = \left(\frac{\mu}{\Lambda}\right)^{\vartheta_i}\ . \tag{2.32}$$

The eigenvalues ϑ_i of $\mathcal{M}_{ij}$ are called *scaling exponents*. The eigenvectors σ_i are called *eigendirections*[19]. One can now classify the eigendirections σ_i in theory space according to the sign of the scaling exponents ϑ_i [53]:

[18] We assume the β-functions are sufficiently well behaved.

[19] Generally, the eigendirections of the stability matrix will not align with the directions of the couplings $\{g_j\}$. One is then interested in the projections onto the couplings $\{g_j\}$.

- $\vartheta_i > 0$: A slight deviation from the fixed point is driven back to the fixed point during the flow towards the IR. At the same time, a slight deviation from the fixed point is driven away from the fixed point during the flow towards the UV. σ_i is then called an *irrelevant direction*.

- $\vartheta_i < 0$: A slight deviation from the fixed point is driven away from the fixed point during the flow towards the IR. At the same time, a slight deviation from the fixed point is driven back to the fixed point during the flow towards the UV. σ_i is then called a *relevant direction*.

- $\vartheta_i = 0$: One has to investigate higher orders to know the behaviour of the couplings. σ_i is then called a *marginal direction*. Depending on the higher order behaviour, one further distinguishes between marginally relevant, marginally irrelevant and – if the scaling exponent is zero at all orders – exactly marginal directions.

Note that the discussion of relevant and irrelevant directions is always meant with respect to a specific FP, namely the FP at which Eq. (2.29) and (2.30) are evaluated.

The relevant directions span the so called *critical manifold*, a submanifold of theory space. It is defined as the set of points in theory space that can be reached by a RG trajectory emanating from the FP[20]. The study of RG flows close to UV critical manifolds is important in order to make statements about the predicivity of a QFT. The physical action of QFT is the *quantum effective action* $\Gamma[\mathbf{\Psi}]$, which takes all quantum corrections into account and includes all possible interactions. In contrast to the (unphysical) bare action $S[\mathbf{\Psi}]$, which is generally polynomial in the fields and contains only a few couplings, the effective action entails infinitely many terms. Given that, in order to fully determine the theory, one would need to fix every of the infinitely many coupling constants by relating them to an amplitude at some kinematic configuration of the external momenta, one would naïvely infer from this that QFT is inherently non-predictive, as we would need infinitely many data points to specify a theory. This is, however, in disagreement with perturbation theory, where one starts from the bare action $S[\mathbf{\Phi}]$ – containing a finite amount of couplings – from which the propagators and vertices of the theory are built. In perturbation theory, all couplings g_n associated with an n-point amplitude $\mathcal{A}_n$ are also non-trivial, but they can be calculated from the finitely many (renormalized) couplings included in the bare action [37]. This makes a perturbatively renormalizable field theory predictive, as only a finite amount of couplings has to be fixed by comparing it to experimental data in order to fully determine the theory.

The explanation for this lies in the characteristics of the RG flow in the vicinity of the critical manifold. Consider some RG trajectory in theory space, starting somewhere off of the critical manifold at some very high UV scale Λ_{UV} (cf. Fig. 2.3). The RG flow is then quickly driven towards the FP along an irrelevant direction (remember that – along an irrelevant direction – small deviations from the FP are driven back to the FP during the flow towards the IR). Close to the FP, the relevant directions become significant

[20] If not stated otherwise, we always consider the direction of the RG flow to be from the UV to the IR. This choice of direction is motivated by the fact that IR physics emerges from the (microscopic) UV physics [61].

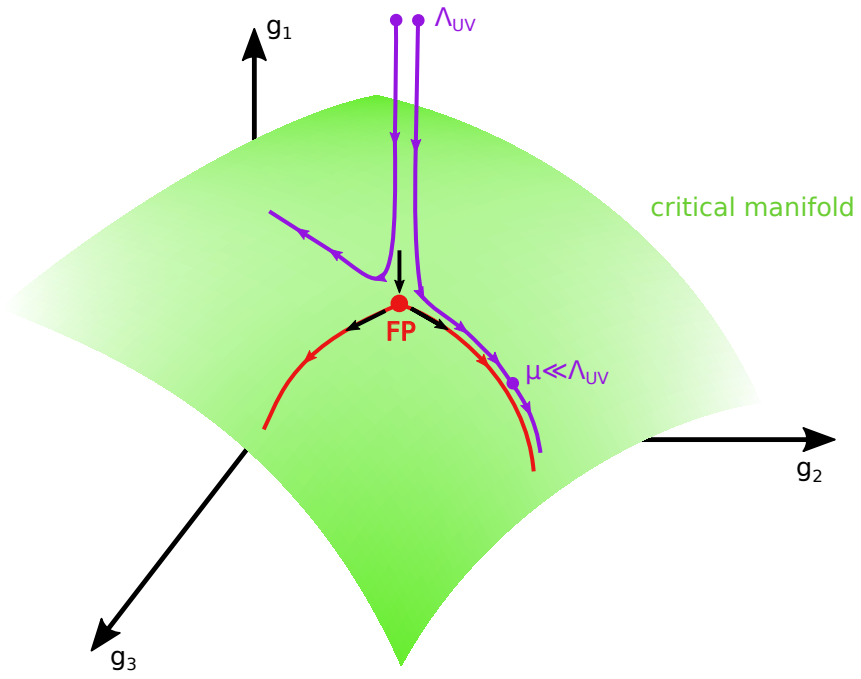

Figure 2.3.: Example of a RG flow in the vicinity of a fixed point. The critical manifold (green) of the FP (red dot) is spanned by the relevant directions. In this example, we have one irrelevant direction (denoted by an in-going black arrow) and two relevant directions (denoted by out-going black arrows). The arrows show the direction of the flow from the UV to the IR. The flow starts off the critical manifold at some high scale Λ_{UV} and is driven towards the FP, from which it flows away again along the critical manifold. For the sake of presentability, we only considered a "truncated", three dimensional theory space. This figure was adapted from [61].

and drive the RG flow away from the FP along the critical manifold. The deviation of the RG flow from the critical manifold is $\mathcal{O}\left(\mu^2/\Lambda_{\mathrm{UV}}^2\right)$ [37], which becomes small for $\mu \ll \Lambda_{\mathrm{UV}}$. Hence, during the flow towards the IR, an interval of values of an irrelevant coupling in the UV is mapped onto a smaller interval of values in the IR [61]. In the limit $\Lambda_{\mathrm{UV}} \to \infty$ the RG flow is confined to the (finite dimensional[21]) critical manifold and the flow is mapped onto a single value in the IR. As the critical manifold is parametrized by the relevant couplings, the flow of the irrelevant couplings can be expressed in terms of the flow of the relevant ones in the limit $\Lambda_{\mathrm{UV}} \to \infty$. Hence, the irrelevant couplings are completely determined and *not* free parameters of the theory. The only free parameters

[21] The critical manifold has a dimension equal to the number of relevant (in the context of perturbation theory: perturbatively renormalizable) couplings [37].

left are the relevant couplings, which have to be fixed using experimental data. This is exactly the justification for only including perturbatively renormalizable – i.e., relevant – terms in perturbation theory, where relevant and irrelevant are meant with respect to a Gaußian UV FP: The irrelevant higher-order couplings are driven towards the free FP and hence no longer play a role in the IR[22] [61]. The fact that irrelevant couplings are not free parameters of the theory will play an important role in the discussion of the top and bottom quark masses within our minimally parametrized bSM model (cf. Chapter 3).

2.3. Perturbative SM β-functions

In this section, we will present all necessary one-loop β-functions within perturbation theory. While this section is intended to demonstrate the overall results as well as important intermediate steps, a detailed derivation is performed in Appendix A. The results of the corresponding two-loop calculations – as performed in [6] – are presented in Appendix B. The β-functions are calculated using dimensional regularization and $\overline{\text{MS}}$-scheme. For a demonstration of the procedure of calculating gauge coupling β-functions using dimensional regularization and MS/$\overline{\text{MS}}$-scheme within non-Abelian gauge theories (specifically, quantum chromodynamics) see, e.g., [62].

2.3.1. Gauge couplings

We start this section with a derivation of the β-functions of the gauge couplings g_Y, g_2 and g_3 for the $\mathsf{U}(1)_\mathsf{Y}$, $\mathsf{SU}(2)_\mathsf{L}$ and $\mathsf{SU}(3)_\mathsf{C}$ gauge groups, respectively. The one-loop β-function of a gauge coupling g of a (simple) gauge group G is given by[23] [1, 19, 20, 55–57, 62, 63]

$$\beta(g) = -\left\{\frac{11}{3}C_2(\mathsf{G}) - \frac{4}{3}\kappa S_2(F) - \frac{1}{3}S_2(S)\right\}\frac{g^3}{16\pi^2}\,. \tag{2.33}$$

Here, $\kappa = \frac{1}{2}$ for 2-component Weyl-fermions[24] and $\kappa = 1$ for 4-component Dirac-fermions, as a Weyl-fermion contributes only as half a Dirac-fermion to the counterterm in the perturbative renormalization procedure. F and S denote the representations of the gauge group G under which the fermion and scalar fields transform. Details on the group theoretical factors appearing in Eq. (2.33) as well as their specific values in the SM are given in Appendix A.1. Using their calculated values given in Tab. A.1, we end

[22] In statistical physics, this is known as *universality*: Certain macroscopic properties of a system are independent of the microscopic details.

[23] The coefficient of the scalar part $S_2(S)$ is $\frac{1}{3}$ for complex scalar fields and $\frac{1}{6}$ for real scalar fields.

[24] As noted by Cvetič et al. [64], Machacek and Vaughn [19, 20] used 2-component spinors as defined in [65].

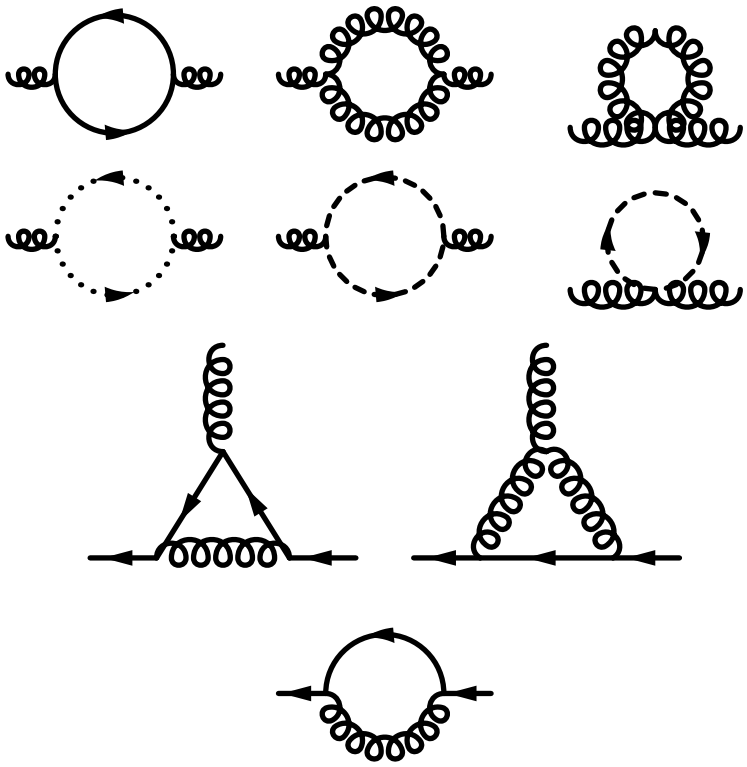

Figure 2.4.: Example of Feynman diagrams contributing to the renormalization constants used in the calculation of the one-loop β-functions of the gauge coupling g in a general gauge theory based on a simple (non-Abelian) gauge group G with scalar, fermion and vector boson fields. Continuous, curly, dotted and dashed lines represent fermions, gauge bosons, ghosts and scalars, respectively.

up with the following one-loop β-functions for the gauge couplings in a SM-like theory[25]:

$$\beta(g_3) = -\left(\frac{11}{3}N_c - \frac{4}{3}N_g\right)\frac{g_3^3}{16\pi^2}\,, \tag{2.34}$$

$$\beta(g_2) = -\left(\frac{22}{3} - \frac{4}{3}N_g - \frac{1}{6}N_H\right)\frac{g_2^3}{16\pi^2}\,, \tag{2.35}$$

$$\begin{aligned}\beta(g_Y) = -\Bigg(&-\frac{2}{3}\sum_{i=1}^{N_g}\Big\{3\left[\left(Y_{u_\mathrm{R}}^{(i)}\right)^2 + 2\left(Y_{q_\mathrm{L}}^{(i)}\right)^2 + \left(Y_{d_\mathrm{R}}^{(i)}\right)^2\right] + \\ &+ \left[\left(Y_{e_\mathrm{R}}^{(i)}\right)^2 + 2\left(Y_{l_\mathrm{L}}^{(i)}\right)^2\right]\Big\} - \frac{2}{3}N_H\left(Y_H\right)^2\Bigg)\frac{g_Y^3}{16\pi^2}\,.\end{aligned} \tag{2.36}$$

Here, N_c is the number of colour charges of the strong interaction, N_g is the number of fermion generations and N_H is the number of complex scalar Higgs doublets. $Y_{u_\mathrm{R}(d_\mathrm{R})}^{(i)}$

[25] In the case of $\mathsf{SU}(5)$ normalization, which is often used in the literature, the hypercharges have to be multiplied by a factor $\sqrt{\frac{3}{5}}$ [66].

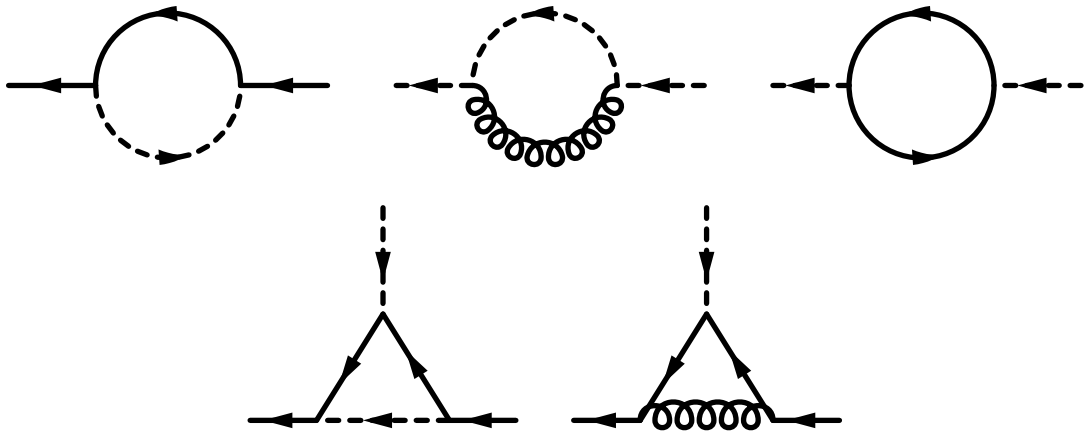

Figure 2.5.: Example of Feynman diagrams contributing to the renormalization constants used in the calculation of the one-loop β-functions of the Yukawa couplings. Continuous, curly and dashed lines represent fermions, gauge bosons and scalars, respectively.

denotes the hypercharge of a right-handed up(down)-type quark, $Y^{(i)}_{e_{\mathrm{R}}}$ denotes the hypercharge of a right-handed charged lepton and $Y^{(i)}_{q_{\mathrm{L}}(l_{\mathrm{L}})}$ denotes the hypercharge of a left-handed quark (lepton).

2.3.2. Yukawa couplings and CKM matrix elements

We now derive the one-loop β-functions of the Yukawa couplings in the mass eigenbasis. As a byproduct of the diagonalization process, we will also obtain the one-loop β-functions of the CKM matrix elements. Details on the calculations are given in Appendices A.2 and A.3.

The one-loop β-functions for the general quark Yukawa matrices[26] $\boldsymbol{\mathcal{Y}}_{u,d}$ read [20, 21, 64, 67–70]:

$$\beta\big(\boldsymbol{\mathcal{Y}}_u\big) = \frac{1}{16\pi^2}\left(-A^{\mathrm{u}}\boldsymbol{\mathcal{Y}}_u + \frac{3}{2}\boldsymbol{\mathcal{Y}}_u\boldsymbol{\mathcal{Y}}_u^\dagger\boldsymbol{\mathcal{Y}}_u - \frac{3}{2}\boldsymbol{\mathcal{Y}}_d\boldsymbol{\mathcal{Y}}_d^\dagger\boldsymbol{\mathcal{Y}}_u + N_c\mathrm{Tr}\left[\boldsymbol{\mathcal{Y}}_u\boldsymbol{\mathcal{Y}}_u^\dagger + \boldsymbol{\mathcal{Y}}_d\boldsymbol{\mathcal{Y}}_d^\dagger\right]\boldsymbol{\mathcal{Y}}_u\right) , \tag{2.37}$$

$$\beta\big(\boldsymbol{\mathcal{Y}}_d\big) = \frac{1}{16\pi^2}\left(-A^{\mathrm{d}}\boldsymbol{\mathcal{Y}}_d + \frac{3}{2}\boldsymbol{\mathcal{Y}}_d\boldsymbol{\mathcal{Y}}_d^\dagger\boldsymbol{\mathcal{Y}}_d - \frac{3}{2}\boldsymbol{\mathcal{Y}}_u\boldsymbol{\mathcal{Y}}_u^\dagger\boldsymbol{\mathcal{Y}}_d + N_c\mathrm{Tr}\left[\boldsymbol{\mathcal{Y}}_u\boldsymbol{\mathcal{Y}}_u^\dagger + \boldsymbol{\mathcal{Y}}_d\boldsymbol{\mathcal{Y}}_d^\dagger\right]\boldsymbol{\mathcal{Y}}_d\right) , \tag{2.38}$$

with

$$A^{\mathrm{u}} = 3\left(\left[Y^2_{u_{\mathrm{R}}} + Y^2_{q_{\mathrm{L}}}\right]g_Y^2 + \frac{3}{4}g_2^2 + \frac{(N_c^2-1)}{N_c}g_3^2\right) , \tag{2.39}$$

$$A^{\mathrm{d}} = 3\left(\left[Y^2_{d_{\mathrm{R}}} + Y^2_{q_{\mathrm{L}}}\right]g_Y^2 + \frac{3}{4}g_2^2 + \frac{(N_c^2-1)}{N_c}g_3^2\right) . \tag{2.40}$$

[26] For the notational convention used here, see Section 2.1.2.

Diagonalization of these equations (cf. Appendix A.2) yields the β-functions of the physical Yukawa couplings (cf. Eq. (2.4)):

$$\beta\left(y_i^u\right) = \frac{y_i^u}{16\pi^2}\left\{-A^{\mathrm{u}} + \frac{3}{2}\left(y_i^u\right)^2 - \frac{3}{2}\sum_j \left(y_j^d\right)^2 |V_{ij}|^2 + N_c \mathrm{Tr}\left[\mathscr{Y}_u\mathscr{Y}_u + \mathscr{Y}_d\mathscr{Y}_d\right]\right\}, \quad (2.41)$$

$$\beta\left(y_i^d\right) = \frac{y_i^d}{16\pi^2}\left\{-A^{\mathrm{d}} + \frac{3}{2}\left(y_i^d\right)^2 - \frac{3}{2}\sum_j \left(y_j^u\right)^2 |V_{ji}|^2 + N_c \mathrm{Tr}\left[\mathscr{Y}_u\mathscr{Y}_u + \mathscr{Y}_d\mathscr{Y}_d\right]\right\}, \quad (2.42)$$

where the superscripts u and d denote whether y_i is the i-th generation up- or down-type quark, respectively. The one-loop β-functions of the quadratic CKM matrix elements $|V_{ij}|^2$ are obtained from diagonalizing Eq. (2.37) and (2.38) (cf. Appendix A.3) and are given by:

$$\begin{aligned}\beta\left(|V_{ij}|^2\right) = {} & \frac{3\left(y_j^d\right)^2}{16\pi^2}\sum_{k\neq j}\frac{1}{\left(y_k^d\right)^2 - \left(y_j^d\right)^2}\left(2\left(y_i^u\right)^2 |V_{ij}|^2 |V_{ik}|^2 + 2\sum_{m\neq i}\left(y_m^u\right)^2 \Re\left\{V_{mj}V_{mk}^* V_{ij}^* V_{ik}\right\}\right) - \\ & - \frac{3\left(y_i^u\right)^2}{16\pi^2}\sum_{k\neq i}\frac{1}{\left(y_i^u\right)^2 - \left(y_k^u\right)^2}\left(2\left(y_j^d\right)^2 |V_{ij}|^2 |V_{kj}|^2 + 2\sum_{m\neq j}\left(y_m^d\right)^2 \Re\left\{V_{im}V_{km}^* V_{ij}^* V_{kj}\right\}\right) + \\ & + \frac{3|V_{ij}|^2}{16\pi^2}\left\{\left(y_{\mathrm{i}}^{\mathrm{u}}\right)^2 + \left(y_j^d\right)^2 - \sum_m \left(y_m^u\right)^2 |V_{mj}|^2 - \sum_m \left(y_m^d\right)^2 |V_{im}|^2\right\}. \end{aligned} \quad (2.43)$$

As shown in Appendix A.3, the differences in the denominators appearing in the β-functions of the squared moduli of the CKM matrix elements are due to the unitarity of the CKM matrix. They lead to poles in the β-functions for degenerate Yukawa couplings, i.e. $y_i^u = y_k^u$ and $y_k^d = y_j^d$. This is a non-perturbative property of the RG flow of the CKM matrix elements, as it is a consequence of the unitarity of the CKM matrix and one would not expect to see (squared) couplings appearing in denominators within a perturbative expansion. The effect of these poles to the running of the Yukawa couplings is discussed in detail in Section 4.3.

3. One Generation Model

This chapter is a summary of refs. [7–9] and serves as a setup for the study of a two generation model.

The Standard Model of particle physics is not UV complete as it suffers from Landau poles in the Abelian $\mathsf{U}(1)_\mathsf{Y}$ gauge coupling [1] as well as in the Higgs-Yukawa sector [2]. As there are hints that this problem persists even beyond perturbation theory [3–5], one has to assume that there must be some beyond-the-Standard-Model (bSM) physics happening at higher energies which renders the SM UV complete. In this thesis, we suppose that there exists such new physics that contributes to the RG evolution of the SM couplings. However, we will not specify what kind of new physics we are dealing with: Neither the field content nor the symmetries of the bSM sector will be defined[1]. Instead, we introduce a set of new scale dependent parameters $\mathfrak{f}_{g,y}(\mu)$ which we use to parametrize the contribution of the aforementioned bSM physics to the RG running of the SM couplings. More specifically, we modify the SM β-functions in the following way [7–9]:

$$\beta(x) = \beta^{\mathrm{SM}}(x) - \mathfrak{f}_x x \ . \tag{3.1}$$

As the work in thesis is restricted to a study of a gauge-Yukawa system, x represents either a gauge coupling g_i or a Yukawa coupling y_j.

The parametrization of the new physics contribution is *minimal* in the sense that it is independent of any internal symmetries [6], i.e. there is one parameter $\mathfrak{f}_g$ for the gauge couplings and one parameter $\mathfrak{f}_y$ for the Yukawa couplings, leaving us with a total of 2 new parameters[2]. The parameters $\mathfrak{f}_{g,y}$ depend on the RG scale μ. In the spirit of effective field theories, we assume that their contribution is significant above a certain mass threshold M_{NP} and negligible below it. Hence, we approximate their scale dependence as

$$\mathfrak{f}_{g,y}(\mu) = f_{g,y} \cdot \Theta(\mu - M_{\mathrm{NP}}) \ , \quad f_{g,y} = \text{const.} > 0 \ . \tag{3.2}$$

Note that these new-physics contributions are scale invariant above M_{NP}. Throughout this thesis, we will use $M_{\mathrm{NP}} = M_{\mathrm{Planck}} = \sqrt{\frac{\hbar c}{8\pi G}} \approx 10^{18}\,\mathrm{GeV}$ for any numerical integrations of the β-functions. The new-physics contribution to the running of the gauge and Yukawa couplings is linear in the couplings, hence it dominates for small values of the couplings. Furthermore, it is strictly negative in the UV regime ($\mu > M_{\mathrm{NP}} = M_{\mathrm{Planck}}$) as $f_{g,y} > 0$.

[1] Mind that in the original works [7–9] the new contributions stem from asymptotically safe quantum gravity. However, we stress that in this thesis we are agnostic about the origin of these bSM contributions.

[2] A study of a model where $\mathfrak{f}_y$ is no longer symmetric with respect to the fermion generations has been done in [6].

This means the new-physics contribution is *antiscreening*. The sign of the new-physics contribution is motivated by the requirement of a UV complete gauge sector. As the one-loop β-function of the Abelian gauge coupling g_Y already has a positive coefficient and hence suffers from a Landau pole problem, we need a negative term to counter the screening character of the SM contribution.

The interplay between the SM β-functions $\beta^{\mathrm{SM}}(x)$ and the new-physics-contribution $-\mathfrak{f}_x x$ generates new zeros of the full β-functions $\beta(x)$, i.e. new fixed points. In the following chapters, we will study the fixed point solutions of this minimally parametrized bSM model and their implications on the structure of the SM model gauge and Yukawa couplings in the IR. We start with a truncated, one generation[3] top-bottom system [7–9], as it will allow us to demonstrate the core mechanism that generates the new fixed point solutions. In the succeeding chapters, we will extend our study to models with more than one generation.

3.1. Fixed Points of Gauge Couplings

Before we investigate the Yukawa sector, it is important to study the gauge sector in detail, as the results we obtain at one-loop order are universal and also hold for the two and three generation models. Upon inserting the SM values of N_c, N_g, N_H and the weak hypercharges in Eq. (2.34) to (2.36) we end up with the following one-loop β-functions:

$$\beta^{\mathrm{SM}}(g_3) = -7\frac{g_3^3}{16\pi^2}\,, \tag{3.3}$$

$$\beta^{\mathrm{SM}}(g_2) = -\frac{19}{6}\frac{g_2^3}{16\pi^2}\,, \tag{3.4}$$

$$\beta^{\mathrm{SM}}(g_Y) = \frac{41}{6}\frac{g_Y^3}{16\pi^2}\,. \tag{3.5}$$

At one-loop order, the β-functions of the gauge couplings are independent of all Yukawa couplings as well as all other gauge couplings. Furthermore, they are monomials in the respective couplings. Hence, only a completely free fixed point is a valid fixed point solution: $g_{3\star} = g_{2\star} = g_{Y\star} = 0$. Furthermore, the coefficients in the β-functions of the non-Abelian gauge couplings are negative, while the coefficient in the β-function of the Abelian gauge coupling is positive. The signs of these coefficients are the reason for the well-known running behaviour of Abelian and non-Abelian gauge couplings: The finite IR values of the non-Abelian couplings are driven towards zero in the UV, resulating in asymptotic freedom [55–57], while the Abelian coupling increases in the UV

[3] A disclaimer on the terms used in the text: By "one generation model", we actually mean a full three generational model but all contributions of the Yukawa couplings from other generations are neglected. Specifically, in the β-functions of the top-bottom system, the values of N_g and N_H appearing in the gauge β-functions Eq. (2.34) to (2.36) are still the same as in the full SM, but the Yukawa couplings of the up-, charm-, down- and strange-quarks are neglected in Eq. (2.41) and (2.42). Also, any leptonic contributions to the running of the Yukawa couplings is completely ignored throughout this thesis. The term "two generation model" used in Chapter 4 has to be understood in an analogous way.

#	$g_{Y\star}^2$	$g_{2\star}^2$	$g_{3\star}^2$	ϑ_Y	ϑ_2	ϑ_3	viable
1	0	0	0	$-f_g$	$-f_g$	$-f_g$	
2	$\frac{96}{41} f_g \pi^2$	0	0	$2f_g$	$-f_g$	$-f_g$	
3	0	$-\frac{96}{19} f_g \pi^2$	0	$-f_g$	$2f_g$	$-f_g$	
4	0	0	$-\frac{16}{7} f_g \pi^2$	$-f_g$	$-f_g$	$2f_g$	
5	$\frac{96}{41} f_g \pi^2$	$-\frac{96}{19} f_g \pi^2$	0	$2f_g$	$2f_g$	$-f_g$	
6	$\frac{96}{41} f_g \pi^2$	0	$-\frac{16}{7} f_g \pi^2$	$2f_g$	$-f_g$	$2f_g$	
7	0	$-\frac{96}{19} f_g \pi^2$	$-\frac{16}{7} f_g \pi^2$	$-f_g$	$2f_g$	$2f_g$	
8	$\frac{96}{41} f_g \pi^2$	$-\frac{96}{19} f_g \pi^2$	$-\frac{16}{7} f_g \pi^2$	$2f_g$	$2f_g$	$2f_g$	

Table 3.1.: UV fixed point solutions in the gauge sector at one-loop level. ϑ_i denote the scaling exponents of the respective couplings g_i. As the β-functions of the gauge couplings are decoupled, the stability matrix $\mathcal{M}_{ij}$ is already diagonal and the eigendirections coincide with the couplings g_i. The last column indicates whether the fixed point is phenomenologically viable or not, according to the discussion in the text.

and subsequently hits a Landau pole at some high scale, resulting in a breakdown of perturbation theory. With respect to the Gaußian UV fixed point, the non-Abelian couplings are marginally relevant, while the Abelian coupling is marginally irrelevant.

If we now modify the SM β-function Eq. (3.3) to (3.5) according to Eq. (3.1) we obtain the following β-functions:

$$\beta(g_3) = -7\frac{g_3^3}{16\pi^2} - \mathfrak{f}_g g_3 \,, \tag{3.6}$$

$$\beta(g_2) = -\frac{19}{6}\frac{g_2^3}{16\pi^2} - \mathfrak{f}_g g_2 \,, \tag{3.7}$$

$$\beta(g_Y) = \frac{41}{6}\frac{g_Y^3}{16\pi^2} - \mathfrak{f}_g g_Y \,. \tag{3.8}$$

In the UV regime ($\mu > M_{\rm NP}$) $\mathfrak{f}_g(\mu > M_{\rm NP}) = f_g = \text{const.} > 0$ and the β-functions are now polynomials in the gauge couplings, which allows for non-trivial fixed point solutions. The full system of UV fixed point solutions for the gauge couplings is shown in Tab. 3.1.

Let us now discuss these fixed point solutions. Each of the three β-functions yields two fixed point solution for the corresponding gauge coupling: a vanishing and a non-vanishing fixed point. All possible fixed point solutions for the gauge sector are the combinations of vanishing and non-vanishing fixed points for the respective gauge couplings, as shown in Tab. 3.1. As the β-functions of the gauge couplings are decoupled,

the stability matrix $\mathcal{M}_{ij}$ is already diagonal ($\sigma_i = \delta g_i$) and its eigenvalues read:

$$\vartheta_Y = \left.\frac{\partial\beta\left(g_Y\right)}{\partial g_Y}\right|_\star = \frac{41}{2}\frac{g_{Y\star}^2}{16\pi^2} - f_g \,, \tag{3.9}$$

$$\vartheta_2 = \left.\frac{\partial\beta\left(g_2\right)}{\partial g_2}\right|_\star = -\frac{19}{2}\frac{g_{2\star}^2}{16\pi^2} - f_g \,, \tag{3.10}$$

$$\vartheta_3 = \left.\frac{\partial\beta\left(g_3\right)}{\partial g_3}\right|_\star = -21\frac{g_{3\star}^2}{16\pi^2} - f_g \,. \tag{3.11}$$

The scaling exponents at the fixed points of the respective gauge couplings are given in Tab. 3.1.

We now discuss the physical viability of these fixed point solutions. We first note that the non-trivial fixed point of the Abelian gauge coupling necessarily has a different sign than the non-trivial fixed points of the non-Abelian gauge couplings. Obviously the fixed points of all couplings have to be real in order to be physical. Hence, all fixed point solutions where the Abelian fixed point as well as at least one non-Abelian fixed point are non-vanishing are inevitably non-physical. This rules out the fixed point solutions 5, 6 and 8 in Tab. 3.1. Since $f_g > 0$, the fixed point solutions 3, 4 and 7 are also ruled out, as they would contain imaginary fixed points. The remaining two fixed points in Tab. 3.1 are then in fact phenomenologically viable. Fixed point number 1 represents a completely free, Gaußian fixed point and can be matched to the observed IR values, as all three gauge couplings are then relevant, i.e., free parameters. Fixed point number 2 has a non-vanishing fixed point of the Abelian gauge coupling. Given that $f_g > 0$, this leaves us with an IR attractive interacting fixed point for the Abelian gauge coupling and asymptotically free non-Abelian couplings.

Out of the two phenomenologically viable fixed point solutions, fixed point #2 is the more interesting one – for two reasons: First of all, the Abelian gauge coupling g_Y is an irrelevant coupling with respect to this fixed point. As its fixed point value is non-zero, i.e. $g_{Y\star} > 0$, there exists an asymptotically safe, non-trivial RG trajectory which is given purely in terms of the relevant couplings. In fact, as we only considered one-loop β-functions, the RG flow is actually constant in the UV regime[4]. Only for scales $\mu < M_{\mathrm{NP}}$ there is a deviation from scale invariance in the Abelian gauge coupling, as the new physics contribution is turned off and $g_{Y\star}$ is no longer a fixed point (cf. Fig. 3.1). As g_Y is an irrelevant coupling with respect to this fixed point, it is no longer a free parameter of the theory (cf. Sec. 2.2.2): In the UV regime, its value at all scales can be calculated purely in terms of the relevant directions (at one-loop order, this dependence is trivial), while in the IR regime, the UV initial condition of the RG flow can be calculated from first principles. Note that fixed point solution #1 in Tab. 3.1 also allows for a UV completion of the gauge sector, but with respect to this fixed point the Abelian gauge coupling is relevant, i.e. it is still a free parameter of the theory.

Beside this enhanced predicitivity, fixed point #2 has another interesting feature: As the Abelian gauge coupling g_Y takes a finite value at the fixed point, there are

[4] In other words, the critical manifold in the "truncated", three-dimensional theory space has no curvature and is parallel to the g_2-g_3-plane.

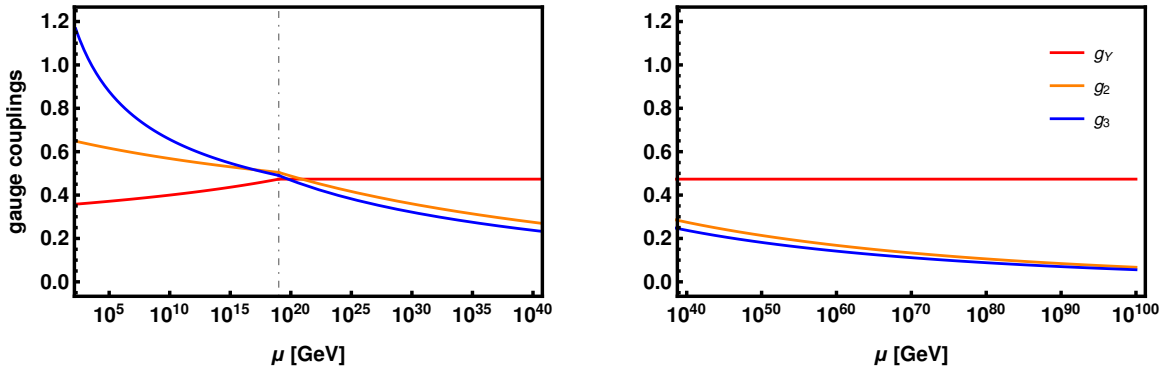

Figure 3.1.: RG flow of gauge couplings for fixed point solution #2 in Tab. 3.1 and $f_g = 9.7 \times 10^{-3}$ [9]. In the UV regime ($\mu > M_{\rm NP} = M_{\rm Planck}$) the Abelian gauge coupling g_Y takes a constant value. The asymptotically free character of the non-Abelian gauge couplings $g_{2,3}$ is amplified by the antiscreening nature of the bSM term $-f_g g_i$. Below the scale of new physics, the RG running of the couplings is governed by the usual SM one-loop β-functions and the Abelian gauge coupling is no longer scale invariant. Choosing suitable initial conditions of the RG flow of the relevant non-Abelian couplings in the UV, their measured IR values can be accomodated. This result was obtained in [7–9].

residual gauge interactions in the far UV. This of course affects the RG evolution of other couplings via diagrams where gauge bosons occur, including the Yukawa couplings. The fact that there is a leftover contribution of the Abelian gauge coupling in the β-functions of the Yukawa couplings results in a breaking of the up-type-down-type symmetry of the fixed point solutions in the Yukawa sector due to the unequal hypercharges of up- and down-type quarks (cf. Sec. 3.2). For these reasons, we will for the rest of this thesis assume that the gauge couplings take the fixed point values of fixed point solution #2 in Tab. 3.1.

In Fig. 3.1 we show a RG trajectory emanating from fixed point #2 in Tab. 3.1. In the UV regime ($\mu > M_{\rm NP} = M_{\rm Planck}$) the Abelian gauge coupling sticks to its fixed point value, while the non-Abelian gauge couplings gain finite values towards the IR. Below the scale of new physics, the usual one-loop SM running sets in and the Abelian gauge coupling is no longer scale invariant. At one-loop level, the β-functions of the gauge couplings are independent of each other. This simplifies the fine-tuning of the initial conditions in the UV in order to accomodate the observed IR values. As the non-Abelian couplings are relevant couplings, we can always recover their IR values by choosing suitable initial conditions of the RG flow. In this case, the initial conditions

are choosen such that one matches the following values[5] at $\mu = m_t$ [63]:

$$g_2\left(m_t\right) = 0.64822\ , \tag{3.12}$$
$$g_3\left(m_t\right) = 1.1666\ . \tag{3.13}$$

The Abelian gauge coupling on the other hand is not a free parameter and is completely fixed by its fixed point value. However, the fixed point value of g_Y dependes on f_g, hence we can accomodate the observed IR value of the Abelian gauge coupling by choosing a suitable value for the parameter f_g. In order to match the value[6] of g_Y at $\mu = m_t$ [63],

$$g_Y\left(m_t\right) = 0.35760 \tag{3.14}$$

we have to choose $f_g = 9.7 \times 10^{-3}$ [7–9].

3.2. Fixed Points of Yukawa Couplings

We are now going to take a look at the Yukawa sector, or more specifically, at a simplified top-bottom system in the style of [7–9]. Inserting the SM values of N_c and the weak hypercharges into Eq. (2.41) and (2.42), ignoring the Yukawa couplings of the lighter quarks (y_u, y_c, y_d, y_s) and adding the linear bSM term according to Eq. (3.1) we end up with the following one-loop β functions:

$$\beta\left(y_t\right) = \frac{y_t}{16\pi^2}\left(-\left[\frac{17}{12}g_Y^2 + \frac{9}{4}g_2^2 + 8g_3^2\right] + \frac{9}{2}y_t^2 + \frac{3}{2}y_b^2\right) - \mathfrak{f}_y y_t\ , \tag{3.15}$$
$$\beta\left(y_b\right) = \frac{y_b}{16\pi^2}\left(-\left[\frac{5}{12}g_Y^2 + \frac{9}{4}g_2^2 + 8g_3^2\right] + \frac{9}{2}y_b^2 + \frac{3}{2}y_t^2\right) - \mathfrak{f}_y y_b\ . \tag{3.16}$$

Notice that the only reason why the above system of equations is not invariant under an exchange of flavour indices $t \leftrightarrow b$ is the coefficient of the Abelian gauge coupling. It is defined as the sum of the squared weak hypercharges of the left-handed $\mathsf{SU}\left(2\right)_\mathsf{L}$ quark doublet and right-handed up- or down-type $\mathsf{SU}\left(2\right)_\mathsf{L}$ quark singlet:

$$\left[Y_{u_\mathrm{R}(d_\mathrm{R})}^2 + Y_{q_\mathrm{L}}^2\right] g_Y^2\ . \tag{3.17}$$

As the hypercharge of the right-handed up-type singlet is different than the hypercharge of the right-handed down-type singlet, this term explicitly breaks the up-type-down-type symmetry of Eq. (3.15) and (3.16). This is an important observation when it comes to the fixed point solutions of the full top-bottom-gauge system.

Let us consider fixed point solution #1 in Tab. 3.1, i.e. the Gaußian fixed point of the gauge couplings. For a RG trajectory emanating from this fixed point, all gauge interactions vanish in the far UV. This means that at the UV fixed point, the symmetry

[5] The value for $g_2(m_t)$ is computed at two loops in the $\overline{\mathrm{MS}}$ scheme in [63]. The value for $g_3(m_t)$ is computed at two loops in the electroweak gauge interactions, four loops in QCD and three loop matching at the top mass m_t to the full SM (cf. [63]).

[6] The value for $g_Y(m_t)$ is computed at two loops in the $\overline{\mathrm{MS}}$ scheme in [63].

#	$y_{t\star}^2$	$y_{b\star}^2$	ϑ_1	ϑ_2
1	0	0	$-f_y$	$-f_y$
2	$\frac{32}{9} f_y \pi^2$	0	$2f_y$	$-\frac{2}{3} f_y$
3	0	$\frac{32}{9} f_y \pi^2$	$2f_y$	$-\frac{2}{3} f_y$
4	$\frac{8}{3} f_y \pi^2$	$\frac{8}{3} f_y \pi^2$	$2f_y$	f_y

Table 3.2.: UV fixed point solutions of the top and bottom Yukawas for asymptotically free gauge couplings, $g_{Y\star} = g_{2\star} = g_{3\star} = 0$. As the β-functions (Eq. (3.15) and (3.16)) are in this case symmetric under an exchange $t \leftrightarrow b$, so is the system of fixed point solutions.

#	$y_{t\star}^2$	$y_{b\star}^2$	ϑ_1	ϑ_2
1	0	0	$-\frac{5}{82} f_g - f_y$	$-\frac{17}{82} f_g - f_y$
2	$\frac{16\pi^2}{9}\left(\frac{17}{41} f_g + 2f_y\right)$	0	$\frac{17}{41} f_g + 2f_y$	$\frac{1}{123}\left(f_g - 82 f_y\right)$
3	0	$\frac{16\pi^2}{9}\left(\frac{5}{41} f_g + 2f_y\right)$	$\frac{5}{41} f_g + 2f_y$	$-\frac{23}{123} f_g - \frac{2}{3} f_y$
4	$4\pi^2\left(\frac{23}{123} f_g + \frac{2}{3} f_y\right)$	$4\pi^2\left(-\frac{1}{123} f_g + \frac{2}{3} f_y\right)$	$\frac{1}{164}(33 f_g + 246 f_y + s_1)$	$\frac{1}{164}(33 f_g + 246 f_y - s_1)$

Table 3.3.: UV fixed point solutions of the top and bottom Yukawas for interacting Abelian gauge coupling, $g_{Y\star} = \frac{96}{41} f_g \pi^2$, $g_{2\star} = g_{3\star} = 0$. Both the β-functions (Eq. (3.15) and (3.16)) and the system of fixed point solutions are not symmetric under an exchange $t \leftrightarrow b$. The square root appearing in the scaling exponents is given by $s_1 = \sqrt{1273 f_g^2 + 1804 f_g f_y + 6724 f_y^2}$.

breaking term $\sim g_Y^2$ does not contribute to the running of the top and bottom Yukawas. Hence, close to the Gaußian fixed point of the gauge couplings, Eq. (3.15) and (3.16) become symmetric under the exchange $t \leftrightarrow b$. This is reflected in the UV fixed point solutions with asymptotically free gauge couplings for the gauge-Yukawa system given in Tab. 3.2: The system of fixed point solutions is also symmetric under the exchange $t \leftrightarrow b$. Note that, while the whole set of fixed point solutions is symmetric under an exchange $t \leftrightarrow b$, a particular choice of fixed point solution may break that symmetry. Also, the RG trajectories themselves will generally *not* be symmetric either. For example, during the flow towards the IR, the Abelian gauge coupling gains a finite value and the symmetry breaking term in the β-functions of the top and bottom Yukawas contributes to the their RG flow.

At the fixed point #2 in Tab. 3.1, the symmetry breaking term $\sim g_Y^2$ is still present in the β-functions of the top and bottom Yukawas. This results in a system of fixed point solutions that itself is not symmetric in the exchange $t \leftrightarrow b$ as shown in Tab. 3.3. Fixed point solution #4 in Tab. 3.3 features IR attractive, interacting UV fixed points for the top and bottom Yukawa couplings. Together with the gauge couplings, out of the five

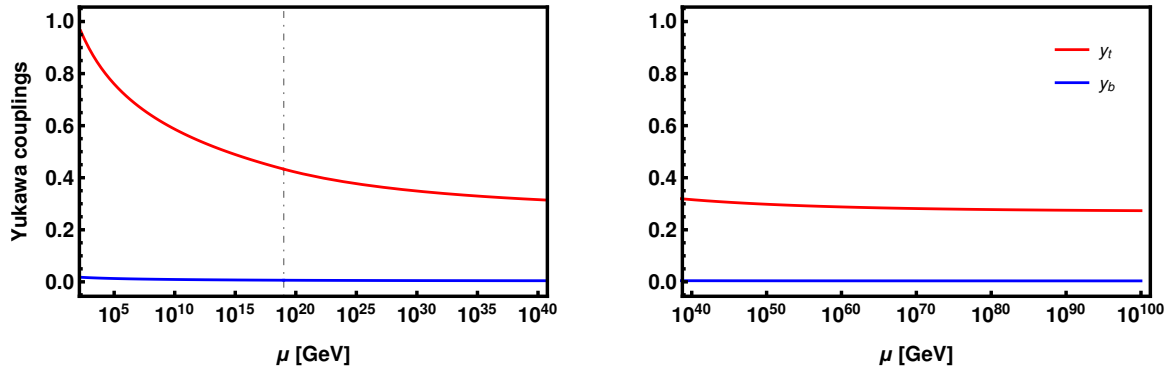

Figure 3.2.: RG flow of the top and bottom Yukawa couplings for fixed point solution #4 in Tab. 3.3. In the UV regime ($\mu > M_{\rm NP} = M_{\rm Planck}$) the Yukawa couplings are not scale invariant. Choosing $f_y = 1.188 \times 10^{-4}$ [9], the measured quark pole masses can be approximately recovered. This result was obtained in [9].

couplings g_Y, g_2, g_3, y_t and y_b, only two couplings – the non-Abelian gauge couplings $g_{2,3}$ – are free parameters. The other couplings are fixed at all scales via the running of $g_{2,3}$.

Fig. 3.2 shows the RG flow of the top and bottom Yukawa couplings emanating from fixed point solution #4 in Tab. 3.3. Both Yukawa couplings take finite values at the UV fixed point and are irrelevant couplings. As the β-functions of the Yukawa couplings Eq. (3.15) and (3.16) depend on both the gauge couplings and other Yukawa couplings, the critical manifold is now curved and – unlike the Abelian gauge coupling at one loop order – the Yukawa couplings are not scale invariant in the UV regime ($\mu > M_{\rm NP} = M_{\rm Planck}$). Their deviation from scale invariance is parametrized by the running of the relevant couplings $g_{2,3}$ and they start to flow away from their fixed points as soon as the non-Abelian couplings gain considerable finite values [9]. Due to the interacting fixed point of the Abelian gauge coupling, the fixed point values of the top and bottom Yukawas in the interacting fixed point solution are no longer equal, as they get a correction from the gauge sector:

$$y_{t\star}^2: \quad \frac{8}{3} f_y \pi^2 \;\to\; \frac{8}{3} f_y \pi^2 + \frac{92}{123} f_g \pi^2 \,, \tag{3.18}$$

$$y_{b\star}^2: \quad \frac{8}{3} f_y \pi^2 \;\to\; \frac{8}{3} f_y \pi^2 - \frac{4}{123} f_g \pi^2 \,. \tag{3.19}$$

This results in a splitting of the fixed point values of the top and bottom Yukawas, which then obey the relation [9]:

$$y_{t\star}^2 - y_{b\star}^2 = \frac{1}{3} g_{Y\star}^2 \,. \tag{3.20}$$

As a last step, we have to convert the running Yukawa couplings in the IR into pole masses to see whether one recovers the correct masses of the quarks from the UV fixed

point structure. The running Yukawa coupling $y_f^{\overline{\text{MS}}}(\mu)$ of a fermion f in the $\overline{\text{MS}}$-scheme is related to the pole mass m_f via the relation [63, 71]:

$$y_f^{\overline{\text{MS}}}(\mu) = 2^{\frac{3}{4}}\sqrt{G_F}\, m_f \left[1 + \delta_f^{(1)}(\mu) + \delta_f^{(2)}(\mu) + \ldots\right] , \tag{3.21}$$

where $G_F = 1.16638 \times 10^{-5}$ GeV^{-2} [14] is the Fermi constant given by $v = \left(2^{1/4}\sqrt{G_F}\right)^{-1}$. The scale dependent terms $\delta_f^{(n)}(\mu)$ describe the n-loop corrections to the tree-level relation $y_f^{\overline{\text{MS}}} = 2^{\frac{3}{4}}\sqrt{G_F}\, m_f$. In this thesis, we consider the first correction to the tree-level relation, i.e. we include $\delta_f^{(1)}(\mu)$. The expressions for $\delta_f^{(1)}(\mu)$ are given in Appendix B.1. For the RG flow of the top and bottom Yukawas emanating from fixed point #4 in Tab. 3.3 shown in Fig. 3.2, we have chosen the value of f_y to be $f_y = 1.188 \times 10^{-4}$ [9]. From this, one obtains $y_t(m_t) = 0.964$ and $y_b(m_t) = 0.0176$. This translates – according to Eq. (3.21) at one-loop order – to pole masses of $m_t = 174.4\,\text{GeV}$ and $m_b = 4.3\,\text{GeV}$, which is reasonably close to the measured values.

4. Two Generation Model

We are now going to extend the study of the one generation model done in [7–9] and presented in Chapter 3 to a two generation model, where we incorporate charm and strange quarks into our theory. This chapter will be the main part of this thesis: We now have to take flavour mixing effects into account, as the CKM matrix for a two generation system is generally no longer trivial. We will discuss the effects of the running mixing parameters on the running of the Yukawa couplings and discuss upper bounds on the masses of the second generation quarks from poles in the β-functions stemming from the unitary of the CKM matrix.

As we restrict this study to a two generation model in the sense that we ignore any contribution of a third generation of quarks, the CKM matrix reduces to a 2×2 matrix parametrized by a single real parameter:

$$\boldsymbol{V} = \begin{pmatrix} V_{11} & V_{12} \\ V_{21} & V_{22} \end{pmatrix} , \qquad \left\{ |V_{ij}|^2 \right\} = \begin{pmatrix} |V_{11}|^2 & 1 - |V_{11}|^2 \\ 1 - |V_{11}|^2 & |V_{11}|^2 \end{pmatrix} . \tag{4.1}$$

Alternatively, one could parametrize this matrix using a rotation angle, i.e., the Cabibbo angle θ_C [10], which is related to V_{11} via

$$V_{11} = \cos\theta_C \, . \tag{4.2}$$

Upon inserting the SM values of the parameters into Eq. (2.41), (2.42) and (2.43) and adding the linear bSM term according to Eq. (3.1), we end up with the following β-functions in the two generation system:

$$\beta\left(y_t\right) = \frac{y_t}{16\pi^2}\left\{-A^{\mathrm{u}} + \frac{9}{2}y_t^2 + \frac{3}{2}y_s^2\left(1 + |V_{11}|^2\right) + \frac{3}{2}y_b^2\left(2 - |V_{11}|^2\right) + 3y_c^2\right\} - \mathfrak{f}_y y_t \, , \tag{4.3}$$

$$\beta\left(y_c\right) = \frac{y_c}{16\pi^2}\left\{-A^{\mathrm{u}} + \frac{9}{2}y_c^2 + \frac{3}{2}y_b^2\left(1 + |V_{11}|^2\right) + \frac{3}{2}y_s^2\left(2 - |V_{11}|^2\right) + 3y_t^2\right\} - \mathfrak{f}_y y_c \, , \tag{4.4}$$

$$\beta\left(y_b\right) = \frac{y_b}{16\pi^2}\left\{-A^{\mathrm{d}} + \frac{9}{2}y_b^2 + \frac{3}{2}y_c^2\left(1 + |V_{11}|^2\right) + \frac{3}{2}y_t^2\left(2 - |V_{11}|^2\right) + 3y_s^2\right\} - \mathfrak{f}_y y_b \, , \tag{4.5}$$

$$\beta\left(y_s\right) = \frac{y_s}{16\pi^2}\left\{-A^{\mathrm{d}} + \frac{9}{2}y_s^2 + \frac{3}{2}y_t^2\left(1 + |V_{11}|^2\right) + \frac{3}{2}y_c^2\left(2 - |V_{11}|^2\right) + 3y_b^2\right\} - \mathfrak{f}_y y_s \, , \tag{4.6}$$

with

$$A^{\mathrm{u}} = \left(\frac{17}{12}g_Y^2 + \frac{9}{4}g_2^2 + 8g_3^2\right) \, , \tag{4.7}$$

$$A^{\mathrm{d}} = \left(\frac{5}{12}g_Y^2 + \frac{9}{4}g_2^2 + 8g_3^2\right) \, , \tag{4.8}$$

#	$y^2_{t\star}$	$y^2_{c\star}$	$y^2_{b\star}$	$y^2_{s\star}$	$\lvert V_{11}\rvert^2_\star$	allowed range
1	$\frac{16}{15}\left(f_g+2f_y\right)\pi^2$	0	$\frac{16}{615}\left(-19f_g+82f_y\right)\pi^2$	0	0	$f_y \geq \frac{19}{82}f_g$
2	$\frac{4}{123}\left(11f_g+82f_y\right)\pi^2$	$\frac{32}{41}f_g\pi^2$	$\frac{4}{123}\left(-13f_g+82f_y\right)\pi^2$	0	1	$f_y \geq \frac{13}{82}f_g$
3	$\frac{4}{123}\left(23f_g+82f_y\right)\pi^2$	0	$\frac{4}{123}\left(-f_g+82f_y\right)\pi^2$	0	1	$f_y \geq \frac{1}{82}f_g$
4	t_4	0	b_4	s_4	V_4	$f_y = \frac{7}{82}f_g$
5	t_5	c_5	b_5	0	V_5	$f_y = \frac{43}{82}f_g$
6	$\frac{4}{123}\left(35f_g+82f_y\right)\pi^2$	0	$\frac{4}{123}\left(11f_g+82f_y\right)\pi^2$	$-\frac{32}{41}f_g$	1	–

Table 4.1.: Classes of discrete fixed point solutions of the two generation model for the partially interacting gauge coupling fixed point $g^2_{Y\star} = \frac{96}{41}f_g\pi^2$ and $g^2_{2\star} = g^2_{3\star} = 0$. Note that each of these fixed point solutions exists in four versions corresponding to a permutation of flavour indices $t \leftrightarrow c$ and $b \leftrightarrow s$. Out of these quartets, only the representatives obeying the phenomenological ordering $y^2_{t\star} > y^2_{c\star}$ and $y^2_{b\star} > y^2_{s\star}$ are presented. In the last column, we state the allowed values of f_y in order to guarantee $y^2_{i\star} \geq 0 \;\; \forall\, i \in \{t,c,b,s\}$. The definitions of the fixed point values $t_{4,5}$, c_5, $b_{4,5}$, s_4 and $V_{4,5}$ are given in the text.

and for the squared modulus of the CKM matrix element $|V_{11}|^2$:

$$\beta\left(|V_{11}|^2\right) = \frac{3}{16\pi^2}|V_{11}|^2\left(1-|V_{11}|^2\right)\left\{\left[\left(y_c^2+y_s^2\right)-\left(y_t^2+y_b^2\right)\right]-2y_c^2\frac{y_s^2-y_b^2}{y_c^2-y_t^2}-2y_s^2\frac{y_c^2-y_t^2}{y_s^2-y_b^2}\right\}, \tag{4.9}$$

where we used, exploiting the unitarity of the CKM matrix $\boldsymbol{V}$,

$$2\Re\left\{V_{im}V_{km}^*V_{ij}^*V_{kj}\right\} = -2\left|V_{im}\right|^2\left|V_{km}\right|^2 . \tag{4.10}$$

for $N_g = 2$.

Regarding the quadratic CKM matrix element, we note that there is no additional new-physics contribution appearing in the β-function. This is because in our ansatz the new physics contribution to Eq. (2.37) and (2.38) is linear in the Yukawa matrices, i.e. $\sim \mathfrak{f}_y\boldsymbol{\mathcal{Y}}_{u,d}$ and hence of the same form as the gauge contribution. The diagonalization of these terms does not introduce any mixing terms, as they do not contain products of up- and down-type matrices (cf. Appendix A.3).

4.1. Fixed Point Solutions

We are now going to discuss the fixed point solutions of this model. Just like in Section 3.2, we assume the gauge couplings take the partially interacting fixed point solution #2 in Tab. 3.1. Again, the consequence of this is the breaking of the up-type-down-type symmetry of the β-functions and hence of the fixed point solutions (cf. discussion in Section 3.2). Upon solving the fixed point equations, one obtains 20 discrete fixed

#	$y^2_{c\star}$	$y^2_{b\star}$	$y^2_{s\star}$	$\lvert V_{11}\rvert^2_\star$	allowed range
0a	$\left(\frac{140}{123}f_g + \frac{8}{3}f_y\right)\pi^2 - y^2_{t\star}$	$\left(\frac{44}{123}f_g + \frac{8}{3}f_y\right)\pi^2 - y^2_{t\star}$	$-\frac{32}{41}f_g\pi^2 + y^2_{t\star}$	0	$f_y \geq \frac{13}{82}f_g$
0b	$\left(\frac{140}{123}f_g + \frac{8}{3}f_y\right)\pi^2 - y^2_{t\star}$	$-\frac{32}{41}f_g\pi^2 + y^2_{t\star}$	$\left(\frac{44}{123}f_g + \frac{8}{3}f_y\right)\pi^2 - y^2_{t\star}$	1	$f_y \geq \frac{13}{82}f_g$

Table 4.2.: One parameter families of solutions (fixed lines) parametrized by the squared top Yukawa fixed point $y^2_{t\star}$. These fixed lines collapse to a quartet of discrete solutions if one includes two-loop terms in the β-functions (cf. discussion in [6]).

#	$y^2_{t\star}/\left(\frac{16}{15}\pi^2\right)$	$y^2_{c\star}/\left(\frac{16}{15}\pi^2\right)$	$y^2_{b\star}/\left(\frac{16}{15}\pi^2\right)$	$y^2_{s\star}/\left(\frac{16}{15}\pi^2\right)$	$\lvert V_{11}\rvert^2_\star$
1a	$f_g + 2f_y$	0	$\frac{1}{41}(-19f_g + 82f_y)$	0	0
1b	$f_g + 2f_y$	0	0	$\frac{1}{41}(-19f_g + 82f_y)$	1
1c	0	$f_g + 2f_y$	0	$\frac{1}{41}(-19f_g + 82f_y)$	0
1d	0	$f_g + 2f_y$	$\frac{1}{41}(-19f_g + 82f_y)$	0	1

Table 4.3.: Quartet of fixed point solution #1 in Tab. 4.1. The solutions are related to each other by permutations of the flavour indices of quarks with equal singlet hypercharge: $t \leftrightarrow c$ and $b \leftrightarrow s$. The fixed point value of the squared modulus of the matrix element, $\lvert V_{11}\rvert^2_\star$, is either 1 or 0, representing a diagonal or anti-diagonal mixing matrix, respectively.

point solutions and two one-parameter families of solutions, i.e., fixed lines. The discrete solutions are given in Tab. 4.1, the two fixed lines in Tab. 4.2. We start by discussing the discrete fixed point solutions and will give a few comments on the fixed lines later on.

As stated above, the up-type-down-type symmetry of the β-functions is broken due to the terms stemming from the Abelian gauge contributions in the case of the partially interacting fixed point in the gauge sector. This observation is independent of the number of generations considered. For $N_g > 1$, however, there exists a permutation symmetry with respect to the interchange of flavour indices with equal singlet hypercharge. For $N_g = 2$, that is $t \leftrightarrow c$ and $b \leftrightarrow s$. This symmetry is reflected in the fixed point solutions: They appear in quartets of $t \leftrightarrow c$ and $b \leftrightarrow s$ permutations. Take, for example, fixed point solution #1 in Tab. 4.1. As given in Tab. 4.1, only the solution with the (phenomenological) ordering $y^2_{t\star} > y^2_{c\star}$ and $y^2_{b\star} > y^2_{s\star}$ is presented. However, there exist three additional permutations of this solution as shown in Tab. 4.3.

Note that in Tab. 4.3, the squared modulus of the CKM parameter is either 1 or 0. These cases correspond to the case of no mixing and have the effect of effectively interchanging the roles of the down-type quarks, $b \leftrightarrow s$. By no mixing, we mean that a flavour eigenstate quark is related to exactly one mass eigenstate quark and is not a superposition of several mass eigenstates. In a two generation model, there are only two

ways of realizing this, namely a diagonal and an anti-diagonal mixing matrix:

$$\boldsymbol{V}_\star = \begin{pmatrix} 1 & 0 \\ 0 & 1 \end{pmatrix} \quad \text{or} \quad \boldsymbol{V}_\star = \begin{pmatrix} 0 & 1 \\ 1 & 0 \end{pmatrix} . \tag{4.11}$$

The two matrices in Eq. (4.11) constitute a faithful representation of the permutation group of two objects [6] – in our specific case, of the two down-type quarks. By virtue of the β-function in Eq. (4.9), $|V_{11}|^2_\star = 0$ and $|V_{11}|^2_\star = 1$ are always fixed point solutions of the squared modulus of the CKM matrix element, independent of the fixed point values of the Yukawa couplings. As the β-function of $|V_{11}|^2$ does not contain any new-physics contributions, the observations made by Pendleton and Ross in [72] also hold here: The fixed point $|V_{11}|^2_\star = 1$ is IR attractive, given that the Yukawa couplings of one generation are strictly larger (smaller) than the Yukawa couplings of the other generation: $y_t^2 > y_c^2$ and $y_b^2 > y_s^2$ (or $y_t^2 < y_c^2$ and $y_b^2 < y_s^2$). Similarly, the fixed point $|V_{11}|^2_\star = 0$ is IR repulsive under these conditions.

Let us now discuss the discrete fixed point solutions given in Tab. 4.1 in more detail. As stated above, each of the solutions presented in the table exists in four permutations of the flavour indices with equal singlet hypercharge (an example was given in Tab. 4.3). Within each of these quartets, the fixed point of the squared modulus of the CKM matrix element takes two values. We will now go through each of the six classes of discrete fixed point solutions one by one and give comments on their phenomenological viability.

Fixed point #1 in Tab. 4.1 is a phenomenologically viable fixed point solution and will be discussed in greater detail in Section 4.2. Here, we will study the RG flow emanating from this fixed point down to the IR and check to what degree one can recover the measured quark masses. This fixed point solution obeys the following relation, which should be compared to Eq. (3.20) for the one-generation case:

$$y_{t\star}^2 - y_{b\star}^2 = \frac{2}{3} g_{Y\star}^2 . \tag{4.12}$$

Fixed point #2 is an endpoint of one of the fixed lines given in Tab. 4.2. One of the fixed point values in this solution, $\frac{32}{41} f_g \pi^2$, only depends on the gauge sector parameter f_g and is hence fixed by the value of f_g from the gauge sector. For the phenomenologically viable choice $f_g = 9.7 \times 10^{-3}$, the numeric value of this fixed point is approximately 0.075, which is a significantly too large value in every permutation of this fixed point solution. Hence, we conclude that this fixed point is phenomenologically not viable.

Fixed point #3 is the trivial extension of the one generation fixed point solution #4 in Tab. 3.3 and has already been studied in [9]. The Yukawa couplings of the second generation quarks have vanishing fixed point values and the quadratic CKM matrix element is equal to 1 at the fixed point. The free fixed point of the strange Yukawa is IR attractive and one exactly recovers $m_s = 0$ in the IR. The vanishing fixed point of the charm quark is IR repulsive. The fixed point of $|V_{11}|^2$ is – as discussed above – also IR attractive as the third generation (top and bottom) is larger than the second generation (charm and strange). This fixed point approximately reproduces the correct phenomenology: The charm Yukawa is a relevant coupling and its IR value can be

accommodated by choosing suitable initial conditions in the UV. The top and bottom Yukawas emerge from the same fixed point as in the one generation case and – due to the smallness of the charm Yukawa throughout the RG flow – their RG trajectories are hardly altered in comparison to the one generation case. The CKM matrix is in this case diagonal at all scales, while small but non-vanishing mixing is observed in experiment. The strange Yukawa is zero at all scales as it corresponds to an irrelevant coupling. This is in contradiction to experiment, where a small but nevertheless finite strange mass was found.

The expressions of the fixed point values in **fixed point #4** are given by:

$$t_4 = \frac{16}{1107}\left(65f_g + 82f_y\right)\pi^2 \,, \tag{4.13}$$

$$b_4 = \frac{8}{1107}\left(-21f_g + 246f_y - r\right)\pi^2 \,, \tag{4.14}$$

$$s_4 = \frac{8}{1107}\left(-21f_g + 246f_y + r\right)\pi^2 \,, \tag{4.15}$$

$$V_4 = \frac{1}{2} + \frac{r}{2\left(65f_g + 82f_y\right)} \,, \tag{4.16}$$

with r given by

$$r = \sqrt{3\left(7f_g - 82f_y\right)\left(65f_g + 82f_y\right)} \,. \tag{4.17}$$

Requiring all Yukawa couplings to be real, i.e., $y_{i\star}^2 \geq 0 \;\; \forall\, i \in \{t, c, b, s\}$ as well as $r \in \mathbb{R}$ and assuming $f_g > 0$, we conclude that $f_y = \frac{7}{82} f_g$ has to be fulfilled. Inserting this value of f_y into the expressions of the fixed point, we end up with:

$$t_4 = \frac{128}{123} f_g \pi^2 = \frac{4}{9} g_{Y\star}^2 \,, \tag{4.18}$$

$$b_4 = 0 \,, \tag{4.19}$$

$$s_4 = 0 \,, \tag{4.20}$$

$$V_4 = \frac{1}{2} \,. \tag{4.21}$$

The expressions of the fixed point values in **fixed point #5** are given by:

$$t_5 = \frac{8}{1107}\left(87f_g + 246f_y - s\right)\pi^2 \,, \tag{4.22}$$

$$c_5 = \frac{8}{1107}\left(87f_g + 246f_y + s\right)\pi^2 \,, \tag{4.23}$$

$$b_5 = \frac{16}{1107}\left(-43f_g + 82f_y\right)\pi^2 \,, \tag{4.24}$$

$$V_5 = \frac{1}{2} - \frac{s}{2\left(43f_g - 82f_y\right)} \,, \tag{4.25}$$

with s given by

$$s = \sqrt{3\left(43f_g - 82f_y\right)\left(29f_g + 82f_y\right)} \,. \tag{4.26}$$

Requiring again all Yukawa couplings to be real, i.e., $y_{i\star}^2 \geq 0 \;\; \forall\, i \in \{t, c, b, s\}$ as well as $s \in \mathbb{R}$ and assuming $f_g > 0$, we conclude that $f_y = \frac{43}{82} f_g$ has to be fulfilled. Inserting this value of f_y into the expressions of the fixed point, we end up with:

$$t_5 = \frac{64}{41} f_g \pi^2 = \frac{2}{3} g_{Y\star}^2 \,, \tag{4.27}$$

$$c_5 = \frac{64}{41} f_g \pi^2 = \frac{2}{3} g_{Y\star}^2 \,, \tag{4.28}$$

$$b_5 = 0 \,. \tag{4.29}$$

Both fixed point solutions #4 and #5 are phenomenologically not viable.

Fixed point #5 can immediately be regarded as phenomenologically not viable, as it contains the strictly negative quadratic fixed point value $-\frac{32}{41} f_g$.

Besides the discrete fixed point solutions, there also exist two one parameter families of solutions, or fixed lines (cf. Tab. 4.2). If one would study the two-loop running of the Yukawa couplings, these fixed lines would collaps into a quartet of discrete fixed point solutions (cf. discussion in [6]). Also, as stated above, fixed point solution #2 in Tab. 4.1 is an endpoint of one of these fixed lines. Hence, treating fixed point solution #2 as an element of one of the fixed lines, we end up with a total of 5 discrete fixed point solution, each of which appears in a quartet. The total number of discrete solutions is therefore 20, while the number of fixed lines is 2.

In Tab. 4.4 we present the scaling exponents for the two generation model at the phenomenologically interesting fixed point solutions #1 and #3. There are three irrelevant directions for fixed point #1 and four irrelevant directions for fixed point #3. These correspond to an IR attractive UV fixed point for the Abelian gauge coupling as well as the top and bottom Yukawa couplings. For fixed point solution #3, we have an additional irrelevant direction, corresponding to the IR attractive Gaußian fixed point of the strange Yukawa.

4.2. An Example of an RG Flow

We are now going to discuss fixed point solution #1 in Tab. 4.1 in greater detail. The four permutations of this fixed point are given in Tab. 4.3. In the following, we will consider the permutation #1a, as this will give us the phenomenologically correct hierarchy of the quark masses in the IR. The reason for this is the fact that the ordering of the up-(down-)type Yukawas at the UV fixed point is preserved throughout the flow to the IR. This is because of the nature of the β-functions of the squared moduli of the CKM matrix elements (Eq. (2.43); (4.9) for $N_g = 2$). Due to the unitarity of the CKM matrix, poles appear in these β-functions if two or more up-(down-)type Yukawas are equal (cf. Section 2.3.2). A thorough discussion of this mechanism will be presented in Section 4.3. For now, we shall be content with the notion that the ordering of the up-(down-)type Yukawa couplings at the UV fixed point will be maintained in the IR.

	FP #1	FP #3
ϑ_1	$2f_g$	$2f_g$
ϑ_2	$-f_g$	$-f_g$
ϑ_3	$-f_g$	$-f_g$
ϑ_4	$-\frac{2}{205}\left(11f_g+82f_y\right)$	$\frac{3}{41}f_g$
ϑ_5	$-\frac{1}{205}\left(11f_g+82f_y\right)$	$-\frac{3}{41}f_g$
ϑ_6	$-\frac{1}{205}\left(11f_g+82f_y\right)$	$\frac{11}{82}f_g+f_y$
ϑ_7	$\frac{1}{205}\Big[3\left(11f_g+82f_y\right)+$	$\frac{1}{164}\Big[3\left(11f_g+82f_y\right)+$
	$+2\sqrt{1246f_g^2+2(11f_g)(82f_y)+(82f_y)^2}\Big]$	$+2\sqrt{1273f_g^2+2(11f_g)(82f_y)+(82f_y)^2}\Big]$
ϑ_8	$\frac{1}{205}\Big[3\left(11f_g+82f_y\right)-$	$\frac{1}{164}\Big[3\left(11f_g+82f_y\right)-$
	$-2\sqrt{1246f_g^2+2(11f_g)(82f_y)+(82f_y)^2}\Big]$	$-2\sqrt{1273f_g^2+2(11f_g)(82f_y)+(82f_y)^2}\Big]$

Table 4.4.: Scaling exponents for the phenomenologically interesting fixed point solutions #1 and #3 in Tab. 4.1. As $f_g > 0$ and $f_y > 0$, most scaling exponents are strictly positive or negative. However, the sign of ϑ_8 for fixed points #1 and #3 depends on the precise values of the parameters f_g and f_y. They are positive for $f_y > \frac{19}{82}f_g$ and $f_y > \frac{1}{82}f_g$, respectively, which are just the allowed ranges for the fixed point solutions #1 and #3 (cf. Tab. 4.1), excluding the lower bound, at which the scaling exponents are zero. There are three irrelevant directions for fixed point #1 and four irrelevant directions for fixed point #3, assuming f_y takes an allowed value.

The full set of (quadratic) fixed point values is given by:

$$g_{Y\star}^2 = \frac{96}{41}f_g\pi^2 \,, \tag{4.30}$$
$$g_{2\star}^2 = g_{3\star}^2 = 0 \,, \tag{4.31}$$

$$y_{t\star}^2 = \frac{16}{15}\left(f_g+2f_y\right)\pi^2 \,, \tag{4.32}$$
$$y_{b\star}^2 = \frac{16}{615}\left(-19f_g+82f_y\right)\pi^2 \,, \tag{4.33}$$
$$y_{c\star}^2 = y_{s\star}^2 = 0 \,, \tag{4.34}$$

$$|V_{11}|_\star^2 = 0 \,. \tag{4.35}$$

As our analysis is at one-loop order, the β-functions in the gauge sector are independent of the Yukawa couplings and CKM matrix elements. Hence, their RG flow is exactly the same as the one in the one generation case (cf. Section 3.1). In the Yukawa sector, the

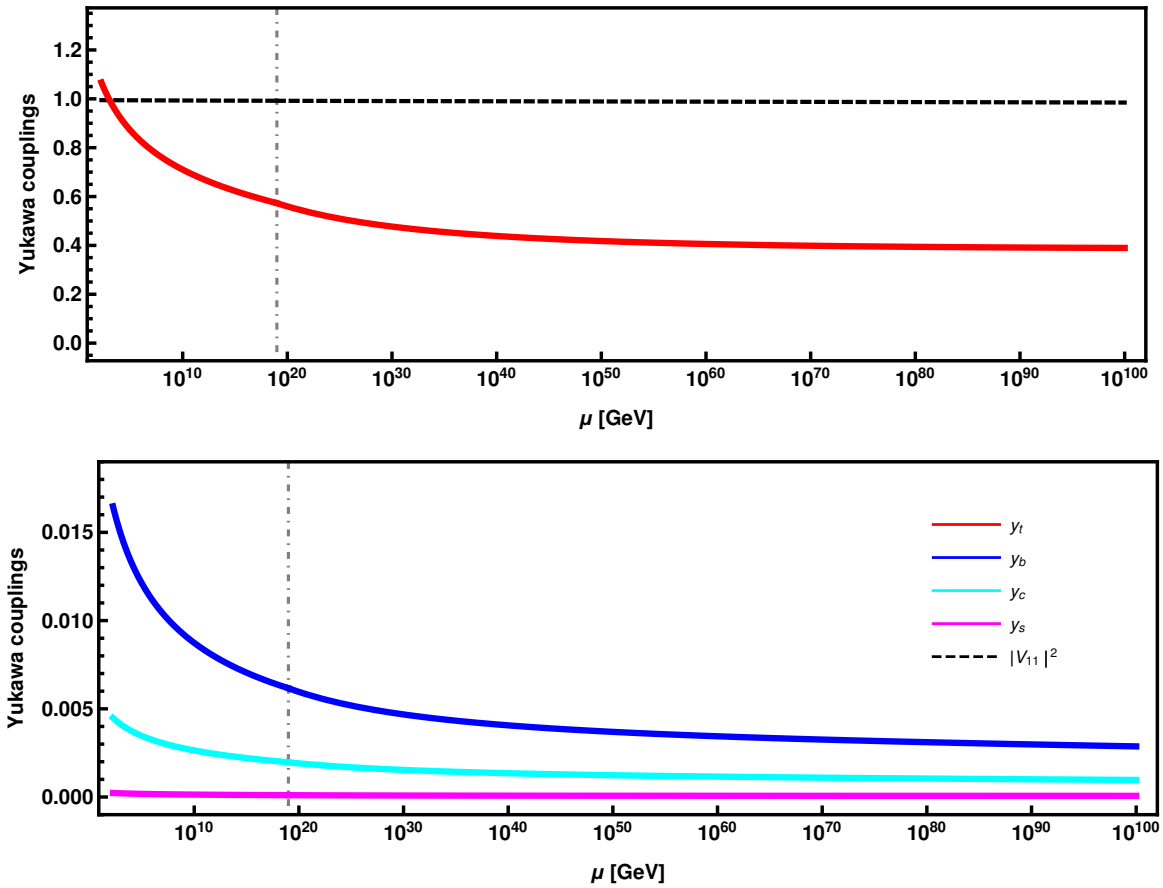

Figure 4.1.: RG flow of Yukawa couplings and quadratic CKM matrix element for fixed point solution #1 in Tab. 4.1. The charm and strange Yukawa as well as the quadratic CKM matrix element are relevant couplings with vanishing fixed point value, while the top and bottom Yukawas are irrelevant couplings with interacting UV fixed points. The top Yukawa is too large, leading to an overestimate of the top mass of about 10%. The running of the CKM parameter is extremely slow (note that $|V_{11}|^2_\star = 0$).

top and bottom Yukawas are again irrelevant couplings just like in the one generation case or at fixed point #3 in Tab. 4.1. For the second generation quarks however, we note that now both of them are relevant couplings. This is due to the fixed point value of the squared CKM matrix element $|V_{11}|^2_\star = 0$: In the β-function of the strange Yukawa, Eq. (4.6), the contribution of the largest Yukawa coupling, the top Yukawa coupling, is of the form $\sim y_t^2 \left(1 + |V_{11}|^2\right)$. If the fixed point value $|V_{11}|^2_\star$ changes from 1 to 0, the screening contribution of the top Yukawa to the running of the strange Yukawa is halved close to the fixed point. This has the effect that the strange Yukawa is now relevant, which means that a correct, finite strange mass can be accommodated as well.

Fig. 4.1 shows an RG flow emanating from fixed point solution #1 in Tab. 4.1. In order to roughly recover the observed quark masses, $f_y = \frac{19}{82} f_g + 5.9 \times 10^{-8} = 2.24762 \times 10^{-3}$ has been chosen. Upon choosing suitable initial conditions for the charm and

strange Yukawas, this leads to the following values of the Yukawa couplings at the top mass scale: $y_t(m_t) = 1.07$, $y_b(m_t) = 0.0165$, $y_c(m_t) = 4.48 \times 10^{-3}$, and $y_s(m_t) = 2.32 \times 10^{-4}$. This translates – according to Eq. (3.21) – to the following pole masses: $m_t = 191.8\,\text{GeV}$, $m_b = 4.1\,\text{GeV}$, $m_c = 1.29\,\text{GeV}$ and $m_s = 96\,\text{MeV}$. As one can see, in comparison to the one generation case, the top mass is overestimated by approximately 10%. This is mainly due to a larger fixed point value: In the one generation case, $y_{t\star} = 0.27$, while in the two generation case $y_{t\star} = 0.39$. Even though the running of the top Yukawa is slower in the two generation case, this significantly larger fixed point value still causes a too large value in the IR, leading to a high top mass. From Fig. 4.1, we further note that the running of the squared modulus $|V_{11}|^2$ is extremely slow. Even though the UV fixed point value of the squared CKM matrix element is 0, one can hardly recognize a deviation from scale invariance in Fig. 4.1 over a range of 10^{100} GeV. The initial condition in the far UV was chosen such that $|V_{11}|^2(m_t) = 0.99$.

4.3. Mass Bounds, Poles and Unitarity

As already mentioned in Section 2.3.2 and Appendix A.3, differences of (squared) Yukawa couplings appear in denominators in the β-functions of the squared moduli $|V_{ij}|^2$ of the CKM matrix elements, Eq. (2.43), which are of the form:

$$\frac{1}{(y_i^u)^2 - (y_k^u)^2}\,, \qquad i \neq k\,, \tag{4.36}$$

$$\frac{1}{\left(y_i^d\right)^2 - \left(y_k^d\right)^2}\,, \qquad i \neq k\,. \tag{4.37}$$

These denominators are non-perturbative in nature: They arise due to the requirement of an unitary CKM matrix and do not stem from a perturbative expansion in the couplings (cf. Appendix A.3). For degenerate Yukawa couplings, the β-functions of $|V_{ij}|^2$ hit a pole[1] and are hence non-analytic on the hypersurfaces in theory space defined by $y_i^{u(d)} = y_k^{u(d)}$ for $i \neq k$.

This has an important consequence: The RG trajectories of the Yukawa couplings emanating from a point in theory space where all Yukawa couplings are non-degenerate (or, at least, all degenerate Yukawas are zero) will never cross each other during the flow towards the IR, i.e. $y_i^{u(d)}(t) \neq y_k^{u(d)}(t)$, $i \neq k$, for $t < \infty$. In order to illustrate this, the RG flow of the bottom and strange Yukawa couplings as well as of the quadratic CKM matrix element $|V_{11}|^2$ as calculated in Fig. 4.1 is shown in Fig. 4.2. In the far UV, the bottom Yukawa stays at its fixed point value, while the strange Yukawa increases towards the IR. As the difference $y_b^2 - y_s^2$ decreases, the running of the quadratic CKM matrix element accelerates. This has the consequence that $|V_{11}|^2$ transitions from the

[1] There is an exception to this: The point in theory space where all or some up-(down-)type Yukawa couplings are zero can be approached continously as long as $y_i^{u(d)}(t) \neq y_k^{u(d)}(t)$, $i \neq k$, for $t < \infty$ [6]. Therefore more than one up-(down-)type quark can be asymptotically free as long as their RG trajectories do not cross at finite scales.

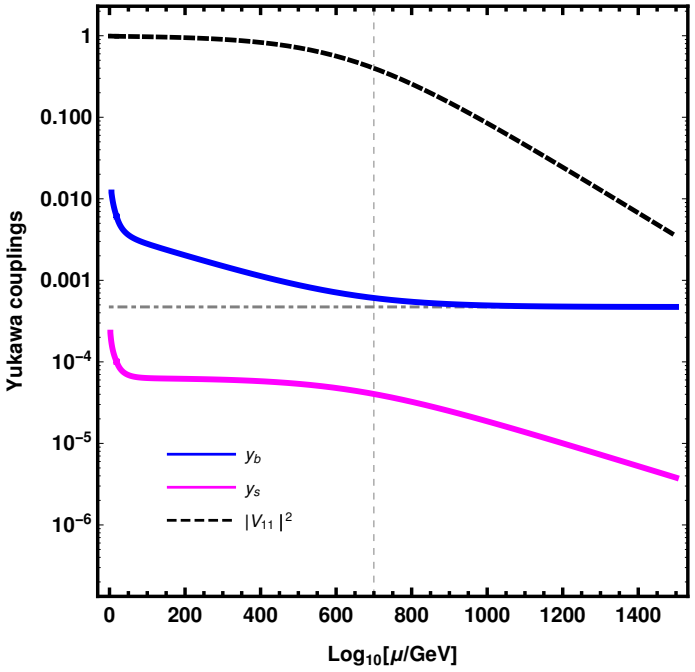

Figure 4.2.: RG flow of bottom and strange Yukawa couplings as well as the squared modulus of the CKM matrix element, $|V_{11}|^2$. In the far UV, the bottom Yukawa sticks to its fixed point value, denoted by a gray dotted-dashed line. As soon as the strange Yukawa comes close to the bottom Yukawa, the denominator in the β-function of $|V_{11}|^2$ becomes small and $|V_{11}|^2$ is driven towards the IR fixed point $|V_{11}|^2_\star = 1$. This reverses the roles of the bottom and strange Yukawas: Now, the running of the strange Yukawa freezes while the running of the bottom Yukawa is accelerated. This has the consequence that the IR value of the strange Yukawa is bounded from above (cf. discussion in the main text). The transition of the fixed point scaling regimes happens around some transition scale $\mu_{\text{trans}} \approx 10^{700}$ GeV, denoted by a gray dashed line.

fixed point $|V_{11}|^2_\star = 0$ in the UV to the fixed point $|V_{11}|^2_\star = 1$ in the IR. As already discussed in previous sections, a change of $|V_{11}|^2$ from 0 to 1 in a two generation model has the effect of interchanging the roles of the bottom and strange Yukawa. In the case of the RG flow shown in Fig. 4.2 we start at a fixed point that is IR attractive in the bottom and IR repulsive in the strange, i.e., fixed point solution #1a in Tab. 4.3. As the CKM matrix transitions from anti-diagonal to diagonal as the denominators become small, the roles of the bottom and strange Yukawa are swapped. Now, the strange Yukawa is irrelevant, while the bottom Yukawa is relevant. As one can see from Fig. 4.2, this happens around a transition scale μ_{trans}.

In order to illustrate this mechanism in a clearer way, we plotted the RG flow of the bottom and strange Yukawa couplings as well as of the quadratic CKM matrix element $|V_{11}|^2$ for exaggerated initial conditions and values of f_y in Fig. 4.3. In this plot, the value of f_y and the initial conditions in the UV were chosen such that they produce

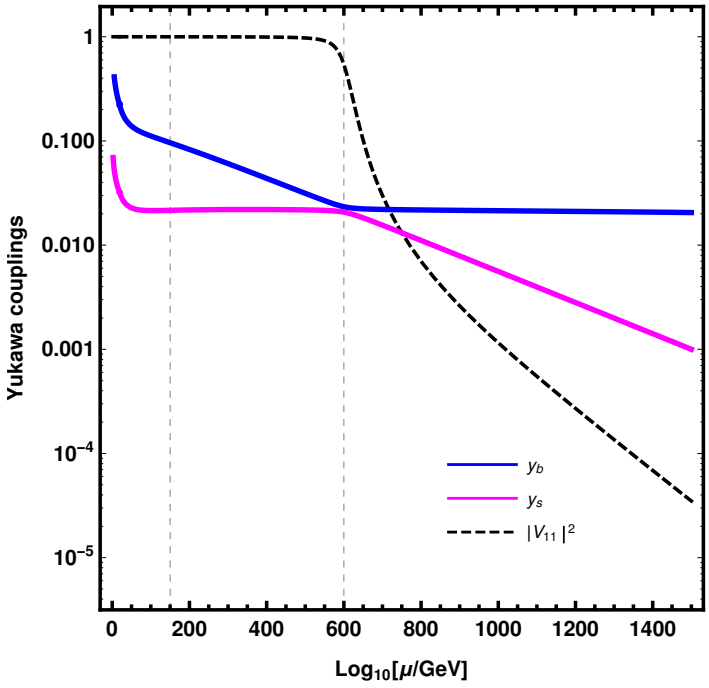

Figure 4.3.: RG flow of bottom and strange Yukawa couplings as well as the squared modulus of the CKM matrix element $|V_{11}|^2$ for exaggerated initial conditions and values of f_y. The flow of the couplings is qualitatively the same as in Fig. 4.2, but the transition between the scaling regimes is much more pronounced. The two gray dotted lines denote the scales at which the flow diagrams in Fig. 4.4 are evaluated: The left dashed line corresponds to $\mu = 10^{150}$ GeV and the right dashed line corresponds to the transition scale of this specific flow, $\mu_{\text{trans}} \approx 10^{600}$ GeV. The value of f_y and the initial conditions in the UV were chosen such that they produce a prominent transition of the scaling behaviour, rather than the correct IR values of the couplings.

a prominent transition of the scaling behaviour, in particular, $f_y = \frac{19}{82} f_g + 1.9 \times 10^{-5}$. One should therefore not be concerned with the IR values of the couplings, as the parameters were not tuned to recover the phenomenological values. However, Fig. 4.3 demonstrates the mechanism that prevents crossing of up-(down-)type Yukawas during the flow towards the IR. In the far UV, the irrelevant bottom Yukawa is effectively scale invariant[2], while the relevant, asymptotically free strange Yukawa increases towards the IR. As soon as the strange Yukawa comes close to the bottom Yukawa at the transition scale μ_{trans}, the quadratic CKM matrix element $|V_{11}|^2$ is rapidly driven towards the IR attractive fixed point $|V_{11}|^2_\star = 1$. In the sub-transtition regime, $\mu < \mu_{\text{trans}}$, the roles of the bottom and strange are inverted.

[2]There are, of course, slight deviations from the fixed point value at all finite scales as the relevant, asymptotically free couplings are all non-zero at finite scales and parametrize the deviation from scale invariance of the irrelevant couplings. However, this deviation is, as can be seen in Fig. 4.3, very small.

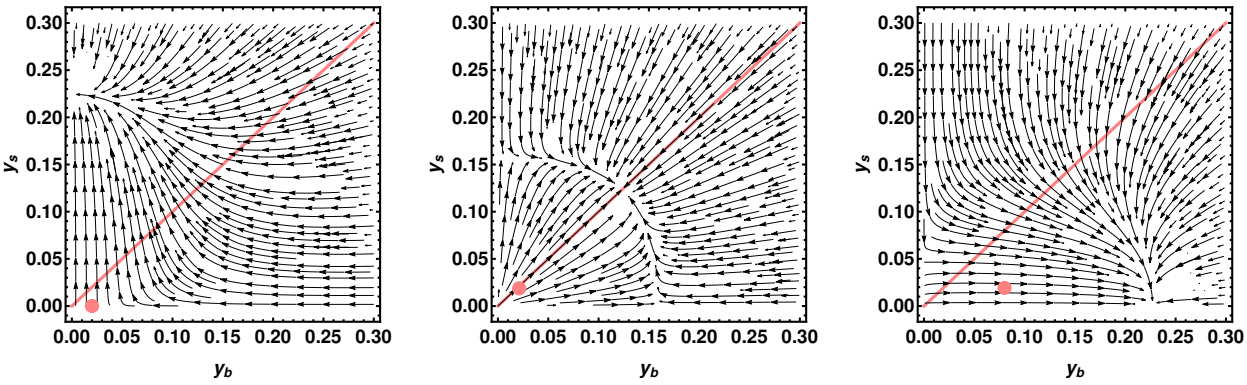

Figure 4.4.: Flow diagrams of the RG flow in Fig. 4.3. In the left panel, the y_b-y_s-plane is shown at the UV fixed point #1 in Tab. 4.1. In the middle panel, we show the flow at the transition scale $\mu_{\text{trans}} = 10^{600}$ GeV. In the left panel, we show the flow in the "IR" at a scale $\mu = 10^{150}$ GeV. The dot represents the current position of the flow shown in Fig. 4.3 in a plane parallel to the y_b-y_s-plane at the respective scale. The diagonal line represents the hypersurface defined by $y_b = y_s$ at which the β-function of $|V_{11}|^2$ becomes non-analytic. The arrows in the flow diagrams all point towards the IR.

We can further illustrate the characteristics of this change in scaling behaviour by looking at the *flow diagrams* of this model at different RG scales μ. In the present two generation model, we have a total of eight running couplings: three gauge couplings, four Yukawa couplings and one squared modulus of the CKM matrix element. In the spirit of the discussion presented in Section 2.2.2, we therefore consider a "truncated" eight-dimensional theory space spanned the aforementioned couplings. The system of β-functions – evaluated at different points in theory space, i.e., at different values of the eight couplings – describes a vector field in theory space governing the RG evolution of the model at hand. Flow diagrams – like, e.g., in Fig. 4.4 – are depiction of such vector fields[3].

In order to provide further inside into the mechanism presented in this section and for the sake of presentability, we will only consider a two-dimensional cut through the eight-dimensional theory space. More precisely, we are interested in planes in theory space that are parallel to the y_b-y_s-plane. A convenient way to imagine such two-dimensional cuts is to consider a three dimensional theory space spanned by the couplings g_x, g_y and g_z. One could then, for example, be interested in the flow diagram in a plane parallel to the g_x-g_y-plane, whose intersection with the g_z-plane is given by the value of g_z at some specific RG scale μ, $g_z(\mu)$. For a different value of the RG scale, μ', the plane might shift along the g_z-axis as, in general, $g_z(\mu) \neq g_z(\mu')$. Hence, – even though the vector field in the full three-dimensional theory space is obviously independent of the RG scale μ – the projection of the vector field onto the two-dimensional cuts parallel to

[3]In flow diagrams presented in this work, arrows always point towards the IR, i.e., the vector field describes the RG flow from the UV towards the IR.

the g_x-g_y-plane generally changes with a change in the RG scale μ.

In Fig. 4.4 we plotted the projections of the vector field onto such two-dimensional cuts parallel to the y_b-y_s-plane, which we will in the following refer to as "flow diagrams in the y_b-y_s-plane", for the flow depicted in Fig. 4.3 at three different values of the RG scale μ. In the left panel, we show the flow diagram in the y_b-y_s-plane at the UV fixed point #1 in Tab. 4.1, i.e., for $\mu \to \infty$. All couplings other than y_b and y_s are set to their respective fixed point values as given in fixed point solution #2 in Tab. 3.1 for the gauge couplings and fixed point solution #1 in Tab. 4.1 for the Yukawa couplings, respectively. The dot represents the position of the RG flow in the two-dimensional cut at the respective scale. In the left panel, the dot marks the UV fixed point values of the bottom and strange Yukawas. As one can see, the y_b- and y_s-axes pretty much align with irrelevant and relevant directions, respectively (cf. Section 2.2.2). As the couplings flow towards the IR, the RG trajectory approaches the hypersurface defined by $y_b = y_s$, denoted by the diagonal line in the flow diagrams. As the RG trajectory gets close to this hypersurface at the transition scale $\mu_{\text{trans}} = 10^{600}\,\text{GeV}$, the quadratic CKM matrix element quickly flows towards its IR fixed point $|V_{11}|^2_\star = 1$. The flow diagram in the y_b-y_s-plane at μ_{trans} is shown in the middle panel. Here, all couplings other than y_b and y_s take their values at the scale μ_{trans} according to their RG evolution for exaggerated values of f_y and initial conditions, specifically:

$$g_Y\left(\mu_{\text{trans}}\right) = 0.473\,, \tag{4.38}$$
$$g_2\left(\mu_{\text{trans}}\right) = 9.45 \times 10^{-7}\,, \tag{4.39}$$
$$g_3\left(\mu_{\text{trans}}\right) = 7.85 \times 10^{-7}\,, \tag{4.40}$$
$$y_t\left(\mu_{\text{trans}}\right) = 0.387\,, \tag{4.41}$$
$$y_c\left(\mu_{\text{trans}}\right) = 1.153 \times 10^{-4}\,, \tag{4.42}$$
$$|V_{11}|^2\left(\mu_{\text{trans}}\right) = 0.503\,. \tag{4.43}$$

At the transition scale, the couplings flow along the hypersurface defined by $y_b = y_s$. Below the transition scale, the roles of the bottom and strange Yukawa are effectively swapped. The right panel in Fig. 4.4 shows the flow diagram in the y_b-y_s-plane at a scale $\mu = 10^{150}\,\text{GeV} < \mu_{\text{trans}}$, where the couplings take the following values:

$$g_Y\left(10^{150}\,\text{GeV}\right) = 0.473\,, \tag{4.44}$$
$$g_2\left(10^{150}\,\text{GeV}\right) = 2.20 \times 10^{-2}\,, \tag{4.45}$$
$$g_3\left(10^{150}\,\text{GeV}\right) = 1.82 \times 10^{-2}\,, \tag{4.46}$$
$$y_t\left(10^{150}\,\text{GeV}\right) = 0.385\,, \tag{4.47}$$
$$y_c\left(10^{150}\,\text{GeV}\right) = 4.91 \times 10^{-4}\,, \tag{4.48}$$
$$|V_{11}|^2\left(10^{150}\,\text{GeV}\right) = 0.99\,. \tag{4.49}$$

This flow diagram looks similar to the flow diagram in the left panel if it was mirrored along the diagonal line $y_b = y_s$. This of course just reflects the effective interchange of

the bottom and strange Yukawa. Note that the flow diagram in the right panel is not exactly a mirrored version of the flow diagram in the left panel. This is due to the fact that during the flow towards the IR, all other couplings – including the relevant ones – have already deviated from their fixed point values. As the values of these couplings influence the flow of the bottom and strange Yukawas, the RG flow at scales below the transition scale, $\mu < \mu_{\text{trans}}$, is *not* related to the RG flow at scales above the transition scale, $\mu > \mu_{\text{trans}}$, by a simple permutation of the flavour indices, $b \leftrightarrow s$.

The non-analyticities at degenerate Yukawa couplings appearing in the β-functions of the squared moduli of the CKM matrix elements are an important piece of non-perturbative information, only emerging if one includes at least a second generation in their study. They impose restrictions on the IR values of the asymptotically free Yukawa couplings in the IR in the form of upper bounds. We will present a more thorough discussion on this topic in the following concluding chapter.

5. Conclusion and Outlook

In this thesis, we have been concerned with two problems of the SM: First of all, how can one achieve an UV completion of the gauge and Yukawa sectors of the SM? Secondly, can we shed light on the intricate flavour structure observed in experiment, i.e., the fermionic mass spectra as well as the mixing patterns, whose roots are not explained by the SM itself? The approach presented in this thesis to tackle both these problems simultaneously was based on modifying the renormalization group running of the gauge and Yukawa couplings, thereby creating new (interacting) renormalization group fixed points in the UV.

The modification of the running was obtained by adding antiscreening terms to the β-functions of the gauge and Yukawa couplings in the style of [7–9], which parametrize the – yet unspecified – bSM physics. By adding an antiscreening new-physics term to the β-functions of the gauge couplings, an UV safe RG trajectory of the Abelian $\mathsf{U}(1)_\mathsf{Y}$ coupling can be achieved[1]. The antiscreening character of the bSM term counters the screening nature of the SM β-function, resulting in – depending of the precise choice of the value of the bSM parameter f_g – either a free or interacting fixed point value of the Abelian gauge coupling. By choosing the bSM parameter f_g such that the SM running and the new-physics term cancel at an interacting fixed point, the value of the Abelian gauge coupling becomes fixed at all scales in terms of the non-Abelian couplings and the parameter f_g. This effectively results in a reparametrization of the gauge sector, which is now UV complete.

Residual Abelian gauge interactions in the far UV give rise to new fixed point structures in the Yukawa sector, as can be demonstrated by a top-bottom-gauge system, the study of which was first performed in [7–9] and is summarized in Chapter 3: Due to the fact that the Abelian gauge contribution to the running of the Yukawa couplings is non-zero at the fixed point, the system of β-functions is no longer symmetric under an interchange of up-type and down-type flavour indices within a generation. This is due to the unequal $\mathsf{U}(1)_\mathsf{Y}$ hypercharges of right-handed up- and down-type quarks and has the effect that also the system of fixed point solutions no longer exhibits this symmetry. In the case where the Abelian gauge coupling is asymptotically free, the fixed point values of the top and bottom Yukawas at the fixed point where both the top and the bottom are interacting are degenerate. In the case where the Abelian gauge coupling emanates from an interacting, IR attractive fixed point in the UV, this degeneracy is lifted. It turns out that – with a suitable choice of the value of the parameter f_y – the splitting of the fixed point values in the UV due to the interacting Abelian gauge coupling results in a phenomenologically viable RG trajectory, where the IR values of the Yukawa couplings

[1] cf. Chapter 3 and [7–9].

translate to the correct pole masses within a reasonable margin. The residual Abelian gauge interactions hence generate a non-trivial flavour structure at the UV fixed point. This structure is not present for vanishing Abelian contributions, as then up- and down-type quarks are indistinguishable at the fixed point. Just like for the Abelian gauge coupling, the interacting fixed point in the Yukawa sector is IR attractive in both the top and the bottom, meaning that the flow of the Yukawa couplings is parametrized in terms of the relevant non-Abelian couplings and the bSM parameters f_g and f_y.

The investigation of the one generation model demonstrates that the antiscreening bSM terms could provide a UV completion of the gauge and Yukawa sector while also generating new, predictive UV fixed points. The predictiveness of the interacting fixed points is a consequence of an enhanced symmetry, in this case of the scale symmetry at the fixed point [6]: As is often the case in physics, a symmetry constrains the interactions of a theory. In the case at hand, the irrelevant couplings are fixed purely in terms of the relevant ones, allowing us to derive the values of the top and bottom Yukawas as well as of the Abelian gauge coupling at all scales from the fixed point structure.

The extension of this study to a system with two generations was the main task performed in this thesis, where we investigated whether the mechanism introduced for the one generation case in [7–9] also works in a multi-generation system. By introducing a second quark generation, we have to take flavour mixing into account, which plays a crucial role in the RG evolution of the Yukawa couplings. A naïve extension of the phenomenologically viable fixed point studied in the one generation case yields a vanishing strange Yukawa coupling at all scales and no finite strange mass can be accommodated[2]. Furthermore, for this fixed point solution the mixing is trivial at all scales and no deviations from a fully diagonal CKM matrix can be achieved. However, there exists a fixed point in the two generation case that yields at least a qualitatively viable RG trajectory (cf. Fig. 4.1): Starting with an anti-diagonal CKM matrix at the UV fixed point, there exists a fixed point with interacting, IR attractive fixed points for the top and bottom Yukawas and asymptotically free charm and strange Yukawas. As the CKM matrix is now anti-diagonal at the UV fixed point, both Yukawas from the second generation are IR repulsive. While viable IR values of the charm and strange Yukawa couplings as well as of the squared modulus of the CKM matrix element can be accommodated, the flows of the top and bottom Yukawas are again fixed by the relevant couplings. While the large mass splitting of the top and bottom quark is again qualitatively described, the top pole mass is predicted to be roughly 10% larger than the experimental value. This is because the fixed point value of the top is significantly larger for this fixed point solution than for the naïve extension of the one generation fixed point.

The study of the two generation case furthermore reveals an important piece of non-perturbative information about the running of the CKM matrix: Due to the unitarity of the CKM matrix, poles appear in the β-functions of the squared moduli $|V_{ij}|^2$ if at least two up-type (down-type) Yukawa couplings are degenerate[3]. This has the consequence

[2]Note, however, that we did not take the dynamically generated mass from strong interactions into account [6].

[3]Mind the exception of vanishing Yukawas as discussed in Section 4.3.

that the trajectories of two up-type (down-type) Yukawas can not cross during the flow towards the IR, meaning that the generational hierarchy of up-type (down-type) quarks at the UV fixed point is conserved at all scales. For the particular case of the two generation model with UV fixed point #1 in Tab. 4.1, this means $y_t(\mu) > y_c(\mu)$ and $y_b(\mu) > y_s(\mu)$ for all values of the RG scale μ. We therefore have – in addition to the predictive, interacting fixed points of the heavy quarks – an additional (albeit weaker) constraint on the flavour structure in the IR. The value of the Yukawa coupling of an up-type (down-type) quark of generation i is effectively bounded from above by the fixed point value of the next heavier up-type (down-type) quark Yukawa. Notice though that this only holds when the deviation of the relevant couplings from their (vanishing) fixed point values is small. As soon as, e.g., the non-Abelian gauge couplings start to deviate from the Gaußian fixed point significantly, the Yukawa couplings may flow to values larger than the fixed point value of the next heavier quark. Finally, we note that the transition scale μ_{trans}, i.e. the scale where the system transitions from one scaling behaviour to another as the denominators in the β-functions of the squared moduli of the CKM matrix elements become small, typically lies several hundred orders of magnitude above the Planck scale, which begs the question how physical they really are and whether these transitions are just mathematical properties of the RG flow of the system.

Before we give an outlook on a study treating the phenomenologically interesting case of three generations, we now briefly discuss the stability of the presented fixed point solutions upon including higher order corrections, following the discussion in [6]. The mechanism that induces fixed points in the model discussed here is the interplay between the SM β-functions and the newly introduced, antiscreening bSM terms. We are only interested in fixed point solutions that arise from this balancing of SM and bSM contributions and not in fixed points that are mere artifacts of the perturbative expansion. As argued in [6], a fixed point that fulfils these conditions must reduce to the free fixed point in the limit $f_g \to 0$ and $f_y \to 0$. Furthermore, for small parameters f_g and f_y, the fixed point solutions should be near Gaußian such that higher order loop contributions do not alter the fixed point values significantly [6]. A study of the effects of two-loop corrections to the one-loop β-functions used in this thesis has been performed in [6], and it was shown that the fixed point solutions discussed in this work are in fact stable upon inclusion of two-loop terms. New fixed point solutions that are artifacts of the perturbative expansion do arise, but their values lie way beyond the perturbative regime. The two-loop β-functions for a two generation model are presented in Appendix B.3.

The next step beyond a two generation model is of course the phenomenologically interesting case of a three generation model. A partial study of such a model has been performed in [6]. The system of one-loop β-functions of a three generation model is significantly more complicated than the system for the two-generation model. In fact, the system of equations is so involved that even with computer algebra systems it is a non-trivial task to find the complete set of analytic fixed point solutions. In [6], the study of the fixed point solutions was hence reduced to solutions where the mixing is minimal, i.e. where the CKM matrix is some unitary matrix with only ones and zeros as entries at the fixed point. The fixed point patterns of the CKM matrix then once

again form a faithful representation of the permutation group, like in the case of two generations. The main findings made in this work also hold for a three generation model: A non-vanishing Abelian gauge coupling breaks the symmetry of up- and down-type flavours within a generation. Furthermore, poles again appear in the β-functions of the squared moduli of the CKM matrix elements, preventing a crossing of up-type (down-type) Yukawa couplings during the flow towards the IR. The one-loop β-functions for a model containing three generations are given in Appendix B.2. For a detailed study of a three generation model see [6].

In summary, we showed in this thesis that the extension of the studies performed in [7–9] to a model containing two generations of quarks where we include flavour mixing effects is possible in the sense that there exists a qualitatively similar RG trajectory: The large splitting between top and bottom quarks due to the unequal Abelian hypercharges at non-vanishing Abelian gauge coupling is still present, while the correct IR values of the charm and strange quark as well as of the CKM matrix element can be accommodated. Hence, the model can in fact yield a phenomenologically viable mass hierarchy in the IR. We also demonstrated how a multi-generational model and the then necessary introduction of flavour mixing effects adds another layer of complexity to the theory: Two fixed point solutions exist for the 2×2 CKM matrix, one at which the matrix is diagonal and one at which the matrix is antidiagonal. These fixed point structures form a representation of the permutation group and have the effect of interchanging the roles of the bottom and strange quarks. This, together with a symmetry of the system of β-functions under the exchange of top and strange quarks results in a quartet structure of the fixed point solutions. Furthermore, the unitarity of the CKM matrix prohibits a crossing of up-type (down-type) Yukawas during the flow towards the IR, which further restricts the flavour structure in the IR. However, unlike in the case of only one generation, the RG study of the two generation model consistently predicts a top mass that is roughly 10% larger than the observed top mass, given that one strarts from the fixed point solution where all other running quantities can can be tuned to reach their phenomenological values in the IR. Another conclusion that we can draw from this work is that the inclusion of a second generation together with mixing effects does not a provide more predictivity than the one generation model: The number of irrelevant, i.e. uniquely fixed directions is the same in the two generation model as in the one generation model. While the Abelian gauge coupling as well as the top and bottom quark Yukawas are still irrelevant, the newly added running couplings (y_c, y_s and $|V_{11}|^2$) have to be relevant with respect to a fixed point where they have vanishing fixed point values in order to accommodate their correct IR values. As discussed in [6], this also seems to be the case for a model containing three generations of quarks. Lastly, we note that the running of the newly added couplings is extremely slow and their sclaing exponents are generally very small. This has the effect that the typical scales where the system changes its running behaviour when one comes close to the poles in the β-functions of $|V_{ij}|^2$ lie hundreds of orders of magnitude above the Planck scale, which might suggest that this transition is rather a methematical property of the system of equations than a truly physical situation. The model we studied in this thesis is hence interesting in detail, but fails to extend the promising results of the one generation model.

As for future work on this topic, we note that so far we completely ignored the leptonic sector of the SM. It would be interesting to study whether the flavour structures for the leptonic sector arise in a similar fashion as they do in the quark sector. Besides the leptonic sector, the research of possible bSM theories that could generate antiscreening terms as studied here is of great interest. Originally, these terms stem from asymptotically safe quantum gravity, but there is no reason to exclude other bSM theories, like, e.g., GUTs, from the considerations.

A. Derivation of β-functions

In this Appendix we show details on the calculation of the β-functions used in the main text.

A.1. Gauge Couplings

In the following, we discuss the group theoretical factors appearing in Eq. (2.33). We follow the definitions given in [19, 20].

The representation matrices τ^a for the generators of the gauge group G satisfy the Lie algebra relation

$$[\tau^a, \tau^b] = i \sum_c f^{abc} \tau^c \ , \tag{A.1}$$

with f^{abc} the structure constants. The quadratic Casimir operator $\boldsymbol{C}_2$ is defined as [73]

$$\boldsymbol{C}_2 \equiv \sum_a \tau^a \tau^a \ . \tag{A.2}$$

Its eigenvalue $C_2(\mathsf{G})$ in the adjoint representation of G is given by

$$\sum_{cd} f^{acd} f^{bcd} = C_2(\mathsf{G}) \delta^{ab} \ . \tag{A.3}$$

The Dynkin index [73, 74] $S_2(R)$ of an irreducible representation R is defined by

$$\mathrm{Tr}\, \tau^a \tau^b = S_2(R) \delta^{ab} \ , \tag{A.4}$$

and satisfies the relation

$$d(\mathsf{G}) S_2(R) = d(R) C_2(R) \ , \tag{A.5}$$

with $d(R)$ the dimension of the representation R and $d(\mathsf{G})$ the dimension of the Lie algebra $\mathfrak{g}$ of G.

We now calculate these group theoretic factors for a SM-like theory with gauge group[1] $\mathsf{SU}(3)_\mathsf{C} \otimes \mathsf{SU}(2)_\mathsf{L} \otimes \mathsf{U}(1)_\mathsf{Y}$. The results are summarized in Tab. A.1. The eigenvalues of the quadratic Casimir operator for a group $\mathsf{SU}(N)$ are given by:

$$C_2\left(\mathsf{SU}(N)\right) = N \ . \tag{A.6}$$

As $\mathsf{U}(1)_\mathsf{Y}$ is an Abelian group, its structure constants vanish and its adjoint representation is zero, hence $C_2\left(\mathsf{U}(1)_\mathsf{Y}\right) = 0$. For $S_2(F)$, i.e. the Dynkin index of the representation

[1] In case that the gauge group is not simple but a direct product group $\mathsf{G} = \bigotimes_i \mathsf{G}_i$, a sum over the index i appears in the definition of the Casimir and Dynkin index, cf. [19, 20].

Group	C_2	$S_2(F)$	$S_2(S)$
$\mathsf{SU}(3)_\mathsf{C}$	3	$2N_g$	0
$\mathsf{SU}(2)_\mathsf{L}$	2	$2N_g$	$\frac{1}{2}N_H$
$\mathsf{U}(1)_\mathsf{Y}$	0	$\sum_{i=1}^{N_g}\left\{3Q^{(i)}+L^{(i)}\right\}$	$2\ N_H\,(Y_H)^2$

Table A.1.: Group theoretic factors for a theory with gauge group $\mathsf{SU}(3)_\mathsf{C}\otimes\mathsf{SU}(2)_\mathsf{L}\otimes\mathsf{U}(1)_\mathsf{Y}$. $Q^{(i)}=\left(Y^{(i)}_{u_\mathrm{R}}\right)^2+2\left(Y^{(i)}_{q_\mathrm{L}}\right)^2+\left(Y^{(i)}_{d_\mathrm{R}}\right)^2$ and $L^{(i)}=\left(Y^{(i)}_{e_\mathrm{R}}\right)^2+2\left(Y^{(i)}_{l_\mathrm{L}}\right)^2$, cf. Eq. (A.10).

of the gauge group under which the fermion fields transform, we have to take a look at the transformation properties of the fields, cf. Tab. 2.2. In case of $\mathsf{G}=\mathsf{SU}(3)_\mathsf{C}$, we note that only the quarks transform in a non-trivial way. Using the usual Gell-Mann matrices $\frac{1}{2}\lambda^A$ as the representation matrices of the generators of $\mathsf{SU}(3)_\mathsf{C}$ in the fundamental representation we obtain

$$S_2(F)=4N_g\ \mathrm{Tr}\left(\frac{\lambda^1}{2}\cdot\frac{\lambda^1}{2}\right)=4N_g\ \mathrm{Tr}\left(\frac{\lambda^2}{2}\cdot\frac{\lambda^2}{2}\right)=\ldots=4N_g\ \mathrm{Tr}\left(\frac{\lambda^8}{2}\cdot\frac{\lambda^8}{2}\right)=2N_g\ , \tag{A.7}$$

where the factor 4 stems from the fact that there are two left-handed and two right-handed quarks per generation. For the $\mathsf{SU}(2)_\mathsf{L}$ group, we find similar results: All left-handed fields transform as $\mathsf{SU}(2)_\mathsf{L}$-doublets, whereas all right-handed fields transform as $\mathsf{SU}(2)_\mathsf{L}$-singlets. There are 3 left-handed quark doublets (3 colours) and 1 left-handed lepton doublet per generation. Using the usual Pauli matrices $\frac{1}{2}\sigma^A$ as the representation matrices of the generators of $\mathsf{SU}(2)_\mathsf{L}$ in the fundamental representation, we obtain

$$S_2(F)=4N_g\ \mathrm{Tr}\frac{\sigma^1}{2}\cdot\frac{\sigma^1}{2}=4N_g\ \mathrm{Tr}\frac{\sigma^2}{2}\cdot\frac{\sigma^2}{2}=4N_g\ \mathrm{Tr}\frac{\sigma^3}{2}\cdot\frac{\sigma^3}{2}=2N_g\ . \tag{A.8}$$

Under local $\mathsf{U}(1)_\mathsf{Y}$ transformations, the left- and right-handed fermions as well as the complex scalar $\mathsf{SU}(2)_\mathsf{L}$ doublets transform as

$$\psi_i\to\psi_i'=\mathrm{e}^{iY_i\theta(x)}\psi_i\ , \tag{A.9}$$

where the ψ_i is any field and Y_i are the generators of $\mathsf{U}(1)_\mathsf{Y}$, the so called (weak) hypercharges [12]. As the generators of $\mathsf{U}(1)_\mathsf{Y}$ are simply numbers, all we have to do to get $S_2(F)$ is to add up the squares of all hypercharges:

$$S_2(F)=\sum_{i=1}^{N_g}\left\{N_c\left[\left(Y^{(i)}_{u_\mathrm{R}}\right)^2+2\left(Y^{(i)}_{q_\mathrm{L}}\right)^2+\left(Y^{(i)}_{d_\mathrm{R}}\right)^2\right]+\left[\left(Y^{(i)}_{e_\mathrm{R}}\right)^2+2\left(Y^{(i)}_{l_\mathrm{L}}\right)^2\right]\right\}\ . \tag{A.10}$$

Here, $Y^{(i)}_{u_\mathrm{R}(d_\mathrm{R})}$ denotes the hypercharge of a right-handed up(down)-type quark, $Y^{(i)}_{e_\mathrm{R}}$ denotes the hypercharge of a right-handed charged lepton and $Y^{(i)}_{q_\mathrm{L}(l_\mathrm{L})}$ denotes the hypercharge of a left-handed quark (lepton), which get an additional factor 2 as there are two

left-handed fields per generation. In addition, every quark hypercharge gets a factor $N_c = 3$, accounting for the number of different colours in which the quarks appear. The superscript i labels the different fermion generations.

For the scalar Dynkin index $S_2(S)$ we note that the complex scalar Higgs doublet is a $\mathsf{SU}(2)_\mathsf{L}$ doublet and hence transforms also as an element of the representation space of the fundamental representation of $\mathsf{SU}(2)_\mathsf{L}$. We conclude that $S_2(S) = \frac{1}{2}N_H$ with N_H the number of complex scalar Higgs doublets in the Lagrangian. For the Abelian group $\mathsf{U}(1)_\mathsf{Y}$ we again have to add up the respective hypercharges which yields $S_2(S) = 2N_H$ where Y_H is the hypercharge of the complex scalar Higgs $(Y_H)^2$. There is also a factor 2 accounting for the doublet structure of the Higgs. As the Higgs doublet transforms trivially under $\mathsf{SU}(3)_\mathsf{C}$ transformations, the respective Dynkin index vanishes.

A.2. Yukawa Couplings

We now demonstrate how to diagonalize Eq. (2.37) and (2.38). The Hermitian matrices $\boldsymbol{\mathcal{Z}}_u(t) = \boldsymbol{\mathcal{Y}}_u\boldsymbol{\mathcal{Y}}_u^\dagger$ and $\boldsymbol{\mathcal{Z}}_d(t) = \boldsymbol{\mathcal{Y}}_d\boldsymbol{\mathcal{Y}}_d^\dagger$ at RG time t_0 can be diagonalized using a unitary transformation:

$$\boldsymbol{\mathcal{Z}}_u(t_0) = \boldsymbol{U}_\mathrm{L}^\dagger \mathscr{Z}_u(t_0)\,\boldsymbol{U}_\mathrm{L}\,, \qquad \boldsymbol{\mathcal{Z}}_d(t_0) = \boldsymbol{D}_\mathrm{L}^\dagger \mathscr{Z}_d(t_0)\,\boldsymbol{D}_\mathrm{L}\,, \tag{A.11}$$

with

$$\mathscr{Z}_u(t) = \mathrm{diag}\left(y_u^2(t), y_c^2(t), y_t^2(t), \ldots\right), \qquad \mathscr{Z}_d(t) = \mathrm{diag}\left(y_d^2(t), y_s^2(t), y_b^2(t), \ldots\right), \tag{A.12}$$

where $t \equiv \log(\mu/\Lambda)$. At another RG time $t_1 \neq t_0$, the Yukawa matrices $\boldsymbol{\mathcal{Y}}_{u,d}$ have evolved according to the β-functions Eq. (2.37) and (2.38) and one needs a different set of unitary transformations given by $\boldsymbol{U}'_\mathrm{L}$ and $\boldsymbol{D}'_\mathrm{L}$ in order to diagonalize the squared Yukawa matrices $\boldsymbol{\mathcal{Z}}_{u,d}$. Hence, the diagonalizing unitary matrices $\boldsymbol{U}_\mathrm{L}$ and $\boldsymbol{D}_\mathrm{L}$ also depend on the RG time t:

$$\boldsymbol{U}_\mathrm{L} \;\to\; \boldsymbol{U}_\mathrm{L}(t)\,, \quad \boldsymbol{D}_\mathrm{L} \;\to\; \boldsymbol{D}_\mathrm{L}(t) \tag{A.13}$$

Assuming that all matrices are smooth functions of the RG time t, after an infinitesimal time step $\mathrm{d}t$ Eq. (A.11) reads:

$$\begin{aligned}
\boldsymbol{\mathcal{Z}}_u(t+\mathrm{d}t) &= \boldsymbol{U}_\mathrm{L}^\dagger(t+\mathrm{d}t)\,\mathscr{Z}_u(t+\mathrm{d}t)\,\boldsymbol{U}_\mathrm{L}(t+\mathrm{d}t) \\
&= \Big(\boldsymbol{U}_\mathrm{L}^\dagger(t) + \mathrm{d}\boldsymbol{U}_\mathrm{L}^\dagger(t)\Big)\Big(\mathscr{Z}_u(t) + \mathrm{d}\mathscr{Z}_u(t)\Big)\Big(\boldsymbol{U}_\mathrm{L}(t) + \mathrm{d}\boldsymbol{U}_\mathrm{L}(t)\Big) \\
&= \Big(\boldsymbol{U}_\mathrm{L}^\dagger(t) + \beta\left(\boldsymbol{U}_\mathrm{L}^\dagger\right)\mathrm{d}t\Big)\Big(\mathscr{Z}_u(t) + \beta\left(\mathscr{Z}_u\right)\mathrm{d}t\Big)\Big(\boldsymbol{U}_\mathrm{L}(t) + \beta\left(\boldsymbol{U}_\mathrm{L}\right)\mathrm{d}t\Big)\,,
\end{aligned} \tag{A.14}$$

and analogous for the down-type matrix:

$$\boldsymbol{\mathcal{Z}}_d(t+\mathrm{d}t) = \Big(\boldsymbol{D}_\mathrm{L}^\dagger(t) + \beta\left(\boldsymbol{D}_\mathrm{L}^\dagger\right)\mathrm{d}t\Big)\Big(\mathscr{Z}_d(t) + \beta\left(\mathscr{Z}_d\right)\mathrm{d}t\Big)\Big(\boldsymbol{D}_\mathrm{L}(t) + \beta\left(\boldsymbol{D}_\mathrm{L}\right)\mathrm{d}t\Big)\,. \tag{A.15}$$

Given that they are unitary at any RG time t, we require the matrices $\boldsymbol{U}_\mathrm{L}$ and $\boldsymbol{D}_\mathrm{L}$ to be unitary after an infinitesimal RG time step $\mathrm{d}t$:

$$\mathbb{1} \overset{!}{=} \boldsymbol{U}_\mathrm{L}(t+\mathrm{d}t)\,\boldsymbol{U}_\mathrm{L}^\dagger(t+\mathrm{d}t) = \boldsymbol{U}_\mathrm{L}^\dagger(t+\mathrm{d}t)\,\boldsymbol{U}_\mathrm{L}(t+\mathrm{d}t) \tag{A.16}$$

$$\begin{aligned}
\Rightarrow \quad \mathbb{1} &= \boldsymbol{U}_\mathrm{L}(t)\,\boldsymbol{U}_\mathrm{L}^\dagger(t) + \Big(\mathrm{d}\boldsymbol{U}_\mathrm{L}(t)\Big)\boldsymbol{U}_\mathrm{L}^\dagger(t) + \boldsymbol{U}_\mathrm{L}(t)\Big(\mathrm{d}\boldsymbol{U}_\mathrm{L}^\dagger(t)\Big) \\
&= \mathbb{1} + \beta(\boldsymbol{U}_\mathrm{L})\,\boldsymbol{U}_\mathrm{L}^\dagger(t)\,\mathrm{d}t + \boldsymbol{U}_\mathrm{L}(t)\Big(\beta(\boldsymbol{U}_\mathrm{L})\Big)^\dagger \mathrm{d}t\,, \qquad \text{(A.17)} \\
\mathbb{1} &= \boldsymbol{U}_\mathrm{L}^\dagger(t)\,\boldsymbol{U}_\mathrm{L}(t) + \Big(\mathrm{d}\boldsymbol{U}_\mathrm{L}^\dagger(t)\Big)\boldsymbol{U}_\mathrm{L}(t) + \boldsymbol{U}_\mathrm{L}^\dagger(t)\Big(\mathrm{d}\boldsymbol{U}_\mathrm{L}(t)\Big) \\
&= \mathbb{1} + \Big(\beta(\boldsymbol{U}_\mathrm{L})\Big)^\dagger \boldsymbol{U}_\mathrm{L}(t)\,\mathrm{d}t + \boldsymbol{U}_\mathrm{L}^\dagger(t)\,\beta(\boldsymbol{U}_\mathrm{L})\,\mathrm{d}t\,. \qquad \text{(A.18)}
\end{aligned}$$

and analogous for the down-type matrix. From this, we can deduce the *unitarity conditions*:

$$\beta\Big(\boldsymbol{U}_\mathrm{L}\boldsymbol{U}_\mathrm{L}^\dagger\Big) = \beta(\boldsymbol{U}_\mathrm{L})\,\boldsymbol{U}_\mathrm{L}^\dagger + \boldsymbol{U}_\mathrm{L}\Big(\beta(\boldsymbol{U}_\mathrm{L})\Big)^\dagger = 0\,, \tag{A.19}$$

$$\beta\Big(\boldsymbol{U}_\mathrm{L}^\dagger\boldsymbol{U}_\mathrm{L}\Big) = \Big(\beta(\boldsymbol{U}_\mathrm{L})\Big)^\dagger \boldsymbol{U}_\mathrm{L} + \boldsymbol{U}_\mathrm{L}^\dagger\beta(\boldsymbol{U}_\mathrm{L}) = 0\,, \tag{A.20}$$

$$\beta\Big(\boldsymbol{D}_\mathrm{L}\boldsymbol{D}_\mathrm{L}^\dagger\Big) = \beta(\boldsymbol{D}_\mathrm{L})\,\boldsymbol{D}_\mathrm{L}^\dagger + \boldsymbol{D}_\mathrm{L}\Big(\beta(\boldsymbol{D}_\mathrm{L})\Big)^\dagger = 0\,, \tag{A.21}$$

$$\beta\Big(\boldsymbol{D}_\mathrm{L}^\dagger\boldsymbol{D}_\mathrm{L}\Big) = \Big(\beta(\boldsymbol{D}_\mathrm{L})\Big)^\dagger \boldsymbol{D}_\mathrm{L} + \boldsymbol{D}_\mathrm{L}^\dagger\beta(\boldsymbol{D}_\mathrm{L}) = 0\,. \tag{A.22}$$

β-functions that satisfy the conditions (A.19) to (A.22) describe a unitary evolution of $\boldsymbol{U}_\mathrm{L}$ and $\boldsymbol{D}_\mathrm{L}$, i.e. matrices that are unitary at an initial RG time t_0 and which evolve according to β-functions that satisfy the conditions (A.19) to (A.22) are unitary at all times. This obviously holds for any unitary matrix $\boldsymbol{A}$:

$$\beta\Big(\boldsymbol{A}\boldsymbol{A}^\dagger\Big) = \beta(\boldsymbol{A})\,\boldsymbol{A}^\dagger + \boldsymbol{A}\Big(\beta(\boldsymbol{A})\Big)^\dagger = 0\,, \tag{A.23}$$

$$\beta\Big(\boldsymbol{A}^\dagger\boldsymbol{A}\Big) = \Big(\beta(\boldsymbol{A})\Big)^\dagger \boldsymbol{A} + \boldsymbol{A}^\dagger\beta(\boldsymbol{A}) = 0\,. \tag{A.24}$$

The CKM matrix $\boldsymbol{V}$ is given by

$$\boldsymbol{V}(t) \equiv \boldsymbol{U}_\mathrm{L}(t)\,\boldsymbol{D}_\mathrm{L}^\dagger(t)\ . \tag{A.25}$$

The general quark Yukawa matrices can be diagonalized by using two unitary matrices:

$$\boldsymbol{\mathcal{Y}}_u = \boldsymbol{U}_\mathrm{L}^\dagger \mathscr{Y}_u \boldsymbol{U}_\mathrm{R}\,, \qquad \boldsymbol{\mathcal{Y}}_d = \boldsymbol{D}_\mathrm{L}^\dagger \mathscr{Y}_d \boldsymbol{D}_\mathrm{R}\,. \tag{A.26}$$

Upon inserting these relations into Eq. (2.37) and (2.38), we can extract the β-functions for the diagonal matrices $\mathscr{Y}_{u,d}$ (following the procedure in [24]):

$$\begin{aligned}\beta\big(\boldsymbol{\mathcal{Y}}_u\big) &= \frac{\mathrm{d}\boldsymbol{\mathcal{Y}}_u}{\mathrm{d}t} = \frac{\mathrm{d}}{\mathrm{d}t}\left[\boldsymbol{U}_{\mathrm{L}}^{\dagger}\mathscr{Y}_u\boldsymbol{U}_{\mathrm{R}}\right] = \\ &= \frac{1}{16\pi^2}\Bigg\{ - A^{\mathrm{u}}\boldsymbol{U}_{\mathrm{L}}^{\dagger}\mathscr{Y}_u\boldsymbol{U}_{\mathrm{R}} + \frac{3}{2}\boldsymbol{U}_{\mathrm{L}}^{\dagger}\mathscr{Y}_u\mathscr{Y}_u\mathscr{Y}_u\boldsymbol{U}_{\mathrm{R}} - \frac{3}{2}\boldsymbol{D}_{\mathrm{L}}^{\dagger}\mathscr{Y}_d\mathscr{Y}_d\boldsymbol{D}_{\mathrm{L}}\boldsymbol{U}_{\mathrm{L}}^{\dagger}\mathscr{Y}_u\boldsymbol{U}_{\mathrm{R}} + \\ &\quad + N_c\mathrm{Tr}\left[\boldsymbol{U}_{\mathrm{L}}^{\dagger}\mathscr{Y}_u\mathscr{Y}_u\boldsymbol{U}_{\mathrm{L}} + \boldsymbol{D}_{\mathrm{L}}^{\dagger}\mathscr{Y}_d\mathscr{Y}_d\boldsymbol{D}_{\mathrm{L}}\right]\boldsymbol{U}_{\mathrm{L}}^{\dagger}\mathscr{Y}_u\boldsymbol{U}_{\mathrm{R}}\Bigg\} . \end{aligned} \tag{A.27}$$

The left-hand side of the above equation can be written as:

$$\frac{\mathrm{d}}{\mathrm{d}t}\left[\boldsymbol{U}_{\mathrm{L}}^{\dagger}\mathscr{Y}_u\boldsymbol{U}_{\mathrm{R}}\right] = \frac{\mathrm{d}\boldsymbol{U}_{\mathrm{L}}^{\dagger}}{\mathrm{d}t}\mathscr{Y}_u\boldsymbol{U}_{\mathrm{R}} + \boldsymbol{U}_{\mathrm{L}}^{\dagger}\frac{\mathrm{d}\mathscr{Y}_u}{\mathrm{d}t}\boldsymbol{U}_{\mathrm{R}} + \boldsymbol{U}_{\mathrm{L}}^{\dagger}\mathscr{Y}_u\frac{\mathrm{d}\boldsymbol{U}_{\mathrm{R}}}{\mathrm{d}t} . \tag{A.28}$$

Now, we can multiply Eq. (A.28) from the left with $\boldsymbol{U}_{\mathrm{L}}$ and from the right with $\boldsymbol{U}_{\mathrm{R}}^{\dagger}$. This yields

$$\boldsymbol{U}_{\mathrm{L}}\frac{\mathrm{d}}{\mathrm{d}t}\left[\boldsymbol{U}_{\mathrm{L}}^{\dagger}\mathscr{Y}_u\boldsymbol{U}_{\mathrm{R}}\right]\boldsymbol{U}_{\mathrm{R}}^{\dagger} = \boldsymbol{U}_{\mathrm{L}}\frac{\mathrm{d}\boldsymbol{U}_{\mathrm{L}}^{\dagger}}{\mathrm{d}t}\mathscr{Y}_u + \frac{\mathrm{d}\mathscr{Y}_u}{\mathrm{d}t} + \mathscr{Y}_u\frac{\mathrm{d}\boldsymbol{U}_{\mathrm{R}}}{\mathrm{d}t}\boldsymbol{U}_{\mathrm{R}}^{\dagger} . \tag{A.29}$$

Adding the Hermitian conjugate of this equation yields

$$\begin{aligned}\boldsymbol{U}_{\mathrm{L}}\frac{\mathrm{d}}{\mathrm{d}t}\left[\boldsymbol{U}_{\mathrm{L}}^{\dagger}\mathscr{Y}_u\boldsymbol{U}_{\mathrm{R}}\right]\boldsymbol{U}_{\mathrm{R}}^{\dagger} + \mathrm{h.c.} &= \boldsymbol{U}_{\mathrm{L}}\frac{\mathrm{d}\boldsymbol{U}_{\mathrm{L}}^{\dagger}}{\mathrm{d}t}\mathscr{Y}_u + \frac{\mathrm{d}\mathscr{Y}_u}{\mathrm{d}t} + \mathscr{Y}_u\frac{\mathrm{d}\boldsymbol{U}_{\mathrm{R}}}{\mathrm{d}t}\boldsymbol{U}_{\mathrm{R}}^{\dagger} + \\ &\quad + \mathscr{Y}_u\frac{\mathrm{d}\boldsymbol{U}_{\mathrm{L}}}{\mathrm{d}t}\boldsymbol{U}_{\mathrm{L}}^{\dagger} + \frac{\mathrm{d}\mathscr{Y}_u}{\mathrm{d}t} + \boldsymbol{U}_{\mathrm{R}}\frac{\mathrm{d}\boldsymbol{U}_{\mathrm{R}}^{\dagger}}{\mathrm{d}t}\mathscr{Y}_u . \end{aligned} \tag{A.30}$$

Performing the same algebraic operations on the r.h.s of $\beta\big(\boldsymbol{\mathcal{Y}}_u\big)$, we get

$$\begin{aligned}\boldsymbol{U}_{\mathrm{L}}\beta\big(\boldsymbol{\mathcal{Y}}_u\big)\boldsymbol{U}_{\mathrm{R}}^{\dagger} + \mathrm{h.c.} &= \boldsymbol{U}_{\mathrm{L}}\frac{\mathrm{d}}{\mathrm{d}t}\left[\boldsymbol{U}_{\mathrm{L}}^{\dagger}\mathscr{Y}_u\boldsymbol{U}_{\mathrm{R}}\right]\boldsymbol{U}_{\mathrm{R}}^{\dagger} + \mathrm{h.c.} = \\ &= \frac{1}{16\pi^2}\Bigg\{ - 2A^{\mathrm{u}}\mathscr{Y}_u + 3\mathscr{Y}_u\mathscr{Y}_u\mathscr{Y}_u - \frac{3}{2}\boldsymbol{U}_{\mathrm{L}}\boldsymbol{D}_{\mathrm{L}}^{\dagger}\mathscr{Y}_d\mathscr{Y}_d\boldsymbol{D}_{\mathrm{L}}\boldsymbol{U}_{\mathrm{L}}^{\dagger}\mathscr{Y}_u - \\ &\quad - \frac{3}{2}\mathscr{Y}_u\boldsymbol{U}_{\mathrm{L}}\boldsymbol{D}_{\mathrm{L}}^{\dagger}\mathscr{Y}_d\mathscr{Y}_d\boldsymbol{D}_{\mathrm{L}}\boldsymbol{U}_{\mathrm{L}}^{\dagger} + 2N_c\mathrm{Tr}\left[\mathscr{Y}_u\mathscr{Y}_u + \mathscr{Y}_d\mathscr{Y}_d\right]\mathscr{Y}_u\Bigg\} , \end{aligned} \tag{A.31}$$

where we also used the invariance of the trace under cyclic permutations. We can now write

$$\begin{aligned}\boldsymbol{U}_{\mathrm{L}}\frac{\mathrm{d}\boldsymbol{U}_{\mathrm{L}}^{\dagger}}{\mathrm{d}t}\mathscr{Y}_u + \mathscr{Y}_u\frac{\mathrm{d}\boldsymbol{U}_{\mathrm{L}}}{\mathrm{d}t}\boldsymbol{U}_{\mathrm{L}}^{\dagger} + 2\frac{\mathrm{d}\mathscr{Y}_u}{\mathrm{d}t} + \boldsymbol{U}_{\mathrm{R}}\frac{\mathrm{d}\boldsymbol{U}_{\mathrm{R}}^{\dagger}}{\mathrm{d}t}\mathscr{Y}_u + \mathscr{Y}_u\frac{\mathrm{d}\boldsymbol{U}_{\mathrm{R}}}{\mathrm{d}t}\boldsymbol{U}_{\mathrm{R}}^{\dagger} &= \\ = \frac{1}{16\pi^2}\Bigg\{ - 2A^{\mathrm{u}}\mathscr{Y}_u + 3\mathscr{Y}_u\mathscr{Y}_u\mathscr{Y}_u - \frac{3}{2}\boldsymbol{U}_{\mathrm{L}}\boldsymbol{D}_{\mathrm{L}}^{\dagger}\mathscr{Y}_d\mathscr{Y}_d\boldsymbol{D}_{\mathrm{L}}\boldsymbol{U}_{\mathrm{L}}^{\dagger}\mathscr{Y}_u - \\ - \frac{3}{2}\mathscr{Y}_u\boldsymbol{U}_{\mathrm{L}}\boldsymbol{D}_{\mathrm{L}}^{\dagger}\mathscr{Y}_d\mathscr{Y}_d\boldsymbol{D}_{\mathrm{L}}\boldsymbol{U}_{\mathrm{L}}^{\dagger} + 2N_c\mathrm{Tr}\left[\mathscr{Y}_u\mathscr{Y}_u + \mathscr{Y}_d\mathscr{Y}_d\right]\mathscr{Y}_u\Bigg\} . \end{aligned} \tag{A.32}$$

As a next step, we want to study the equations for the diagonal elements of the above matrix differential equation. In order to do so, we rewrite the above equation as

$$\begin{aligned}
&\boldsymbol{U}_{\mathrm{L}}\frac{\mathrm{d}\boldsymbol{U}_{\mathrm{L}}^{\dagger}}{\mathrm{d}t}\mathscr{Y}_u+\mathscr{Y}_u\frac{\mathrm{d}\boldsymbol{U}_{\mathrm{L}}}{\mathrm{d}t}\boldsymbol{U}_{\mathrm{L}}^{\dagger}+2\frac{\mathrm{d}\mathscr{Y}_u}{\mathrm{d}t}+\boldsymbol{U}_{\mathrm{R}}\frac{\mathrm{d}\boldsymbol{U}_{\mathrm{R}}^{\dagger}}{\mathrm{d}t}\mathscr{Y}_u+\mathscr{Y}_u\frac{\mathrm{d}\boldsymbol{U}_{\mathrm{R}}}{\mathrm{d}t}\boldsymbol{U}_{\mathrm{R}}^{\dagger}=\\
&=\boldsymbol{U}_{\mathrm{L}}\frac{\mathrm{d}\boldsymbol{U}_{\mathrm{L}}^{\dagger}}{\mathrm{d}t}\mathscr{Y}_u+\frac{\mathrm{d}\boldsymbol{U}_{\mathrm{L}}}{\mathrm{d}t}\boldsymbol{U}_{\mathrm{L}}^{\dagger}\mathscr{Y}_u+2\frac{\mathrm{d}\mathscr{Y}_u}{\mathrm{d}t}+\boldsymbol{U}_{\mathrm{R}}\frac{\mathrm{d}\boldsymbol{U}_{\mathrm{R}}^{\dagger}}{\mathrm{d}t}\mathscr{Y}_u+\frac{\mathrm{d}\boldsymbol{U}_{\mathrm{R}}}{\mathrm{d}t}\boldsymbol{U}_{\mathrm{R}}^{\dagger}\mathscr{Y}_u-\\
&-\left[\frac{\mathrm{d}\boldsymbol{U}_{\mathrm{L}}}{\mathrm{d}t}\boldsymbol{U}_{\mathrm{L}}^{\dagger},\mathscr{Y}_u\right]-\left[\frac{\mathrm{d}\boldsymbol{U}_{\mathrm{R}}}{\mathrm{d}t}\boldsymbol{U}_{\mathrm{R}}^{\dagger},\mathscr{Y}_u\right]\\
&=2\frac{\mathrm{d}\mathscr{Y}_u}{\mathrm{d}t}-\left[\frac{\mathrm{d}\boldsymbol{U}_{\mathrm{L}}}{\mathrm{d}t}\boldsymbol{U}_{\mathrm{L}}^{\dagger},\mathscr{Y}_u\right]-\left[\frac{\mathrm{d}\boldsymbol{U}_{\mathrm{R}}}{\mathrm{d}t}\boldsymbol{U}_{\mathrm{R}}^{\dagger},\mathscr{Y}_u\right] \qquad \text{(A.33)}
\end{aligned}$$

and

$$\begin{aligned}
&\frac{1}{16\pi^2}\Bigg\{-2A^{\mathrm{u}}\mathscr{Y}_u+3\mathscr{Y}_u\mathscr{Y}_u\mathscr{Y}_u-\frac{3}{2}\boldsymbol{U}_{\mathrm{L}}\boldsymbol{D}_{\mathrm{L}}^{\dagger}\mathscr{Y}_d\mathscr{Y}_d\boldsymbol{D}_{\mathrm{L}}\boldsymbol{U}_{\mathrm{L}}^{\dagger}\mathscr{Y}_u-\\
&\qquad-\frac{3}{2}\mathscr{Y}_u\boldsymbol{U}_{\mathrm{L}}\boldsymbol{D}_{\mathrm{L}}^{\dagger}\mathscr{Y}_d\mathscr{Y}_d\boldsymbol{D}_{\mathrm{L}}\boldsymbol{U}_{\mathrm{L}}^{\dagger}+2N_c\mathrm{Tr}\left[\mathscr{Y}_u\mathscr{Y}_u+\mathscr{Y}_d\mathscr{Y}_d\right]\mathscr{Y}_u\Bigg\}=\\
&=\frac{1}{16\pi^2}\Bigg\{-2A^{\mathrm{u}}\mathscr{Y}_u+3\mathscr{Y}_u\mathscr{Y}_u\mathscr{Y}_u-3\mathscr{Y}_d\mathscr{Y}_d\mathscr{Y}_u+2N_c\mathrm{Tr}\left[\mathscr{Y}_u\mathscr{Y}_u+\mathscr{Y}_d\mathscr{Y}_d\right]\mathscr{Y}_u+\\
&\qquad+\frac{3}{2}\left\{\boldsymbol{V}\left[\boldsymbol{V}^{\dagger},\mathscr{Y}_d\mathscr{Y}_d\right],\mathscr{Y}_u\right\}\Bigg\}. \qquad \text{(A.34)}
\end{aligned}$$

Next we note that the commutator of a diagonal matrix $\boldsymbol{\Lambda}=\mathrm{diag}(\lambda_1,\lambda_2,\lambda_3,\ldots)$ and an arbitrary matrix $\boldsymbol{M}$ has vanishing diagonal entries:

$$S_{ij}=\sum_k\Lambda_{ik}M_{kj}=\sum_k\lambda_i\delta_{ik}M_{kj}=\lambda_iM_{ij}\ , \qquad \text{(A.35)}$$

$$\tilde{S}_{ij}=\sum_k M_{ik}\Lambda_{kj}=\sum_k M_{ik}\delta_{kj}\lambda_j=\lambda_jM_{ij}\ , \qquad \text{(A.36)}$$

$$\begin{aligned}
&\Rightarrow\ S_{ii}=\tilde{S}_{ii}\ ,\\
&\Rightarrow\ [\boldsymbol{\Lambda},\boldsymbol{M}]_{ii}=S_{ii}-\tilde{S}_{ii}=0\ , \qquad \text{(A.37)}\\
&\Rightarrow\ \{\boldsymbol{\Lambda},\boldsymbol{M}\}_{ii}=S_{ii}+\tilde{S}_{ii}=2S_{ii}=2\tilde{S}_{ii}\ . \qquad \text{(A.38)}
\end{aligned}$$

This allows us to write down the one-loop β-functions of the diagonal elements of the Yukawa matrix $\mathscr{Y}_u$ from Eq. (A.33) and (A.34):

$$\beta\left(y_i^u\right)=\frac{y_i^u}{16\pi^2}\left\{-A^{\mathrm{u}}+\frac{3}{2}\left(y_i^u\right)^2-\frac{3}{2}\sum_j\left(y_j^d\right)^2|V_{ij}|^2+N_c\mathrm{Tr}\left[\mathscr{Y}_u\mathscr{Y}_u+\mathscr{Y}_d\mathscr{Y}_d\right]\right\}\ , \qquad \text{(A.39)}$$

which is the same result as in [25]. An analogous calculation for the down-type Yukawa matrix yields [25]:

$$\beta\left(y_i^d\right) = \frac{y_i^d}{16\pi^2}\left\{-A^{\mathrm{d}} + \frac{3}{2}\left(y_i^d\right)^2 - \frac{3}{2}\sum_j\left(y_j^u\right)^2|V_{ji}|^2 + N_c\mathrm{Tr}\left[\mathscr{Y}_u\mathscr{Y}_u + \mathscr{Y}_d\mathscr{Y}_d\right]\right\} . \quad \text{(A.40)}$$

A.3. CKM Matrix Elements

In order to calculate the one-loop β-functions of the quadratic matrix elements $|V_{ij}|^2 = V_{ij}V_{ij}^*$, we first note that

$$\frac{\mathrm{d}\,|V_{ij}|^2}{\mathrm{d}t} = V_{ij}^*\frac{\mathrm{d}V_{ij}}{\mathrm{d}t} + V_{ij}\frac{\mathrm{d}V_{ij}^*}{\mathrm{d}t} = V_{ij}^*\frac{\mathrm{d}V_{ij}}{\mathrm{d}t} + \left(V_{ij}^*\frac{\mathrm{d}V_{ij}}{\mathrm{d}t}\right)^* = 2\Re\left\{V_{ij}^*\frac{\mathrm{d}V_{ij}}{\mathrm{d}t}\right\} . \quad \text{(A.41)}$$

Furthermore, derivation of $\boldsymbol{V}$ with respect to the RG time t yields

$$\begin{aligned}
\frac{\mathrm{d}\boldsymbol{V}}{\mathrm{d}t} &= \boldsymbol{U}_{\mathrm{L}}\frac{\mathrm{d}\boldsymbol{D}_{\mathrm{L}}^\dagger}{\mathrm{d}t} + \frac{\mathrm{d}\boldsymbol{U}_{\mathrm{L}}}{\mathrm{d}t}\boldsymbol{D}_{\mathrm{L}}^\dagger \\
&= \boldsymbol{U}_{\mathrm{L}}\boldsymbol{D}_{\mathrm{L}}^\dagger\boldsymbol{D}_{\mathrm{L}}\frac{\mathrm{d}\boldsymbol{D}_{\mathrm{L}}^\dagger}{\mathrm{d}t} + \boldsymbol{U}_{\mathrm{L}}\boldsymbol{U}_{\mathrm{L}}^\dagger\frac{\mathrm{d}\boldsymbol{U}_{\mathrm{L}}}{\mathrm{d}t}\boldsymbol{D}_{\mathrm{L}}^\dagger \\
&= \boldsymbol{U}_{\mathrm{L}}\boldsymbol{D}_{\mathrm{L}}^\dagger\boldsymbol{D}_{\mathrm{L}}\frac{\mathrm{d}\boldsymbol{D}_{\mathrm{L}}^\dagger}{\mathrm{d}t} + \boldsymbol{U}_{\mathrm{L}}\left(\frac{\mathrm{d}\boldsymbol{U}_{\mathrm{L}}^\dagger}{\mathrm{d}t}\boldsymbol{U}_{\mathrm{L}}\right)^\dagger\boldsymbol{D}_{\mathrm{L}}^\dagger \\
&= \boldsymbol{U}_{\mathrm{L}}\boldsymbol{D}_{\mathrm{L}}^\dagger\boldsymbol{D}_{\mathrm{L}}\frac{\mathrm{d}\boldsymbol{D}_{\mathrm{L}}^\dagger}{\mathrm{d}t} - \boldsymbol{U}_{\mathrm{L}}\left(\boldsymbol{U}_{\mathrm{L}}^\dagger\frac{\mathrm{d}\boldsymbol{U}_{\mathrm{L}}}{\mathrm{d}t}\right)^\dagger\boldsymbol{D}_{\mathrm{L}}^\dagger \\
&= \boldsymbol{U}_{\mathrm{L}}\boldsymbol{D}_{\mathrm{L}}^\dagger\boldsymbol{D}_{\mathrm{L}}\frac{\mathrm{d}\boldsymbol{D}_{\mathrm{L}}^\dagger}{\mathrm{d}t} - \boldsymbol{U}_{\mathrm{L}}\frac{\mathrm{d}\boldsymbol{U}_{\mathrm{L}}^\dagger}{\mathrm{d}t}\boldsymbol{U}_{\mathrm{L}}\boldsymbol{D}_{\mathrm{L}}^\dagger \\
&= \boldsymbol{V}\boldsymbol{D}_{\mathrm{L}}\frac{\mathrm{d}\boldsymbol{D}_{\mathrm{L}}^\dagger}{\mathrm{d}t} - \boldsymbol{U}_{\mathrm{L}}\frac{\mathrm{d}\boldsymbol{U}_{\mathrm{L}}^\dagger}{\mathrm{d}t}\boldsymbol{V} \qquad \text{(A.42)} \\
\Rightarrow \frac{\mathrm{d}V_{ij}}{\mathrm{d}t} &= \sum_k\left[V_{ik}\left(\boldsymbol{D}_{\mathrm{L}}\frac{\mathrm{d}\boldsymbol{D}_{\mathrm{L}}^\dagger}{\mathrm{d}t}\right)_{kj} - \left(\boldsymbol{U}_{\mathrm{L}}\frac{\mathrm{d}\boldsymbol{U}_{\mathrm{L}}^\dagger}{\mathrm{d}t}\right)_{ik}V_{kj}\right] , \qquad \text{(A.43)}
\end{aligned}$$

where we used Eq. (A.19) to (A.22). Multiplying with the complex conjugate matrix element V_{ij}^* yields

$$\begin{aligned}
V_{ij}^*\frac{\mathrm{d}V_{ij}}{\mathrm{d}t} &= |V_{ij}|^2\left(\boldsymbol{D}_{\mathrm{L}}\frac{\mathrm{d}\boldsymbol{D}_{\mathrm{L}}^\dagger}{\mathrm{d}t}\right)_{jj} - |V_{ij}|^2\left(\boldsymbol{U}_{\mathrm{L}}\frac{\mathrm{d}\boldsymbol{U}_{\mathrm{L}}^\dagger}{\mathrm{d}t}\right)_{ii} + \\
&\quad + \sum_{k\neq j}V_{ij}^*V_{ik}\left(\boldsymbol{D}_{\mathrm{L}}\frac{\mathrm{d}\boldsymbol{D}_{\mathrm{L}}^\dagger}{\mathrm{d}t}\right)_{kj} - \sum_{k\neq i}\left(\boldsymbol{U}_{\mathrm{L}}\frac{\mathrm{d}\boldsymbol{U}_{\mathrm{L}}^\dagger}{\mathrm{d}t}\right)_{ik}V_{ij}^*V_{kj} . \qquad \text{(A.44)}
\end{aligned}$$

As a next step, we need to calculate the expressions for the non-diagonal elements of $\boldsymbol{U}_{\mathrm{L}}\frac{\mathrm{d}\boldsymbol{U}_{\mathrm{L}}^\dagger}{\mathrm{d}t}$ and $\boldsymbol{D}_{\mathrm{L}}\frac{\mathrm{d}\boldsymbol{D}_{\mathrm{L}}^\dagger}{\mathrm{d}t}$. In order to do so, we use

$$\frac{\mathrm{d}\boldsymbol{\mathcal{Z}}_u}{\mathrm{d}t} = \frac{\mathrm{d}\boldsymbol{U}_{\mathrm{L}}^\dagger}{\mathrm{d}t}\mathscr{Z}_u\boldsymbol{U}_{\mathrm{L}} + \boldsymbol{U}_{\mathrm{L}}^\dagger\frac{\mathrm{d}\mathscr{Z}_u}{\mathrm{d}t}\boldsymbol{U}_{\mathrm{L}} + \boldsymbol{U}_{\mathrm{L}}^\dagger\mathscr{Z}_u\frac{\mathrm{d}\boldsymbol{U}_{\mathrm{L}}}{\mathrm{d}t} . \quad \text{(A.45)}$$

Multiplying this with $\boldsymbol{U}_{\mathrm{L}}$ from the right and $\boldsymbol{U}_{\mathrm{L}}^{\dagger}$ from the left, we obtain:

$$\boldsymbol{U}_{\mathrm{L}}\frac{\mathrm{d}\boldsymbol{\mathcal{Z}}_u}{\mathrm{d}t}\boldsymbol{U}_{\mathrm{L}}^{\dagger}-\frac{\mathrm{d}\mathscr{Z}_u}{\mathrm{d}t}=\boldsymbol{U}_{\mathrm{L}}\frac{\mathrm{d}\boldsymbol{U}_{\mathrm{L}}^{\dagger}}{\mathrm{d}t}\mathscr{Z}_u+\mathscr{Z}_u\frac{\mathrm{d}\boldsymbol{U}_{\mathrm{L}}}{\mathrm{d}t}\boldsymbol{U}_{\mathrm{L}}^{\dagger}\,. \tag{A.46}$$

Using Eq. (A.19) and (A.20), this can be written as:

$$\boldsymbol{U}_{\mathrm{L}}\frac{\mathrm{d}\boldsymbol{\mathcal{Z}}_u}{\mathrm{d}t}\boldsymbol{U}_{\mathrm{L}}^{\dagger}-\frac{\mathrm{d}\mathscr{Z}_u}{\mathrm{d}t}=\left[\boldsymbol{U}_{\mathrm{L}}\frac{\mathrm{d}\boldsymbol{U}_{\mathrm{L}}^{\dagger}}{\mathrm{d}t},\mathscr{Z}_u\right]\,. \tag{A.47}$$

We are interested in the off-diagonal elements of the above equation. The off-diagonal elements of a commutator of a diagonal matrix $\boldsymbol{\Lambda}=\mathrm{diag}(\lambda_1,\lambda_2,\lambda_3,\ldots)$ and an arbitrary matrix $\boldsymbol{M}$ are given by $(i\neq j)$:

$$\begin{aligned}\left[\boldsymbol{M},\boldsymbol{\Lambda}\right]_{ij}&=\sum_k\left(M_{ik}\Lambda_{kj}-\Lambda_{ik}M_{kj}\right)\\&=\sum_k\left(M_{ik}\delta_{kj}\lambda_j-\lambda_i\delta_{ik}M_{kj}\right)\\&=\lambda_jM_{ij}-\lambda_iM_{ij}\\&=\left(\lambda_j-\lambda_i\right)M_{ij}\,.\end{aligned} \tag{A.48}$$

Hence:

$$\begin{aligned}&\left[\boldsymbol{U}_{\mathrm{L}}\frac{\mathrm{d}\boldsymbol{U}_{\mathrm{L}}^{\dagger}}{\mathrm{d}t},\mathscr{Z}_u\right]_{ij}=-\left[\left(y_i^u\right)^2-\left(y_j^u\right)^2\right]\left(\boldsymbol{U}_{\mathrm{L}}\frac{\mathrm{d}\boldsymbol{U}_{\mathrm{L}}^{\dagger}}{\mathrm{d}t}\right)_{ij}=\left(\boldsymbol{U}_{\mathrm{L}}\frac{\mathrm{d}\boldsymbol{\mathcal{Z}}_u}{\mathrm{d}t}\boldsymbol{U}_{\mathrm{L}}^{\dagger}\right)_{ij}\\\Rightarrow\quad&\left(\boldsymbol{U}_{\mathrm{L}}\frac{\mathrm{d}\boldsymbol{U}_{\mathrm{L}}^{\dagger}}{\mathrm{d}t}\right)_{ij}=\frac{-1}{\left(y_i^u\right)^2-\left(y_j^u\right)^2}\left(\boldsymbol{U}_{\mathrm{L}}\frac{\mathrm{d}\boldsymbol{\mathcal{Z}}_u}{\mathrm{d}t}\boldsymbol{U}_{\mathrm{L}}^{\dagger}\right)_{ij}\,,\qquad i\neq j\,,\end{aligned} \tag{A.49}$$

where we used that $\beta\left(\mathscr{Z}_u\right)$ has vanishing off-diagonal elements. After evaluating $\left(\boldsymbol{U}_{\mathrm{L}}\frac{\mathrm{d}\boldsymbol{\mathcal{Z}}_u}{\mathrm{d}t}\boldsymbol{U}_{\mathrm{L}}^{\dagger}\right)_{ij}$ using Eq. (2.37) and (2.38) and performing the same calculation for the down type matrices, one obtains the relations [25]:

$$\left(\boldsymbol{U}_{\mathrm{L}}\frac{\mathrm{d}\boldsymbol{U}_{\mathrm{L}}^{\dagger}}{\mathrm{d}t}\right)_{ij}=\frac{3}{32\pi^2}\frac{\left(y_i^u\right)^2+\left(y_j^u\right)^2}{\left(y_i^u\right)^2-\left(y_j^u\right)^2}\left(\boldsymbol{V}\mathscr{Y}_d\mathscr{Y}_d\boldsymbol{V}^{\dagger}\right)_{ij}\,,\qquad i\neq j\,, \tag{A.50}$$

$$\left(\boldsymbol{D}_{\mathrm{L}}\frac{\mathrm{d}\boldsymbol{D}_{\mathrm{L}}^{\dagger}}{\mathrm{d}t}\right)_{ij}=\frac{3}{32\pi^2}\frac{\left(y_i^d\right)^2+\left(y_j^d\right)^2}{\left(y_i^d\right)^2-\left(y_j^d\right)^2}\left(\boldsymbol{V}^{\dagger}\mathscr{Y}_u\mathscr{Y}_u\boldsymbol{V}\right)_{ij}\,,\qquad i\neq j\,, \tag{A.51}$$

for the non-diagonal elements. This yields

$$\begin{aligned}V_{ij}^*\frac{\mathrm{d}V_{ij}}{\mathrm{d}t}=&\left|V_{ij}\right|^2\left(\boldsymbol{D}_{\mathrm{L}}\frac{\mathrm{d}\boldsymbol{D}_{\mathrm{L}}^{\dagger}}{\mathrm{d}t}\right)_{jj}-\left|V_{ij}\right|^2\left(\boldsymbol{U}_{\mathrm{L}}\frac{\mathrm{d}\boldsymbol{U}_{\mathrm{L}}^{\dagger}}{\mathrm{d}t}\right)_{ii}+\\&+\frac{3}{32\pi^2}\sum_{k\neq j}V_{ij}^*V_{ik}\frac{\left(y_k^d\right)^2+\left(y_j^d\right)^2}{\left(y_k^d\right)^2-\left(y_j^d\right)^2}\left(\boldsymbol{V}^{\dagger}\mathscr{Y}_u\mathscr{Y}_u\boldsymbol{V}\right)_{kj}-\\&-\frac{3}{32\pi^2}\sum_{k\neq i}\frac{\left(y_i^u\right)^2+\left(y_k^u\right)^2}{\left(y_i^u\right)^2-\left(y_k^u\right)^2}\left(\boldsymbol{V}\mathscr{Y}_d\mathscr{Y}_d\boldsymbol{V}^{\dagger}\right)_{ik}V_{ij}^*V_{kj}\,.\end{aligned} \tag{A.52}$$

The difference of squared Yukawa couplings appears in the denominators of Eq. (A.50) and (A.51) because of the commutator in Eq. (A.47). We can write Eq. (A.47) using a commutator because of Eq. (A.19) to (A.22), which in turn are due to the unitarity of $\boldsymbol{U}_\mathrm{L}$ and $\boldsymbol{D}_\mathrm{L}$. The poles in the β-functions of the CKM matrix elements are therefore a consequence of unitarity.

Next, we use

$$\begin{aligned}
\left(\boldsymbol{V}^\dagger \mathscr{Y}_u \mathscr{Y}_u \boldsymbol{V}\right)_{kj} &= \sum_{l,m,n} V_{kl}^\dagger \left(\mathscr{Y}_u\right)_{lm} \left(\mathscr{Y}_u\right)_{mn} V_{nj} \\
&= \sum_{l,m,n} V_{kl}^\dagger \, \delta_{lm} \, y_m^u \, y_m^u \, \delta_{mn} \, V_{nj} \\
&= \sum_m \left(y_m^u\right)^2 \, V_{mj} V_{mk}^* \,, \qquad \text{(A.53)} \\
\left(\boldsymbol{V} \mathscr{Y}_d \mathscr{Y}_d \boldsymbol{V}^\dagger\right)_{ik} &= \sum_{l,m,n} V_{il} \left(\mathscr{Y}_d\right)_{lm} \left(\mathscr{Y}_d\right)_{mn} V_{nk}^\dagger \\
&= \sum_{l,m,n} V_{il} \, \delta_{lm} \, y_m^d \, y_m^d \, \delta_{mn} \, V_{nk}^\dagger \\
&= \sum_m \left(y_m^d\right)^2 \, V_{im} V_{km}^* \,. \qquad \text{(A.54)}
\end{aligned}$$

Hence,

$$
\begin{aligned}
V_{ij}^{*}\frac{\mathrm{d}V_{ij}}{\mathrm{d}t} &= |V_{ij}|^2\left(\boldsymbol{D}_{\mathrm{L}}\frac{\mathrm{d}\boldsymbol{D}_{\mathrm{L}}^{\dagger}}{\mathrm{d}t}\right)_{jj} - |V_{ij}|^2\left(\boldsymbol{U}_{\mathrm{L}}\frac{\mathrm{d}\boldsymbol{U}_{\mathrm{L}}^{\dagger}}{\mathrm{d}t}\right)_{ii} + \\
&+ \frac{3}{32\pi^2}\sum_{k\neq j}\frac{\left(y_k^d\right)^2+\left(y_j^d\right)^2}{\left(y_k^d\right)^2-\left(y_j^d\right)^2}\sum_m \left(y_m^u\right)^2 V_{mj}V_{mk}^{*}V_{ij}^{*}V_{ik} - \\
&- \frac{3}{32\pi^2}\sum_{k\neq i}\frac{\left(y_i^u\right)^2+\left(y_k^u\right)^2}{\left(y_i^u\right)^2-\left(y_k^u\right)^2}\sum_m \left(y_m^d\right)^2 V_{im}V_{km}^{*}V_{ij}^{*}V_{kj} \qquad \text{(A.55)} \\
&= |V_{ij}|^2\left(\boldsymbol{D}_{\mathrm{L}}\frac{\mathrm{d}\boldsymbol{D}_{\mathrm{L}}^{\dagger}}{\mathrm{d}t}\right)_{jj} - |V_{ij}|^2\left(\boldsymbol{U}_{\mathrm{L}}\frac{\mathrm{d}\boldsymbol{U}_{\mathrm{L}}^{\dagger}}{\mathrm{d}t}\right)_{ii} + \\
&+ \frac{3}{32\pi^2}\sum_{k\neq j}\frac{\left(y_k^d\right)^2+\left(y_j^d\right)^2}{\left(y_k^d\right)^2-\left(y_j^d\right)^2}\left(\left(y_i^u\right)^2|V_{ij}|^2|V_{ik}|^2 + \sum_{m\neq i}\left(y_m^u\right)^2 V_{mj}V_{mk}^{*}V_{ij}^{*}V_{ik}\right) - \\
&- \frac{3}{32\pi^2}\sum_{k\neq i}\frac{\left(y_i^u\right)^2+\left(y_k^u\right)^2}{\left(y_i^u\right)^2-\left(y_k^u\right)^2}\left(\left(y_j^d\right)^2|V_{ij}|^2|V_{kj}|^2 + \sum_{m\neq j}\left(y_m^d\right)^2 V_{im}V_{km}^{*}V_{ij}^{*}V_{kj}\right) \\
&= |V_{ij}|^2\left(\boldsymbol{D}_{\mathrm{L}}\frac{\mathrm{d}\boldsymbol{D}_{\mathrm{L}}^{\dagger}}{\mathrm{d}t}\right)_{jj} - |V_{ij}|^2\left(\boldsymbol{U}_{\mathrm{L}}\frac{\mathrm{d}\boldsymbol{U}_{\mathrm{L}}^{\dagger}}{\mathrm{d}t}\right)_{ii} + \\
&+ \frac{3\left(y_j^d\right)^2}{16\pi^2}\sum_{k\neq j}\frac{1}{\left(y_k^d\right)^2-\left(y_j^d\right)^2}\left(\left(y_i^u\right)^2|V_{ij}|^2|V_{ik}|^2 + \sum_{m\neq i}\left(y_m^u\right)^2 V_{mj}V_{mk}^{*}V_{ij}^{*}V_{ik}\right) - \\
&- \frac{3\left(y_i^u\right)^2}{16\pi^2}\sum_{k\neq i}\frac{1}{\left(y_i^u\right)^2-\left(y_k^u\right)^2}\left(\left(y_j^d\right)^2|V_{ij}|^2|V_{kj}|^2 + \sum_{m\neq j}\left(y_m^d\right)^2 V_{im}V_{km}^{*}V_{ij}^{*}V_{kj}\right) + \\
&+ \frac{3|V_{ij}|^2}{32\pi^2}\left\{\left(y_i^u\right)^2+\left(y_j^d\right)^2 - \sum_m\left(y_m^u\right)^2|V_{mj}|^2 - \sum_m\left(y_m^d\right)^2|V_{im}|^2\right\} + \\
&+ \frac{3}{32\pi^2}\sum_k\left(\sum_{m\neq j}\left(y_m^d\right)^2 V_{im}V_{km}^{*}V_{ij}^{*}V_{kj} + \sum_{m\neq i}\left(y_m^u\right)^2 V_{mj}V_{mk}^{*}V_{ij}^{*}V_{ik}\right) . \qquad \text{(A.56)}
\end{aligned}
$$

The last line vanishes, as

$$
\begin{aligned}
&\sum_k\left(\sum_{m\neq j}\left(y_m^d\right)^2 V_{im}V_{km}^{*}V_{ij}^{*}V_{kj} + \sum_{m\neq i}\left(y_m^u\right)^2 V_{mj}V_{mk}^{*}V_{ij}^{*}V_{ik}\right) = \\
&= \sum_{m\neq j}\sum_k\left(y_m^d\right)^2 V_{im}V_{km}^{*}V_{ij}^{*}V_{kj} + \sum_{m\neq i}\sum_k\left(y_m^u\right)^2 V_{mj}V_{mk}^{*}V_{ij}^{*}V_{ik} \\
&= \sum_{m\neq j}\left(y_m^d\right)^2 V_{im}V_{ij}^{*}\left(\boldsymbol{V}^{\dagger}\boldsymbol{V}\right)_{mj} + \sum_{m\neq i}\left(y_m^u\right)^2 V_{mj}V_{ij}^{*}\left(\boldsymbol{V}\boldsymbol{V}^{\dagger}\right)_{im} \\
&= \sum_{m\neq j}\left(y_m^d\right)^2 V_{im}V_{ij}^{*}\delta_{mj} + \sum_{m\neq i}\left(y_m^u\right)^2 V_{mj}V_{ij}^{*}\delta_{im} = 0 , \qquad \text{(A.57)}
\end{aligned}
$$

where we used the unitarity of $\boldsymbol{V}$. We further note that because of the relations in Eq. (A.19) to (A.22), $\boldsymbol{U}_{\mathrm{L}}\frac{\mathrm{d}\boldsymbol{U}_{\mathrm{L}}^{\dagger}}{\mathrm{d}t}$ and $\boldsymbol{D}_{\mathrm{L}}\frac{\mathrm{d}\boldsymbol{D}_{\mathrm{L}}^{\dagger}}{\mathrm{d}t}$ are anti-Hermitian matrices, hence there diagonal elements are purely imaginary. Taking the real part of the expression for $V_{ij}^{*}\frac{\mathrm{d}V_{ij}}{\mathrm{d}t}$ then finally yields the β-function for the quadratic CKM matrix element $|V_{ij}|^2$:

$$\begin{aligned}\beta\left(|V_{ij}|^2\right) = {} & \frac{3\left(y_j^d\right)^2}{16\pi^2}\sum_{k\neq j}\frac{1}{\left(y_k^d\right)^2-\left(y_j^d\right)^2}\left(2\left(y_i^u\right)^2\,|V_{ij}|^2\,|V_{ik}|^2+2\sum_{m\neq i}\left(y_m^u\right)^2\,\Re\left\{V_{mj}V_{mk}^{*}V_{ij}^{*}V_{ik}\right\}\right)- \\ & -\frac{3\left(y_i^u\right)^2}{16\pi^2}\sum_{k\neq i}\frac{1}{\left(y_i^u\right)^2-\left(y_k^u\right)^2}\left(2\left(y_j^d\right)^2\,|V_{ij}|^2\,|V_{kj}|^2+2\sum_{m\neq j}\left(y_m^d\right)^2\,\Re\left\{V_{im}V_{km}^{*}V_{ij}^{*}V_{kj}\right\}\right)+ \\ & +\frac{3\,|V_{ij}|^2}{16\pi^2}\left\{\left(y_{\mathrm{i}}^{\mathrm{u}}\right)^2+\left(y_j^d\right)^2-\sum_m\left(y_m^u\right)^2\,|V_{mj}|^2-\sum_m\left(y_m^d\right)^2\,|V_{im}|^2\right\}\,, \end{aligned} \tag{A.58}$$

which is the same result as in [25].

We now show that this β-function guarantees a unitary RG-evolution of the CKM matrix. First, we recall the unitarity conditions for a $N_g \times N_g$ matrix:

$$\sum_i V_{ij}V_{ik}^{*}=\delta_{jk}\,,\qquad \sum_j V_{ij}V_{kj}^{*}=\delta_{ik}\,,\qquad \forall\, i,j,k=1,\ldots,N_g\,. \tag{A.59}$$

In order to guarantee a unitary RG-evolution, we require:

$$\beta\left(\sum_i |V_{ij}|^2\right)=\sum_i\beta\left(|V_{ij}|^2\right)\stackrel{!}{=}0\,,\qquad \forall j=1,\ldots,N_g\,, \tag{A.60}$$

$$\beta\left(\sum_j |V_{ij}|^2\right)=\sum_j\beta\left(|V_{ij}|^2\right)\stackrel{!}{=}0\,,\qquad \forall i=1,\ldots,N_g\,. \tag{A.61}$$

We start by writing $\beta\left(|V_{ij}|^2\right)$ using Eq. (A.55) and summing over rows:

$$\begin{aligned}
\sum_i \beta\left(|V_{ij}|^2\right) &= 2\sum_i \Re\left\{V_{ij}^* \frac{\mathrm{d}V_{ij}}{\mathrm{d}t}\right\} \\
&= \frac{3}{16\pi^2}\sum_i \sum_{k\neq j} \frac{\left(y_k^d\right)^2+\left(y_j^d\right)^2}{\left(y_k^d\right)^2-\left(y_j^d\right)^2} \sum_m \left(y_m^u\right)^2 \Re\left\{V_{mj}V_{mk}^* V_{ij}^* V_{ik}\right\} - \\
&\quad - \frac{3}{16\pi^2}\sum_i \sum_{k\neq i} \frac{\left(y_i^u\right)^2+\left(y_k^u\right)^2}{\left(y_i^u\right)^2-\left(y_k^u\right)^2} \sum_m \left(y_m^d\right)^2 \Re\left\{V_{im}V_{km}^* V_{ij}^* V_{kj}\right\} \\
&= \frac{3}{32\pi^2}\sum_{k\neq j} \frac{\left(y_k^d\right)^2+\left(y_j^d\right)^2}{\left(y_k^d\right)^2-\left(y_j^d\right)^2} \sum_m \left(y_m^u\right)^2 \sum_i \left(V_{mj}V_{mk}^* V_{ij}^* V_{ik} + V_{mj}^* V_{mk} V_{ij} V_{ik}^*\right) - \\
&\quad - \frac{3}{32\pi^2}\sum_m \left(y_m^d\right)^2 \sum_i \sum_{k\neq i} \frac{\left(y_i^u\right)^2+\left(y_k^u\right)^2}{\left(y_i^u\right)^2-\left(y_k^u\right)^2} \left(V_{im}V_{km}^* V_{ij}^* V_{kj} + V_{im}^* V_{km} V_{ij} V_{kj}^*\right) \\
&= \frac{3}{32\pi^2}\sum_m \left(y_m^u\right)^2 \sum_{k\neq j} \frac{\left(y_k^d\right)^2+\left(y_j^d\right)^2}{\left(y_k^d\right)^2-\left(y_j^d\right)^2} \left(V_{mj}V_{mk}^* + V_{mj}^* V_{mk}\right)\delta_{jk} - \\
&\quad - \frac{3}{32\pi^2}\sum_m \left(y_m^d\right)^2 \sum_i \sum_{k\neq i} \frac{\left(y_i^u\right)^2+\left(y_k^u\right)^2}{\left(y_i^u\right)^2-\left(y_k^u\right)^2} \left(V_{im}V_{km}^* V_{ij}^* V_{kj} + V_{im}^* V_{km} V_{ij} V_{kj}^*\right) \ .
\end{aligned}$$

The first term is zero because of the Kronecker delta δ_{jk} and the sum $\sum_{k\neq j}$. In the second term, every combination of indices i and k appears two times, due to the double sum $\sum_i \sum_{k\neq i}$. However, because of the minus in denominator, the members of such pairs differ in their sign. Hence, the individual terms cancel each other and we conclude that

$$\sum_i \beta\left(|V_{ij}|^2\right) = 0 \ . \tag{A.62}$$

The same holds if we sum over columns.

We conclude that the β-function in Eq. (A.58) describes a unitary RG evolution. A set of mixing parameters $|V_{ij}|^2$ that satisfy the unitarity conditions in Eq. (A.59) at an initial RG time t_0 and evolve according to eq. (A.58) satisfy the unitarity conditions at all times. The fact that Eq. (A.58) satisfies the unitarity conditions in Eq. (A.60) and (A.61) is again due to the minus sign in the denominators.

B. Miscellaneous Expressions

In this Appendix we present the full expressions of quantities which are used in the main text.

B.1. One-loop Expressions of δ_f

The running Yukawa coupling $y_f^{\overline{\rm MS}}(\mu)$ of a fermion f in the $\overline{\rm MS}$-scheme is related to the pole mass m_f via the relation [63, 71]:

$$y_f^{\overline{\rm MS}}(\mu) = 2^{\frac{3}{4}}\sqrt{G_F}\, m_f \left[1 + \delta_f^{(1)}(\mu) + \delta_f^{(2)}(\mu) + \ldots\right] . \tag{B.1}$$

The one-loop contribution $\delta_f^{(1)}(\mu)$ can be split into a weak, electromagnetic and strong part:

$$\delta_f^{(1)}(\mu) = \delta_f^{\rm W}(\mu) + \delta_f^{\rm QED}(\mu) + \delta_f^{\rm QCD}(\mu) . \tag{B.2}$$

These contributions are given by [71]:

$$\delta_f^{\rm QCD}(\mu) = \frac{N_c^2-1}{2N_c}\frac{g_3^2(\mu)}{16\pi^2}\left(3\log\frac{m_f^2}{\mu^2} - 4\right) , \tag{B.3}$$

$$\delta_f^{\rm QED}(\mu) = Q_f^2\frac{g_2^2(\mu)}{16\pi^2}\left(1 - \frac{M_W^2}{M_Z^2}\right)\left(3\log\frac{m_f^2}{\mu^2} - 4\right) , \tag{B.4}$$

$$\begin{aligned}\delta_t^{\rm W}(\mu) = \frac{G_F m_t^2}{8\pi^2\sqrt{2}}\Big[&-\left(N_c + \frac{3}{2}\right)\log\frac{m_t^2}{\mu^2} + \frac{N_c}{2} + 4 - \frac{M_H^2}{4m_t^2} + \frac{M_H^2}{2m_t^2}\left(\frac{M_H^2}{2m_t^2} - 3\right)\log\frac{M_H^2}{m_t^2} - \\ &- 8\left(\frac{M_H^2}{4m_t^2}\right)^2\left(\frac{4m_t^2}{M_H^2} - 1\right)^{\frac{3}{2}}\arccos\frac{M_H}{2m_t}\Big] ,\end{aligned} \tag{B.5}$$

$$\delta_b^{\rm W}(\mu) = \frac{G_F}{8\pi^2\sqrt{2}}\left\{m_t^2\left[\left(-N_c + \frac{3}{2}\right)\log\frac{m_t^2}{\mu^2} + \frac{N_c}{2} - \frac{5}{4}\right] + \frac{M_H^2}{4}\right\} , \tag{B.6}$$

$$\delta_f^{\rm W}(\mu) = \frac{G_F}{8\pi^2\sqrt{2}}\left[N_c m_t^2\left(-\log\frac{m_t^2}{\mu^2} + \frac{1}{2}\right) + \frac{M_H^2}{4}\right] , \qquad (f = u, d, s, c) , \tag{B.7}$$

where Q_f is the electric charge of the fermion f and $M_{W,Z,H}$ are the masses of the W boson, Z boson and Higgs boson, respectively. Note that these expressions were calculated in [71] in the limit were M_H and m_t are large in comparison to the masses of all other fermions in the SM. Also, we have ignored any threshold effects (for details, see [71]).

B.2. One-loop β-functions for $N_g = 3$

In this section of the Appendix we present the one-loop β-functions for a three generation model. We write all β-functions in terms of the four squared moduli of the CKM matrix elements $|V_{11}|^2$, $|V_{22}|^2$, $|V_{12}|^2$ and $|V_{21}|^2$.

$$\beta\left(y_t\right) = \frac{y_t}{16\pi^2}\Bigg\{ - A^{\mathrm{u}} + \frac{9}{2}y_t^2 + 3y_u^2 + 3y_c^2 + \frac{3}{2}y_d^2\left(1 + |V_{11}|^2 + |V_{21}|^2\right) + \frac{3}{2}y_s^2\left(1 + |V_{12}|^2 + |V_{22}|^2\right) + \\ + \frac{3}{2}y_b^2\left(3 - |V_{11}|^2 - |V_{22}|^2 - |V_{12}|^2 - |V_{21}|^2\right)\Bigg\} - f_y y_t \ , \tag{B.8}$$

$$\beta\left(y_c\right) = \frac{y_c}{16\pi^2}\Bigg\{ - A^{\mathrm{u}} + \frac{9}{2}y_c^2 + 3y_u^2 + 3y_t^2 + \frac{3}{2}y_d^2\left(2 - |V_{21}|^2\right) + \frac{3}{2}y_s^2\left(2 - |V_{22}|^2\right) + \\ + \frac{3}{2}y_b^2\left(1 + |V_{21}|^2 + |V_{22}|^2\right)\Bigg\} - f_y y_c \ , \tag{B.9}$$

$$\beta\left(y_u\right) = \frac{y_u}{16\pi^2}\Bigg\{ - A^{\mathrm{u}} + \frac{9}{2}y_u^2 + 3y_c^2 + 3y_t^2 + \frac{3}{2}y_d^2\left(2 - |V_{11}|^2\right) + \frac{3}{2}y_s^2\left(2 - |V_{12}|^2\right) + \\ + \frac{3}{2}y_b^2\left(1 + |V_{11}|^2 + |V_{12}|^2\right)\Bigg\} - f_y y_u \ , \tag{B.10}$$

$$\beta\left(y_b\right) = \frac{y_b}{16\pi^2}\Bigg\{ - A^{\mathrm{d}} + \frac{9}{2}y_b^2 + 3y_d^2 + 3y_s^2 + \frac{3}{2}y_u^2\left(1 + |V_{11}|^2 + |V_{12}|^2\right) + \frac{3}{2}y_c^2\left(1 + |V_{21}|^2 + |V_{22}|^2\right) + \\ + \frac{3}{2}y_t^2\left(3 - |V_{11}|^2 - |V_{22}|^2 - |V_{12}|^2 - |V_{21}|^2\right)\Bigg\} - f_y y_b \ , \tag{B.11}$$

$$\beta\left(y_s\right) = \frac{y_s}{16\pi^2}\Bigg\{ - A^{\mathrm{d}} + \frac{9}{2}y_s^2 + 3y_d^2 + 3y_b^2 + \frac{3}{2}y_u^2\left(2 - |V_{12}|^2\right) + \frac{3}{2}y_c^2\left(2 - |V_{22}|^2\right) + \\ + \frac{3}{2}y_t^2\left(1 + |V_{12}|^2 + |V_{22}|^2\right)\Bigg\} - f_y y_s \ , \tag{B.12}$$

$$\beta\left(y_d\right) = \frac{y_d}{16\pi^2}\Bigg\{ - A^{\mathrm{d}} + \frac{9}{2}y_d^2 + 3y_s^2 + 3y_b^2 + \frac{3}{2}y_u^2\left(2 - |V_{11}|^2\right) + \frac{3}{2}y_c^2\left(2 - |V_{21}|^2\right) + \\ + \frac{3}{2}y_t^2\left(1 + |V_{11}|^2 + |V_{21}|^2\right)\Bigg\} - f_y y_d \ , \tag{B.13}$$

with

$$A^{\mathrm{u}} = \left(\frac{17}{12}g_Y^2 + \frac{9}{4}g_2^2 + 8g_3^2\right) \ , \tag{B.14}$$

$$A^{\mathrm{d}} = \left(\frac{5}{12}g_Y^2 + \frac{9}{4}g_2^2 + 8g_3^2\right) \ . \tag{B.15}$$

$$
\begin{aligned}
\beta\left(|V_{11}|^2\right) = \frac{3y_d^2}{16\pi^2}\Bigg\{ & \frac{1}{y_s^2 - y_d^2}\Big[2y_u^2 |V_{11}|^2 |V_{12}|^2 + \\
& + y_c^2\left(1 - |V_{11}|^2 - |V_{22}|^2 - |V_{12}|^2 - |V_{21}|^2 + |V_{21}|^2 |V_{12}|^2 + |V_{11}|^2 |V_{22}|^2\right) + \\
& + y_t^2\left(|V_{11}|^2 + |V_{22}|^2 + |V_{12}|^2 + |V_{21}|^2 - 2|V_{12}|^2 |V_{11}|^2 - |V_{12}|^2 |V_{21}|^2 - |V_{22}|^2 |V_{11}|^2 - 1\right)\Big] + \\
& + \frac{1}{y_b^2 - y_d^2}\Big[2y_u^2 |V_{11}|^2\left(1 - |V_{11}|^2 - |V_{12}|^2\right) + \\
& + y_c^2\left(|V_{11}|^2 + |V_{22}|^2 + |V_{12}|^2 + |V_{21}|^2 - 2|V_{21}|^2 |V_{11}|^2 - |V_{12}|^2 |V_{21}|^2 - |V_{22}|^2 |V_{11}|^2 - 1\right) + \\
& + y_t^2\Big(1 - 3|V_{11}|^2 - |V_{22}|^2 - |V_{12}|^2 - |V_{21}|^2 + 2|V_{11}|^2 |V_{12}|^2 + 2|V_{11}|^2 |V_{21}|^2 + \\
& \quad + |V_{12}|^2 |V_{21}|^2 + |V_{11}|^2 |V_{22}|^2 + 2|V_{11}|^4\Big)\Big]\Bigg\} + \\
& + \frac{3y_u^2}{16\pi^2}\Bigg\{ \frac{1}{y_c^2 - y_u^2}\Big[2y_d^2 |V_{11}|^2 |V_{21}|^2 + \\
& + y_s^2\left(1 - |V_{11}|^2 - |V_{22}|^2 - |V_{12}|^2 - |V_{21}|^2 + |V_{21}|^2 |V_{12}|^2 + |V_{11}|^2 |V_{22}|^2\right) + \\
& + y_b^2\left(|V_{11}|^2 + |V_{22}|^2 + |V_{12}|^2 + |V_{21}|^2 - 2|V_{21}|^2 |V_{11}|^2 - |V_{12}|^2 |V_{21}|^2 - |V_{22}|^2 |V_{11}|^2 - 1\right)\Big] + \\
& + \frac{1}{y_t^2 - y_u^2}\Big[2y_d^2 |V_{11}|^2\left(1 - |V_{11}|^2 - |V_{21}|^2\right) + \\
& + y_s^2\left(|V_{11}|^2 + |V_{22}|^2 + |V_{12}|^2 + |V_{21}|^2 - 2|V_{12}|^2 |V_{11}|^2 - |V_{12}|^2 |V_{21}|^2 - |V_{22}|^2 |V_{11}|^2 - 1\right) + \\
& + y_b^2\Big(1 - 3|V_{11}|^2 - |V_{22}|^2 - |V_{12}|^2 - |V_{21}|^2 + 2|V_{11}|^2 |V_{12}|^2 + 2|V_{11}|^2 |V_{21}|^2 + \\
& \quad + |V_{12}|^2 |V_{21}|^2 + |V_{11}|^2 |V_{22}|^2 + 2|V_{11}|^4\Big)\Big]\Bigg\} + \\
& + \frac{3|V_{11}|^2}{16\pi^2}\Big\{y_u^2\left(1 - |V_{11}|^2\right) + y_d^2\left(1 - |V_{11}|^2\right) - y_c^2 |V_{21}|^2 - y_t^2\left(1 - |V_{11}|^2 - |V_{21}|^2\right) - \\
& \quad - y_s^2 |V_{12}|^2 - y_b^2\left(1 - |V_{11}|^2 - |V_{12}|^2\right)\Big\}\,, \qquad \text{(B.16)}
\end{aligned}
$$

$$
\begin{aligned}
\beta\left(|V_{22}|^2\right) = \frac{3y_s^2}{16\pi^2}\Bigg\{ & \frac{1}{y_d^2 - y_s^2}\Big[2y_c^2\,|V_{22}|^2\,|V_{21}|^2 + \\
& + y_u^2\left(1 - |V_{11}|^2 - |V_{22}|^2 - |V_{12}|^2 - |V_{21}|^2 + |V_{21}|^2\,|V_{12}|^2 + |V_{11}|^2\,|V_{22}|^2\right) + \\
& + y_t^2\left(|V_{11}|^2 + |V_{22}|^2 + |V_{12}|^2 + |V_{21}|^2 - 2\,|V_{21}|^2\,|V_{22}|^2 - |V_{12}|^2\,|V_{21}|^2 - |V_{22}|^2\,|V_{11}|^2 - 1\right)\Big] + \\
& + \frac{1}{y_b^2 - y_s^2}\Big[2y_c^2\,|V_{22}|^2\left(1 - |V_{21}|^2 - |V_{22}|^2\right) + \\
& + y_u^2\left(|V_{11}|^2 + |V_{22}|^2 + |V_{12}|^2 + |V_{21}|^2 - 2\,|V_{12}|^2\,|V_{22}|^2 - |V_{12}|^2\,|V_{21}|^2 - |V_{22}|^2\,|V_{11}|^2 - 1\right) + \\
& + y_t^2\Big(1 - 3\,|V_{22}|^2 - |V_{11}|^2 - |V_{12}|^2 - |V_{21}|^2 + 2\,|V_{12}|^2\,|V_{22}|^2 + 2\,|V_{21}|^2\,|V_{22}|^2 + \\
& \quad + |V_{12}|^2\,|V_{21}|^2 + |V_{11}|^2\,|V_{22}|^2 + 2\,|V_{22}|^4\Big)\Big]\Bigg\} + \\
& + \frac{3y_c^2}{16\pi^2}\Bigg\{\frac{1}{y_u^2 - y_c^2}\Big[2y_s^2\,|V_{22}|^2\,|V_{12}|^2 + \\
& + y_d^2\left(1 - |V_{11}|^2 - |V_{22}|^2 - |V_{12}|^2 - |V_{21}|^2 + |V_{21}|^2\,|V_{12}|^2 + |V_{11}|^2\,|V_{22}|^2\right) + \\
& + y_b^2\left(|V_{11}|^2 + |V_{22}|^2 + |V_{12}|^2 + |V_{21}|^2 - 2\,|V_{12}|^2\,|V_{22}|^2 - |V_{12}|^2\,|V_{21}|^2 - |V_{22}|^2\,|V_{11}|^2 - 1\right)\Big] + \\
& + \frac{1}{y_t^2 - y_c^2}\Big[2y_s^2\,|V_{22}|^2\left(1 - |V_{12}|^2 - |V_{22}|^2\right) + \\
& + y_d^2\left(|V_{11}|^2 + |V_{22}|^2 + |V_{12}|^2 + |V_{21}|^2 - 2\,|V_{21}|^2\,|V_{22}|^2 - |V_{12}|^2\,|V_{21}|^2 - |V_{22}|^2\,|V_{11}|^2 - 1\right) + \\
& + y_b^2\Big(1 - 3\,|V_{22}|^2 - |V_{11}|^2 - |V_{12}|^2 - |V_{21}|^2 + 2\,|V_{12}|^2\,|V_{22}|^2 + 2\,|V_{21}|^2\,|V_{22}|^2 + \\
& \quad + |V_{12}|^2\,|V_{21}|^2 + |V_{11}|^2\,|V_{22}|^2 + 2\,|V_{22}|^4\Big)\Big]\Bigg\} + \\
& + \frac{3\,|V_{22}|^2}{16\pi^2}\Big\{y_c^2\left(1 - |V_{22}|^2\right) + y_s^2\left(1 - |V_{22}|^2\right) - y_u^2\,|V_{12}|^2 - y_t^2\left(1 - |V_{12}|^2 - |V_{22}|^2\right) - \\
& \quad - y_d^2\,|V_{21}|^2 - y_b^2\left(1 - |V_{21}|^2 - |V_{22}|^2\right)\Big\}\,, \qquad \text{(B.17)}
\end{aligned}
$$

$$
\begin{aligned}
\beta\left(|V_{12}|^2\right) = \frac{3y_s^2}{16\pi^2}\Bigg\{ & \frac{1}{y_d^2 - y_s^2}\Big[2y_u^2 \left|V_{12}\right|^2 \left|V_{11}\right|^2 + \\
& + y_c^2\left(1 - \left|V_{11}\right|^2 - \left|V_{22}\right|^2 - \left|V_{12}\right|^2 - \left|V_{21}\right|^2 + \left|V_{21}\right|^2\left|V_{12}\right|^2 + \left|V_{11}\right|^2\left|V_{22}\right|^2\right) + \\
& + y_t^2\left(\left|V_{11}\right|^2 + \left|V_{22}\right|^2 + \left|V_{12}\right|^2 + \left|V_{21}\right|^2 - 2\left|V_{11}\right|^2\left|V_{12}\right|^2 - \left|V_{12}\right|^2\left|V_{21}\right|^2 - \left|V_{22}\right|^2\left|V_{11}\right|^2 - 1\right)\Big] + \\
& + \frac{1}{y_b^2 - y_s^2}\Big[2y_u^2\left|V_{12}\right|^2\left(1 - \left|V_{11}\right|^2 - \left|V_{12}\right|^2\right) + \\
& + y_c^2\left(\left|V_{11}\right|^2 + \left|V_{22}\right|^2 + \left|V_{12}\right|^2 + \left|V_{21}\right|^2 - 2\left|V_{12}\right|^2\left|V_{22}\right|^2 - \left|V_{12}\right|^2\left|V_{21}\right|^2 - \left|V_{22}\right|^2\left|V_{11}\right|^2 - 1\right) + \\
& + y_t^2\Big(1 - 3\left|V_{12}\right|^2 - \left|V_{11}\right|^2 - \left|V_{22}\right|^2 - \left|V_{21}\right|^2 + 2\left|V_{12}\right|^2\left|V_{22}\right|^2 + 2\left|V_{11}\right|^2\left|V_{12}\right|^2 + \\
& \quad + \left|V_{12}\right|^2\left|V_{21}\right|^2 + \left|V_{11}\right|^2\left|V_{22}\right|^2 + 2\left|V_{12}\right|^4\Big)\Big]\Bigg\} + \\
& + \frac{3y_u^2}{16\pi^2}\Bigg\{\frac{1}{y_c^2 - y_u^2}\Big[2y_s^2\left|V_{12}\right|^2\left|V_{22}\right|^2 + \\
& + y_d^2\left(1 - \left|V_{11}\right|^2 - \left|V_{22}\right|^2 - \left|V_{12}\right|^2 - \left|V_{21}\right|^2 + \left|V_{21}\right|^2\left|V_{12}\right|^2 + \left|V_{11}\right|^2\left|V_{22}\right|^2\right) + \\
& + y_b^2\left(\left|V_{11}\right|^2 + \left|V_{22}\right|^2 + \left|V_{12}\right|^2 + \left|V_{21}\right|^2 - 2\left|V_{12}\right|^2\left|V_{22}\right|^2 - \left|V_{12}\right|^2\left|V_{21}\right|^2 - \left|V_{22}\right|^2\left|V_{11}\right|^2 - 1\right)\Big] + \\
& + \frac{1}{y_t^2 - y_u^2}\Big[2y_s^2\left|V_{12}\right|^2\left(1 - \left|V_{12}\right|^2 - \left|V_{22}\right|^2\right) + \\
& + y_d^2\left(\left|V_{11}\right|^2 + \left|V_{22}\right|^2 + \left|V_{12}\right|^2 + \left|V_{21}\right|^2 - 2\left|V_{11}\right|^2\left|V_{12}\right|^2 - \left|V_{12}\right|^2\left|V_{21}\right|^2 - \left|V_{22}\right|^2\left|V_{11}\right|^2 - 1\right) + \\
& + y_b^2\Big(1 - 3\left|V_{12}\right|^2 - \left|V_{11}\right|^2 - \left|V_{22}\right|^2 - \left|V_{21}\right|^2 + 2\left|V_{12}\right|^2\left|V_{22}\right|^2 + 2\left|V_{11}\right|^2\left|V_{12}\right|^2 + \\
& \quad + \left|V_{12}\right|^2\left|V_{21}\right|^2 + \left|V_{11}\right|^2\left|V_{22}\right|^2 + 2\left|V_{12}\right|^4\Big)\Big]\Bigg\} + \\
& + \frac{3\left|V_{12}\right|^2}{16\pi^2}\Big\{y_{\mathrm{u}}^2\left(1 - \left|V_{12}\right|^2\right) + y_{\mathrm{s}}^2\left(1 - \left|V_{12}\right|^2\right) - y_{\mathrm{c}}^2\left|V_{22}\right|^2 - y_t^2\left(1 - \left|V_{12}\right|^2 - \left|V_{22}\right|^2\right) - \\
& \quad - y_d^2\left|V_{11}\right|^2 - y_b^2\left(1 - \left|V_{11}\right|^2 - \left|V_{12}\right|^2\right)\Big\}\,, \qquad \text{(B.18)}
\end{aligned}
$$

$$
\begin{aligned}
\beta\left(|V_{21}|^2\right) = \frac{3y_d^2}{16\pi^2}\Bigg\{ & \frac{1}{y_s^2-y_d^2}\Big[2y_c^2\,|V_{21}|^2\,|V_{22}|^2 + \\
& + y_u^2\left(1-|V_{11}|^2-|V_{22}|^2-|V_{12}|^2-|V_{21}|^2+|V_{21}|^2\,|V_{12}|^2+|V_{11}|^2\,|V_{22}|^2\right) + \\
& + y_t^2\left(|V_{11}|^2+|V_{22}|^2+|V_{12}|^2+|V_{21}|^2-2\,|V_{21}|^2\,|V_{22}|^2-|V_{12}|^2\,|V_{21}|^2-|V_{22}|^2\,|V_{11}|^2-1\right)\Big] + \\
& + \frac{1}{y_b^2-y_d^2}\Big[2y_c^2\,|V_{21}|^2\left(1-|V_{21}|^2-|V_{22}|^2\right) + \\
& + y_u^2\left(|V_{11}|^2+|V_{22}|^2+|V_{12}|^2+|V_{21}|^2-2\,|V_{21}|^2\,|V_{11}|^2-|V_{12}|^2\,|V_{21}|^2-|V_{22}|^2\,|V_{11}|^2-1\right) + \\
& + y_t^2\Big(1-3\,|V_{21}|^2-|V_{11}|^2-|V_{22}|^2-|V_{12}|^2+2\,|V_{11}|^2\,|V_{21}|^2+2\,|V_{21}|^2\,|V_{22}|^2 + \\
& \quad + |V_{12}|^2\,|V_{21}|^2+|V_{11}|^2\,|V_{22}|^2+2\,|V_{21}|^4\Big)\Big]\Bigg\} + \\
+ \frac{3y_c^2}{16\pi^2}\Bigg\{ & \frac{1}{y_u^2-y_c^2}\Big[2y_d^2\,|V_{21}|^2\,|V_{11}|^2 + \\
& + y_s^2\left(1-|V_{11}|^2-|V_{22}|^2-|V_{12}|^2-|V_{21}|^2+|V_{21}|^2\,|V_{12}|^2+|V_{11}|^2\,|V_{22}|^2\right) + \\
& + y_b^2\left(|V_{11}|^2+|V_{22}|^2+|V_{12}|^2+|V_{21}|^2-2\,|V_{21}|^2\,|V_{11}|^2-|V_{12}|^2\,|V_{21}|^2-|V_{22}|^2\,|V_{11}|^2-1\right)\Big] + \\
& + \frac{1}{y_t^2-y_c^2}\Big[2y_d^2\,|V_{21}|^2\left(1-|V_{11}|^2-|V_{21}|^2\right) + \\
& + y_s^2\left(|V_{11}|^2+|V_{22}|^2+|V_{12}|^2+|V_{21}|^2-2\,|V_{21}|^2\,|V_{22}|^2-|V_{12}|^2\,|V_{21}|^2-|V_{22}|^2\,|V_{11}|^2-1\right) + \\
& + y_b^2\Big(1-3\,|V_{21}|^2-|V_{11}|^2-|V_{22}|^2-|V_{12}|^2+2\,|V_{11}|^2\,|V_{21}|^2+2\,|V_{21}|^2\,|V_{22}|^2 + \\
& \quad + |V_{12}|^2\,|V_{21}|^2+|V_{11}|^2\,|V_{22}|^2+2\,|V_{21}|^4\Big)\Big]\Bigg\} + \\
+ \frac{3\,|V_{21}|^2}{16\pi^2}\Big\{ & y_c^2\left(1-|V_{21}|^2\right)+y_d^2\left(1-|V_{21}|^2\right)-y_u^2\,|V_{11}|^2-y_t^2\left(1-|V_{11}|^2-|V_{21}|^2\right) - \\
& - y_s^2\,|V_{22}|^2-y_b^2\left(1-|V_{21}|^2-|V_{22}|^2\right)\Big\}\,. \qquad \text{(B.19)}
\end{aligned}
$$

Here, we used the following expression for the real parts $\Re\left\{V_{im}V_{km}^*V_{ij}^*V_{kj}\right\}$ for $N_g = 3$ [25]:

$$
2\Re\left\{V_{im}V_{km}^*V_{ij}^*V_{kj}\right\} = 1-|V_{im}|^2-|V_{km}|^2-|V_{kj}|^2-|V_{ij}|^2+|V_{im}|^2\,|V_{kj}|^2+|V_{km}|^2\,|V_{ij}|^2\ . \qquad \text{(B.20)}
$$

B.3. Two-loop β-functions for $N_g = 2$

For the sake of completeness, we present the two-loop β-functions of the gauge and Yukawa couplings as well as the quadratic CKM matrix element for $N_g = 2$ as calculated in [6].

$$\beta\left(g_Y^2\right) = \frac{g_Y^2}{16\pi^2}\left(\frac{41}{3}g_Y^2 + \frac{g_Y^2}{16\pi^2}\left[\frac{199}{9}g_Y^2 + 9g_2^2 + 88g_3^2 - \frac{17}{3}(y_t^2+y_c^2) - \frac{5}{3}(y_b^2+y_c^2)\right]\right), \quad \text{(B.21)}$$

$$\beta\left(g_2^2\right) = \frac{g_2^2}{16\pi^2}\left(-\frac{19}{3}g_2^2 + \frac{g_2^2}{16\pi^2}\left[3g_Y^2 + \frac{35}{3}g_2^2 + 24g_3^2 - 3(y_t^2+y_c^2) + 3(y_b^2+y_c^2)\right]\right), \quad \text{(B.22)}$$

$$\beta\left(g_3^2\right) = \frac{g_3^2}{16\pi^2}\left(-14g_3^2 + \frac{g_3^2}{16\pi^2}\left[\tfrac{11}{3}g_1^2 + 9g_2^2 - 52g_3^2 - 4(y_t^2+y_c^2) - 4(y_b^2+y_c^2)\right]\right), \quad \text{(B.23)}$$

$$\begin{aligned}\beta\left(y_t^2\right) = {} & \frac{y_t^2}{16\pi^2}\left[2(Y_2(S) - G^{\mathrm{u}}) + 3y_t^2 - 3y_b^2\left|V_{11}\right|^2 - 3y_s^2(1-\left|V_{11}\right|^2)\right] + \\ & + \frac{y_t^2}{(16\pi^2)^2}\Big[3y_t^4 - \tfrac{5}{2}y_t^2\left(y_b^2\left|V_{11}\right|^2 + y_s^2(1-\left|V_{11}\right|^2)\right) + \frac{11}{2}y_b^4\left|V_{11}\right|^2 + \frac{11}{2}y_s^4(1-\left|V_{11}\right|^2) + \\ & \qquad + 2A^{\mathrm{uu}}y_t^2 + 2A^{\mathrm{ud}}\left(y_b^2\left|V_{11}\right|^2 + y_s^2(1-\left|V_{11}\right|^2)\right) + 2B^{\mathrm{u}}\Big], \end{aligned} \quad \text{(B.24)}$$

$$\begin{aligned}\beta\left(y_c^2\right) = {} & \frac{y_c^2}{16\pi^2}\left[2(Y_2(S) - G^{\mathrm{u}}) + 3y_c^2 - 3y_s^2\left|V_{11}\right|^2 - 3y_b^2(1-\left|V_{11}\right|^2)\right] + \\ & + \frac{y_c^2}{(16\pi^2)^2}\Big[3y_c^4 - \frac{5}{2}y_c^2\left(y_s^2\left|V_{11}\right|^2 + y_b^2(1-\left|V_{11}\right|^2)\right) + \frac{11}{2}y_s^4\left|V_{11}\right|^2 + \frac{11}{2}y_b^4(1-\left|V_{11}\right|^2) + \\ & \qquad + 2A^{\mathrm{uu}}y_c^2 + 2A^{\mathrm{ud}}\left(y_s^2\left|V_{11}\right|^2 + y_b^2(1-\left|V_{11}\right|^2)\right) + 2B^{\mathrm{u}}\Big], \end{aligned} \quad \text{(B.25)}$$

$$\begin{aligned}\beta\left(y_b^2\right) = {} & \frac{y_b^2}{16\pi^2}\left[2(Y_2(S) - G^{\mathrm{d}}) + 3y_b^2 - 3y_t^2\left|V_{11}\right|^2 - 3y_c^2(1-\left|V_{11}\right|^2)\right] + \\ & + \frac{y_b^2}{(16\pi^2)^2}\Big[3y_b^4 - \frac{5}{2}y_b^2\left(y_t^2\left|V_{11}\right|^2 + y_c^2(1-\left|V_{11}\right|^2)\right) + \frac{11}{2}y_t^4\left|V_{11}\right|^2 + \frac{11}{2}y_c^4(1-\left|V_{11}\right|^2) + \\ & \qquad + 2A^{\mathrm{dd}}y_b^2 + 2A^{\mathrm{du}}\left(y_t^2\left|V_{11}\right|^2 + y_c^2(1-\left|V_{11}\right|^2)\right) + 2B^{\mathrm{d}}\Big], \end{aligned} \quad \text{(B.26)}$$

$$\begin{aligned}\beta\left(y_s^2\right) = {} & \frac{y_s^2}{16\pi^2}\left[2(Y_2(S) - G^{\mathrm{d}}) + 3y_s^2 - 3y_c^2\left|V_{11}\right|^2 - 3y_t^2(1-\left|V_{11}\right|^2)\right] + \\ & + \frac{y_s^2}{(16\pi^2)^2}\Big[3y_s^4 - \frac{5}{2}y_s^2\left(y_c^2\left|V_{11}\right|^2 + y_t^2(1-\left|V_{11}\right|^2)\right) + \frac{11}{2}y_c^4X + \frac{11}{2}y_t^4(1-\left|V_{11}\right|^2) + \\ & \qquad + 2A^{\mathrm{dd}}y_s^2 + 2A^{\mathrm{du}}\left(y_c^2\left|V_{11}\right|^2 + y_t^2(1-\left|V_{11}\right|^2)\right) + 2B^{\mathrm{d}}\Big]. \end{aligned} \quad \text{(B.27)}$$

$$\beta\left(|V_{11}|^2\right) = \frac{3}{16\pi^2}|V_{11}|^2\left(1-|V_{11}|^2\right)\left\{\left[\left(y_c^2+y_s^2\right)-\left(y_t^2+y_b^2\right)\right]-2y_c^2\frac{y_s^2-y_b^2}{y_c^2-y_t^2}-2y_s^2\frac{y_c^2-y_t^2}{y_s^2-y_b^2}\right\}-$$
$$-\frac{2}{(16\pi^2)^2}|V_{11}|^2\left(1-|V_{11}|^2\right)\left[\frac{1}{y_t^2-y_c^2}\left\{(y_b^2-y_s^2)\left(\frac{1}{2}y_t^2y_c^2+y_t^4+y_c^4-A^{\mathrm{ud}}(y_t^2+y_c^2)\right)-\right.\right.$$
$$\left.\left.-(y_b^4-y_s^4)(y_t^2+y_c^2)\right\}+\right.$$
$$\left.+\frac{1}{y_b^2-y_s^2}\left\{(y_t^2-y_c^2)\left(\frac{1}{2}y_b^2y_s^2+y_b^4+y_s^4-A^{\mathrm{du}}(y_b^2+y_s^2)\right)-(y_t^4-y_c^4)(y_b^2+y_s^2)\right\}\right], \tag{B.28}$$

with

$$G^{\mathrm{u}} = \frac{17}{12}g_1^2+\frac{9}{4}g_2^2+8g_3^2 \tag{B.29}$$
$$G^{\mathrm{d}} = \frac{5}{12}g_1^2+\frac{9}{4}g_2^2+8g_3^2\,, \tag{B.30}$$
$$Y_2(S) = 3(y_t^2+y_c^2)+3(y_b^2+y_s^2)\,, \tag{B.31}$$

$$A^{\mathrm{uu}} = \left(\tfrac{223}{48}g_1^2+\tfrac{135}{16}g_2^2+16g_3^2\right)-\tfrac{9}{4}Y_2(S)\,, \tag{B.32}$$
$$A^{\mathrm{dd}} = \left(\tfrac{187}{48}g_1^2+\tfrac{135}{16}g_2^2+16g_3^2\right)-\tfrac{9}{4}Y_2(S)\,, \tag{B.33}$$
$$A^{\mathrm{ud}} = \tfrac{5}{4}Y_2(S)-\left(\tfrac{43}{48}g_1^2-\tfrac{9}{16}g_2^2+16g_3^2\right)\,, \tag{B.34}$$
$$A^{\mathrm{du}} = \tfrac{5}{4}Y_2(S)-\left(\tfrac{79}{48}g_1^2-\tfrac{9}{16}g_2^2+16g_3^2\right)\,, \tag{B.35}$$

$$B^{\mathrm{u}} = -\chi_4(S)+\tfrac{1187}{216}g_1^4-\tfrac{23}{4}g_2^4-108g_3^4-\tfrac{3}{4}g_1^2g_2^2+\tfrac{19}{9}g_1^2g_2^3+9g_2^2g_3^2+\tfrac{5}{2}Y_4(S)\,, \tag{B.36}$$
$$B^{\mathrm{d}} = -\chi_4(S)-\tfrac{127}{216}g_1^4-\tfrac{23}{4}g_2^4-108g_3^4-\tfrac{9}{4}g_1^2g_2^2+\tfrac{31}{9}g_1^2g_2^3+9g_2^2g_3^2+\tfrac{5}{2}Y_4(S)\,, \tag{B.37}$$

$$\chi_4(S) = \frac{9}{4}\Big[3\left(y_t^4+y_c^4\right)+3\left(y_b^4+y_s^4\right)-$$
$$-\frac{2}{3}\left(y_t^2y_b^2|V_{11}|^2+y_t^2y_s^2(1-|V_{11}|^2)+y_c^2y_s^2|V_{11}|^2+y_c^2y_s^2(1-|V_{11}|^2)\right)\Big]\,, \tag{B.38}$$
$$Y_4(S) = \left(\frac{17}{12}g_1^2+\frac{9}{4}g_2^2+8g_3^2\right)\left(y_t^2+y_c^2\right)+\left(\frac{5}{12}g_1^2+\frac{9}{4}g_2^2+8g_3^2\right)\left(y_b^2+y_s^2\right)\,. \tag{B.39}$$

Acknowledgement

Firstly, I would like to express my gratitude to my supervisor Reinhard Alkofer for his guidance and valuable support during the creation of this thesis. Furthermore, I would like to offer my special thanks to Astrid Eichhorn, Aaron Held, Carlos M. Nieto and Roberto Percacci for the fruitful collaboration and giving me the chance to work with them on this exciting topic. I am grateful to the Paul-Urban foundation for financial support.

List of Figures

List of Tables

Bibliography

[1] M. Gell-Mann and F. E. Low, Phys. Rev. **95**, 1300 (1954).

[2] L. Maiani, G. Parisi, and R. Petronzio, Nuclear Physics B **136**, 115 (1978).

[3] M. Göckeler, R. Horsley, V. Linke, P. Rakow, G. Schierholz, and H. Stüben, Phys. Rev. Lett. **80**, 4119 (1998).

[4] M. Göckeler, R. Horsley, V. Linke, P. Rakow, G. Schierholz, and H. Stüben, Nuclear Physics B - Proceedings Supplements **63**, 694 (1998).

[5] H. Gies and J. Jaeckel, Phys. Rev. Lett. **93**, 110405 (2004).

[6] R. Alkofer, A. Eichhorn, A. Held, C. M. Nieto, R. Percacci, and M. Schröfl, *in preparation* .

[7] A. Eichhorn and F. Versteegen, JHEP **1801**, 30 (2018).

[8] A. Eichhorn and A. Held, Phys. Lett. B **777**, 217 (2018).

[9] A. Eichhorn and A. Held, Phys. Rev. Lett. **121**, 151302 (2018).

[10] N. Cabibbo, Phys. Rev. Lett. **10**, 531 (1963).

[11] M. Kobayashi and T. Maskawa, Progress of Theoretical Physics **49**, 652 (1973).

[12] A. Pich, in *The Standard model of electroweak interactions* (2008) arXiv:0705.4264 [hep-ph] .

[13] A. Pich, CERN Yellow Rep. School Proc. **4**, 65 (2018), arXiv:1805.08597 [hep-ph] .

[14] M. Tanabashi *et al.* (Particle Data Group), Phys. Rev. D **98**, 030001 (2018) and 2019 update.

[15] M. Böhm, A. Denner, and H. Joos, *Gauge Theories of the Strong and Electroweak Interaction*, edited by Springer (Vieweg+Teubner Verlag, 2001).

[16] F. Englert and R. Brout, Phys. Rev. Lett. **13**, 321 (1964).

[17] P. W. Higgs, Phys. Rev. Lett. **13**, 508 (1964).

[18] G. S. Guralnik, C. R. Hagen, and T. W. B. Kibble, Phys. Rev. Lett. **13**, 585 (1964).

[19] M. E. Machacek and M. T. Vaughn, Nuclear Physics B **222**, 83 (1983).

[20] M. E. Machacek and M. T. Vaughn, Nuclear Physics B **236**, 221 (1984).

[21] H. Arason, D. J. Castaño, B. Kesthelyi, S. Mikaelian, E. J. Piard, P. Ramond, and B. D. Wright, Phys. Rev. D **46**, 3945 (1992).

[22] Z. Maki, M. Nakagawa, and S. Sakata, Progress of Theoretical Physics **28**, 870 (1962).

[23] B. Pontecorvo, Sov. Phys. JETP **7**, 172 (1958), originally published in Zh. Eksp. Teor. Fiz. 34, 247 (1957).

[24] P. Kielanowski, S. R. Juárez W., and J. H. Montes de Oca Y., Phys. Rev. D **78**, 116010 (2008).

[25] K. Sasaki, Zeitschrift für Physik C Particles and Fields **32**, 149 (1986).

[26] H. Fritzsch, Nucl. Phys. **B155**, 189 (1979).

[27] H. Fritzsch and Z.-z. Xing, Prog. Part. Nucl. Phys. **45**, 1 (2000), arXiv:hep-ph/9912358 [hep-ph] .

[28] H. Fritzsch and Z.-Z. Xing, Phys. Lett. **B372**, 265 (1996), arXiv:hep-ph/9509389 [hep-ph] .

[29] C. G. Callan, Phys. Rev. D **2**, 1541 (1970).

[30] K. Symanzik, Communications in Mathematical Physics **18**, 227 (1970).

[31] K. Symanzik, Communications in Mathematical Physics **23**, 49 (1971).

[32] M. E. Peskin and D. V. Schroeder, *An Introduction to quantum field theory* (Addison-Wesley, Reading, USA, 1995).

[33] J. C. Collins, *Renormalization: An Introduction to Renormalization, the Renormalization Group and the Operator-Product Expansion*, Cambridge Monographs on Mathematical Physics (Cambridge University Press, 1984).

[34] P. Kopietz, L. Bartosch, and F. Schütz, Lect. Notes Phys. **798**, 1 (2010).

[35] T. J. Hollowood, *Renormalization Group and Fixed Points: in Quantum Field Theory (SpringerBriefs in Physics)* (Springer, 2013).

[36] B. Delamotte, Am. J. Phys. **72**, 170 (2004), arXiv:hep-th/0212049 [hep-th] .

[37] B. Delamotte, Lect. Notes Phys. **852**, 49 (2012), arXiv:cond-mat/0702365 [cond-mat.stat-mech] .

[38] G. 't Hooft and M. Veltman, Nuclear Physics B **44**, 189 (1972).

[39] G. 't Hooft, Nucl. Phys. **B61**, 455 (1973).

[40] J. C. Collins, in *QCD and beyond. Proceedings, Theoretical Advanced Study Institute in Elementary Particle Physics, TASI-95, Boulder, USA, June 4-30, 1995* (1995) pp. 269–326, arXiv:hep-ph/9510276 [hep-ph] .

[41] M. E. Fisher, *Conceptual foundations of quantum field theory. Proceedings, Symposium and Workshop, Boston, USA, March 1-3, 1996*, Rev. Mod. Phys. **70**, 653 (1998).

[42] E. C. G. Stueckelberg de Breidenbach and A. Petermann, Helv. Phys. Acta **26**, 499 (1953).

[43] K. G. Wilson, Phys. Rev. B **4**, 3174 (1971).

[44] K. G. Wilson, Phys. Rev. B **4**, 3184 (1971).

[45] K. G. Wilson, Rev. Mod. Phys. **47**, 773 (1975).

[46] H. Kleinert and V. Schulte-Frohlinde, *Critical Properties of ϕ^4-Theories* (World Scientific, 2001).

[47] C. Wetterich, Physics Letters B **301**, 90 (1993).

[48] T. R. Morris, Int. J. Mod. Phys. **A9**, 2411 (1994), arXiv:hep-ph/9308265 [hep-ph] .

[49] J. Polchinski, Nucl. Phys. **B231**, 269 (1984).

[50] J. Berges, N. Tetradis, and C. Wetterich, Phys. Rept. **363**, 223 (2002), arXiv:hep-ph/0005122 [hep-ph] .

[51] H. Gies, Lect. Notes Phys. **852**, 287 (2012), arXiv:hep-ph/0611146 [hep-ph] .

[52] S. Weinberg, *The Quantum Theory of Fields, Volume 2: Modern Applications* (Cambridge University Press, 2005).

[53] D. Barducci, M. Fabbrichesi, C. M. Nieto, R. Percacci, and V. Skrinjar, JHEP **11**, 057 (2018), arXiv:1807.05584 [hep-ph] .

[54] S. Weinberg, in *General Relativity: An Einstein Centenary Survey* (1980) pp. 790–831.

[55] D. J. Gross and F. Wilczek, Phys. Rev. Lett. **30**, 1343 (1973).

[56] D. J. Gross and F. Wilczek, Phys. Rev. **D8**, 3633 (1973).

[57] H. D. Politzer, Phys. Rev. Lett. **30**, 1346 (1973).

[58] D. F. Litim and F. Sannino, JHEP **12**, 178 (2014), arXiv:1406.2337 [hep-th] .

[59] A. D. Bond and D. F. Litim, Phys. Rev. **D97**, 085008 (2018), arXiv:1707.04217 [hep-th] .

[60] A. D. Bond, G. Hiller, K. Kowalska, and D. F. Litim, JHEP **08**, 004 (2017), arXiv:1702.01727 [hep-ph] .

[61] A. Eichhorn, Front. Astron. Space Sci. **5**, 47 (2019), arXiv:1810.07615 [hep-th] .

[62] P. Pascual and R. Tarrach, *QCD: Renormalization for the Practitioner*, 1st ed., edited by S.-V. B. Heidelberg, Lecture Notes in Physics, Vol. 194 (Springer-Verlag Berlin Heidelberg, 1984).

[63] D. Buttazzo, G. Degrassi, P. P. Giardino, G. F. Giudice, F. Sala, A. Salvio, and A. Strumia, JHEP **12**, 089 (2013), arXiv:1307.3536 [hep-ph] .

[64] G. Cvetič, S. S. Hwang, and C. S. Kim, Phys. Rev. D **58**, 116003 (1998).

[65] P. Sikivie and F. Gürsey, Phys. Rev. D **16**, 816 (1977).

[66] T. Cheng and L. Li, *Gauge Theory of Elementary Particle Physics*, Oxford science publications (Clarendon Press, 1984).

[67] T. P. Cheng, E. Eichten, and L.-F. Li, Phys. Rev. D **9**, 2259 (1974).

[68] M. E. Machacek and M. T. Vaughn, Physics Letters B **103**, 427 (1981).

[69] M. Luo and Y. Xiao, Physical Review Letters **90**, 011601 (2003), hep-ph/0207271 .

[70] V. Barger, M. S. Berger, and P. Ohmann, Phys. Rev. D **47**, 1093 (1993).

[71] R. Hempfling and B. A. Kniehl, Phys. Rev. **D51**, 1386 (1995), arXiv:hep-ph/9408313 [hep-ph] .

[72] B. Pendleton and G. Ross, Physics Letters B **98**, 291 (1981).

[73] R. Slansky, Phys. Rept. **79**, 1 (1981).

[74] E. B. Dynkin, Trans. Am. Math. Soc. Ser.2 **6**, 111 (1957).